﴿ وأنزل الله عليك الكتاب والحكمة وعلمك

مالم تكن تعلم وكان فضل الله عليك عظيما ﴾

صدق الله العظيم

النساء / الآية (113)

CHAPTER ONE

INTRODUCTION

1.1 General

The engineering of modern composite materials has had a significant impact on the technology of design and construction. The high-quality composite materials are lighter, stiffer and stronger than any other structural material used in construction. Composite materials are ideal for structural applications where high stiffness per unit weight and potentially low unit cost are required. Aircrafts and spacecrafts are typical weight–sensitive structures in which composite materials are cost–effective.

A composite material can be defined as a material that is composed of two or more distinct phases, usually a reinforcing material supported in compatible matrix, assembled in prescribed amounts to achieve specific physical and chemical properties (***Stegmann*** and ***Lund, 2001***) [(14)].

Composite materials have many characteristics that are different from many conventional engineering materials. Most common engineering materials are homogeneous and isotropic while the composite materials are often heterogeneous and anisotropic. Such materials have physical properties varying with respect to position and orientation (***Lekhnitskii, 1981***) [(21).]

Layered plates are extensively used in the construction of aerospace, civil, marine, automotive and other high performance structures, and during the operation of these structures they are subject to static and dynamic loads. Therefore, there exists a need for the investigation of the response of layered (laminated) composite–material plates subjected to such types of loading.

1.2 Classification of composite materials

In order to classify and characterize the composite materials, a distinction between the following four types is commonly accepted:

A. ***Fibrous composite materials*** that consist of fibers in a matrix, e. g.

- Orthotropic aligned reinforced materials: stiffeners, wires, and fibers in matrix.

B. ***Laminated composite materials*** that consist of layers of various materials, e. g.

- Laminated glass, plywood and clad metals.

C. ***Particulate composite materials*** that are composed of particles in a matrix, e. g.

- Quasi–isotropic random reinforced materials: Powder or particles in a matrix like ceramics.

D. ***Combinations of some or all of the first three types***, e. g.

- Laminated fiber–reinforced materials: Orthotropic lamina bonded together to form an anisotropic material.
- Sandwich constructions: face sheets bonded to a lightweight core.

The fiber–reinforced laminates have increasingly found applications in many engineering structures because of their anisotropic material properties that can be tailored through variation of the fiber orientation and stacking sequence of lamina that give the designer an added degree of flexibility.

1.3 Analysis of composite material plates

The modeling techniques associated with the finite element method for the analysis of composite plates have been based on the following approaches (***Ferreira*** and ***Fernandes, 2003***) [8]:

A. Equivalent single–layer theories (2–D Layered approach)
   - Classical lamination theory (CLT).
   - First order shear deformation theory (FSDT).
   - High order shear deformation theory (HOST).

B. Three–dimensional elasticity theory (3–D).
   - Traditional three-dimensional elasticity formulation.
   - Layerwise theories.

The equivalent single–layer theories are derived from the three-dimensional elasticity theory by making suitable assumptions concerning the kinematics of deformation of the stress state through the thickness of the composite plates. These assumptions allow the reduction of three-dimensional problem to two-dimensional problem. The equivalent single–layer theories are suitable for thin to moderately thick layered composite plates. In the three–dimensional or layerwise theories each layer is treated as three-dimensional solid and these theories are suitable for thick composite plates.

In the present study, the higher order shear deformation theory of **Reddy [**mentioned in ***Reddy (1999)*** [33] and ***Santos et al. (1998)*** [38]**]** with seven and nine degrees of freedom per node is adopted. This theory (sometimes called "third order theory") is better than the classical lamination theory and first order shear deformation theory, because it represents the plate kinematics better, does not require shear correction factors, and yields more accurate inter–laminar stress distributions through the plate thickness.

1.4 Applications of composite materials

The procession road in ancient Babylon, one of the most wonders of the ancient world, was made of bitumen reinforced with straw. Straw and horsehair have been used to reinforce mud bricks for at least 5000 years (***Ashby*** and ***Jones, 1988***) [3].

The composite materials industry however is new. It has grown rapidly in the past fifty years with development of fibrous composites; to begin with glass fiber-reinforced polymers and more recently carbon fiber-reinforced polymers. Fiber reinforced polymer composites with high strength to weight and high stiffness to weight ratios have become more important in light weight applications such as aircraft, aerospace, sports and boats application….etc. Their use in such systems is a revolution in materials usage, which is still accelerating. Some of composite materials applications today are listed in Table (1.1).

Table (1.1): Applications of composite materials in some industries [1].

Application	***Parts***
Marine	Boats, fairings, deck houses, tanks, deep submergence objects, vehicles, etc.
Aircraft	Rudder, fuselage, landing – gear, fairings, etc.
Automobile	Tires, drive shaft, window glass, etc.
Chemical Industries	Pipes, pressure vessels, tanks, etc.
Sport	Tennis rackets, sports equipments.
Medical	Dental materials, joints in human bodies, denture bases.

1.5 Objective and scope

In this study the focus will be on a hybrid class, namely ***laminated fiber–reinforced composite materials*** and ***sandwich constructions*** as they are the basic building element of ***plate structures***, taking into account that these structures are subject to static as well as dynamic loads.

A computer program (coded ***FEDALP*** in this study) has been written and numerical applications on plate structures for testing the accuracy of the program are studied. Also, the results are compared with those reported by other researches.

A parametric study is presented for the dynamic analysis in order to determine the effect of several influencing parameters on the behavior of layered plates with various boundary conditions.

1.6 Thesis layout

This thesis is organized in seven chapters:

Chapter one: introduces and explains briefly the problem within hand, the aim of the study and the subjects included in other chapters.

Chapter two: contains a brief review of previous studies on the subject under consideration.

Chapter three: presents a description of different theories to analyze layered plates and establishes the derivations of the basic equations of the macromechanical behavior of such structures. Also, the chapter shows the classification of the laminated plates.

Chapter four: contains a complete formulation of the stiffness, mass and damping matrices in case of plate bending element. Also, it includes a discussion of the solution techniques which are adapted to solve the eignvalue problems as well as the dynamic equilibrium equations.

Chapter five: describes the flow chart of the computer program (***FEDALP***) which has been written in this study using ***Fortran-77*** language with several applications.

Chapter six: includes a parametric study that was done on different variables which affect the dynamic response of fiber–reinforced laminated composite plates.

Chapter seven: gives a summary of the conclusions which can be drawn from this study and the suggestions for future related works.

CHAPTER TWO

REVIEW OF LITERATURE

2.1 General

Laminated fiber-reinforced composite material plates have continuous increasing usage in primary and secondary aerospace and aircraft structures owing to their superior mechanical properties as mentioned previously. One form of these materials, being used in current design studies, is the unidirectional fiber-reinforced lamina. In addition, anisotropy, non-homogeneity and larger ratio of longitudinal to transverse modulus of these materials supply an improvement in the existing analytical tools. As a result, the analysis of laminated composite plates has attracted many research workers and has been considerably improved to achieve realistic results.

The present review covers three aspects. The first includes the developments in the analysis of laminated composite plates subjected to static load. The second aspect is concerned with the developments in the free vibration analysis of such plates. The third deals with those plates under dynamic loads.

2.2 Static analysis

Pryor and **Barker** [29] **(1971)** used the finite element analysis technique, which included the effect of transverse shear deformation, and they found that it is readily adaptable to arbitrary laminated plates. The discrete element employed is a rectangle with five degrees of freedom per node (i.e. u, v, w, θ_x and θ_y) which include extension, bending and transverse shear deformation states. The displacement formulation is based on a refined first order shear deformation

theory for laminates, which assumes constant shear strain through thickness, thus a shear correction coefficient is used. The theory allows the deformed normal to rotate, independently, to include transverse shear deformations. Results for plate deformations and internal stress distribution, including transverse shear stresses, were shown to compare quantitatively with the theory of elasticity for selected example problems.

Maweneya and **Davies** [23] **(1974)** presented a development for a general quadratic multilayer plate element for the analysis of arbitrary layered curved plates. In the formulation, each layer of the multilayer plate can have different orthotropic properties and can be deformed locally, i.e., the formulation depends on the layerwise first order shear deformation theory. Examples of bending problems were presented which demonstrated the applicability of the formulation.

Turvey [44] **(1977)** presented an exact and approximate analysis for the flexural response, including transverse shear deformations, of rectangular, simply supported, moderately thick, antisymmetrically laminated plates subjected to a variety of load distributions. He demonstrated that the approximate analysis was accurate for cross-ply lay-ups but less so for angle-ply lay-ups. Thereafter the exact analysis, incorporating a shear correction factor used previously in an approximate analysis, is used to provide detailed results for four different types of loads, namely a uniform load, a central patch load, a central point load and a hydrostatic load.

Panda and **Natarajan** [24] **(1979)** described a finite element analysis technique for an arbitrary laminated anisotropic plate. A superparametric plate element with five degrees of freedom per node was used in the analysis. A stress-strain relation was derived to the problem from a three-dimensional approach. The volume integration of the stiffness matrix was evaluated

numerically by using the Gauss quadrature formula with **2*2*2** sampling points. A variety of laminated plate problems were solved and the results are compared with the exact solutions, which demonstrated the validity of the method.

Reddy [34] **(1984)** presented a higher order shear deformation theory. This theory contains the same dependent unknowns as in Mindlin type theory and accounts for parabolic distribution of the transverse shear strains through the thickness of the plate. The results were compared with the exact solutions of three-dimensional elasticity theory, the first order shear deformation theory and classical plate theory. The comparison showed that the higher order theory predicted the deflections, stresses and frequencies more accurately when compared to the first order theory and the classical plate theory.

Sciuva (1986) [39] developed several triangular and quadrilateral multilayered anisotropic plate elements, based on Mindlin theory, which included extension, bending and transverse shear deformation. To show the accuracy and the relative merits of the developed finite elements, results were presented for some sampling problems of bending and free undamped vibrations of three layers, symmetric cross-ply square plate that was simply-supported on all edges.

Pandya and **Kant** [25] **(1988)** presented a C^o-continuous displacement finite element formulation of a higher order theory for flexure of thick arbitrary laminated composite plates under transverse loads. The displacement mode accounts for constant non-linear and variation of in-plane and transverse displacements respectively through the plate thickness. The discrete element chosen was a nine-noded quadrilateral element with nine degrees of freedom per node. Results for plate deformation and stresses for selected examples were compared with available solutions.

Pandya and **Kant** [26] **(1988)** presented a simple, isoparametric finite element formulation based on higher order displacement model for flexure analysis of multilayer symmetric sandwich plates. This formulation does not require the use of shear correction factor (s) generally associated with the first order shear deformation theory. Two sandwich plate theories were developed; one, in which the free shear stress conditions on the top and bottom bounding planes were imposed and another, in which such conditions were not imposed. A comparison of results of first order theory and classical plate theory with the exact three-dimensional analysis indicated high percentage error in the results of thick sandwich or laminated plates, especially in the analysis of sandwich plates with highly stiff top and bottom layers. But the results of higher order two-dimensional theory had good agreement with those of three-dimensional elasticity theory.

2.3 Free vibration analysis

Khatua and **Chang** [17] **(1973)** presented a finite element displacement analysis of multilayer sandwich beams and plates, each with **n** stiff layers and **n-1** weak cores. Each layer of the sandwich structure may have individual orthotropic properties of its own, and the bending rigidities of the stiff layers are taken into account while direct stresses in core are neglected in the analysis. Several free vibration problems were solved, and the results were compared with the exact solutions, demonstrating the validity of the method.

Phan and **Reddy** [28] **(1985)** used a higher order shear deformation theory to analyze laminated anisotropic composite plates for deflections, stresses natural frequencies and buckling loads. The theory accounts for parabolic distribution of the transverse shear stresses, and requires no shear correction coefficient. A displacement finite element model for the theory was developed, and applications of the element to bending, vibration and stability of laminated

plates were discussed. The results of higher order theory and classical plate theory were compared with those obtained by using the three-dimensional elasticity theory. The maximum percentage differences of higher order theory and classical lamination theory with three-dimensional elasticity theory were **0.326%** and **70.19%** respectively, for a four layer square, simply supported, antisymmetric angle-ply laminated plate.

Khdeir [18] **(1988)** developed a generalized Levy- type solution in conjunction with the state space concept for the bending, buckling, and vibration of antisymmetric angle-ply laminated plates. The solution was applicable to rectangular plates with two opposite edges simply supported and the remaining edges subjected to a combination of clamped, simply supported and free boundary conditions. Comparisons were made with exact and finite element solutions to demonstrate the validity of the method.

Kant and **Mallikarjuna** [16] **(1989)** formulated a refined higher order theory for free vibration analysis of unsymmetrically laminated multilayered plates. The theory accounts for parabolic distribution of the transverse shear strains through the thickness of the plate and also for rotary inertia effects. A simple C^o-finite element formulation is used and the nine-noded Lagrangian element is chosen with seven degrees of freedom per node. The adopted theory predicts the frequencies more accurately when compared with the first order and classical plate theories.

Santos, et al. [38] **(1998)** proposed a numerical model for the analysis of the free vibration of multilayerd, fully free rectangular plate with arbitrary lay-ups. The method is based on a displacement field that assumes a non-linear distribution of the in-plane displacement with respect to the thickness coordinate, and a constant transverse displacement through the thickness of the plate. The displacement field accounts for a parabolic distribution of transverse

shear strains and satisfies the condition of zero transverse shear stresses on the top and bottom surfaces of the plate. The mathematical problem is solved by Ritz technique. The results show that the adopted higher order Ritz model predicts more accurate solution than the first order theory and the classical plate theory when compared with those obtained from a three-dimensional finite element analysis.

Singh and **Rao**[40] **(2000)** studied free vibration behavior of unsymmetrically laminated plates. They used four-noded shear flexible rectangular element with six degrees of freedom per node [three displacements (u, v and w), two rotations (θx and θy) and twist (θxy)]. A series of numerical examples were solved to demonstrate the efficiency of the adopted element.

2.4 Dynamic analysis

Reddy [37] **(1982)** presented two different lamination schemes under appropriate boundary conditions and sinusoidal distribution of the transverse load. The exact form of the spatial variation of the solution was obtained, and the problem was reduced to the solution of a system of ordinary deferential equations in time, which were integrated numerically using Newmark integration method. The adopted theory was first order shear deformation theory. Numerical results for deflection and stresses of a rectangular plate were presented showing the effect of plate side-to-thickness ratio, aspect ratio, material orthotropy and lamination scheme.

Reddy [36] **(1983)** investigated the transient response of isotropic, orthotropic and layered anisotropic composite plates by using a shear flexible finite element solution depending on using first order shear deformation theory. Numerical convergence and stability of the adopted element was established using Newmark integration method. Numerical results for deflection and stresses were

presented for rectangular plates under various boundary conditions and loading. The effects of time step, finite elements mesh and lamination schemes of the transient response were investigated.

Khdeir and **Reddy** [19] **(1988)** investigated the transient response of simply supported antisymmetric angle-ply rectangular plates subjected to arbitrary loading. They presented an exact solution for equation of motion of the first order transverse shear deformation theory as well as the classical lamination theory. The solutions of these two theories were considered to bring out the influence of the transverse shear deformation, the degree of anisotropy and the number of layers.

Mallikarjuna and **Kant** [22] **(1988)** formulated a simple isoparametric finite element with five degrees of freedom per node based on a higher order displacement model for dynamic analysis of multilayer symmetric composite plates with an explicit time marching scheme. A special mass lumping scheme was adopted which conserves the total mass of the element and includes the effects due to rotary inertia terms. Several numerical examples were presented and compared with results from other sources. The comparison showed that higher order theory is more accurate than the Mindlin theory for the evaluation of plate response to different types of dynamic loads. The effects of the time step, finite elements mesh and lamination schemes on the transient response were studied.

Kommineni and **Kant** [20] **(1993)** presented a C^o continuous finite element formulation of a higher order displacement theory with nine degrees of freedom per node for predicting linear and geometrically non-linear (in the sense of **Von-Karman** concept**)** transient response of composite and sandwich plates. The displacement model accounts for non-linear cubic variation of in-plane displacement components through the thickness of the laminate and the theory

requires no shear correction coefficients. The explicit central difference integration scheme was used for solution. Numerical results for center transverse deflection and stresses were presented for square and rectangular composite and sandwich plates under various boundary conditions and loading and the results compared with the results of other sources. The effects of time step, finite element mesh on linear and non-linear response were investigated.

From the preceding review of literature, it is clear that there is no study, which considers the dynamic analysis of laminated composite plates by taking into account the effect of damping. Also, there is a little literature that takes into account the higher order displacement model of nine degrees of freedom per node with different types of lamination, different geometrical dimensions, different boundary conditions and aspect ratio effect. Thus, the present study will cover the above research fields.

CHAPTER THREE

THEORY AND DERIVATIONS

3.1 Introduction

The basic building element of laminated fiber–reinforced composite plates is the composite lamina. Thus, the knowledge of the mechanical behavior of a lamina is essential to study the laminated composite structures.

In the design of laminated fiber–reinforced plates, layers of fiber–reinforced material are bonded together with the fibers in each layer typically oriented in different directions in order to give strengths and stiffness in the various directions and to match the requirements of the structural elements to be built.

In this chapter, stress–strain relations of anisotropic, orthotropic material are summarized. Stresses and stress resultants formulations are explained for the theory of the present study. Classification of laminated plates is also given.

3.2 Stress–strain relations for a composite lamina

A lamina (ply) is a flat (or sometimes curved as in shells) arrangement of unidirectional or woven fibers in a supporting matrix. The following demands must be made on fibers used in reinforced composite materials ***(Stegmann*** and ***Lund, 2001)*** [14]**:**

- High tensile strength.
- High modulus of elasticity.
- Lower ultimate elongation than the matrix.

- Good adhesion to the matrix.
- Good resistance to the matrix and its additives.

The influence of the matrix on the composite is as follows:

- Binding the reinforcement and distributing the load.
- Protecting the fibers from physical and mechanical damage.
- Dominant factor in determining transverse shear and through–thickness properties.
- Dominant factor in determining impact resistance and fracture toughness.
- Dominant factor in determining long time (creep) response.
- Dominant factor in determining service temperature.

The purpose of this section is to provide a basic understanding of the macromechanical behavior of a lamina when averaged apparent mechanical properties are considered.

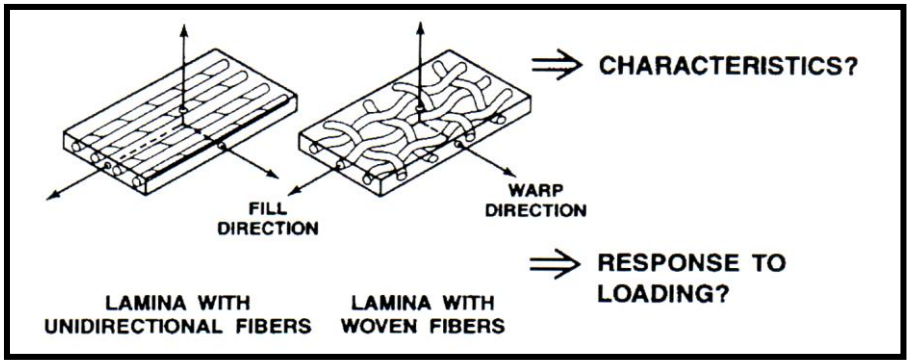

Figure (3.1): Basic questions of lamina macromechanics [14].

The basic questions of lamina macromechanics as illustrated by Figure (3.1) are:

1. What are the characteristics of a lamina?
2. How does a lamina respond to loading?

The materials are assumed to behave linearly elastic, i. e., the generalized **Hooke's** law is used for relating the stresses to strains. Figure (3.2) shows transformation of plane **x** and **y**-coordinates into principal **1** and **2**-coordinates.

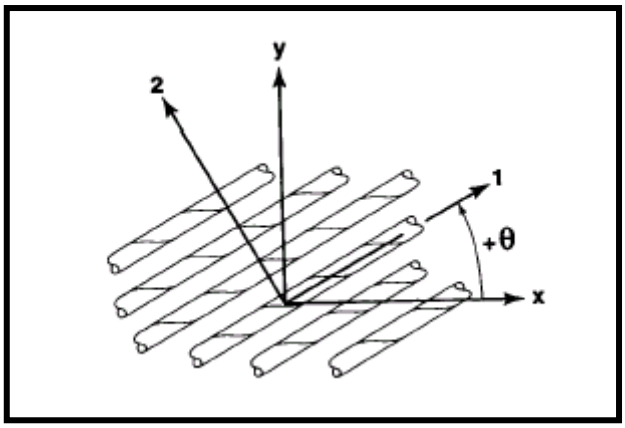

Figure (3.2): Positive rotation of principal material axes 1-2 from x-y axes [14].

Hooke's law gives the general ***anisotropic*** constitutive relation with respect to a material coordinate system **1–2–3** as follows:

$$\begin{Bmatrix} \sigma_1 \\ \sigma_2 \\ \sigma_3 \\ \tau_{23} \\ \tau_{13} \\ \tau_{12} \end{Bmatrix} = \begin{bmatrix} c_{11}\ c_{12}\ c_{13}\ c_{14}\ c_{15}\ c_{16} \\ c_{21}\ c_{22}\ c_{23}\ c_{24}\ c_{25}\ c_{26} \\ c_{31}\ c_{32}\ c_{33}\ c_{34}\ c_{35}\ c_{36} \\ c_{41}\ c_{42}\ c_{43}\ c_{44}\ c_{45}\ c_{46} \\ c_{51}\ c_{52}\ c_{53}\ c_{54}\ c_{55}\ c_{56} \\ c_{61}\ c_{62}\ c_{63}\ c_{64}\ c_{65}\ c_{66} \end{bmatrix} \begin{Bmatrix} \varepsilon_1 \\ \varepsilon_2 \\ \varepsilon_3 \\ \gamma_{23} \\ \gamma_{13} \\ \gamma_{12} \end{Bmatrix} \qquad \textit{…(3.1)}$$

i.e., twenty-one independent material constants are used to describe the material.

For the composite lamina illustrated in Figure (3.2), there are two orthogonal planes of material property symmetry and the material is termed ***orthotropic***. The stress–strain relations in coordinates aligned with principal material directions are given by:

$$\begin{Bmatrix}\sigma_1\\ \sigma_2\\ \sigma_3\\ \tau_{23}\\ \tau_{13}\\ \tau_{12}\end{Bmatrix}=\begin{bmatrix}c_{11}\,c_{12}\,c_{13} & 0 & 0 & 0\\ c_{21}\,c_{22}\,c_{23} & 0 & 0 & 0\\ c_{13}\,c_{23}\,c_{33} & 0 & 0 & 0\\ 0\;\;0\;\;0 & c_{44} & 0 & 0\\ 0\;\;0\;\;0 & 0 & c_{55} & 0\\ 0\;\;0\;\;0 & 0 & 0 & c_{66}\end{bmatrix}\begin{Bmatrix}\varepsilon_1\\ \varepsilon_2\\ \varepsilon_3\\ \gamma_{23}\\ \gamma_{13}\\ \gamma_{12}\end{Bmatrix} \qquad \textbf{\textit{…(3.2)}}$$

If a moderately thick plate with orthotropic laminae is assumed, i. e., $\varepsilon_3 = 0$, the stress–strain relations are as follows:

$$\begin{Bmatrix}\sigma_1\\ \sigma_2\\ \tau_{12}\\ \tau_{13}\\ \tau_{23}\end{Bmatrix}=\begin{bmatrix}c_{11}\,c_{12}\,0 & 0 & 0\\ c_{21}\,c_{22}\,0 & 0 & 0\\ 0\;\;0\;\;c_{66} & 0 & 0\\ 0\;\;0\;\;0 & c_{55} & 0\\ 0\;\;0\;\;0 & 0 & c_{44}\end{bmatrix}\begin{Bmatrix}\varepsilon_1\\ \varepsilon_2\\ \gamma_{12}\\ \gamma_{13}\\ \gamma_{23}\end{Bmatrix} \qquad \textbf{\textit{…(3.3a)}}$$

or

$$\{\sigma\}=[\mathbb{E}]\{\varepsilon\} \qquad \textbf{\textit{…(3.3b)}}$$

where

$$c_{11} = E_1 / 1 - \nu_{12}\nu_{21} \qquad c_{44} = \mathbb{G}_{23}$$

$$c_{12} = \nu_{12}\, E_2 / 1 - \nu_{12}\nu_{21} \qquad c_{55} = \mathbb{G}_{13} \qquad \textbf{\textit{…(3.4)}}$$

$$c_{22} = E_2 / 1 - \nu_{12}\nu_{21} \qquad c_{66} = \mathbb{G}_{12}$$

To express the stress–strain relations for the lamina of arbitrary orientation as illustrated in Figure (3.2), the transformation equations are used for expressing stresses in ***x–y*** coordinate system in terms of stresses in ***1–2*** coordinate system ***(Jones, 1975)*** [15]:

$$\begin{Bmatrix}\sigma_x\\ \sigma_y\\ \tau_{xy}\\ \tau_{xz}\\ \tau_{yz}\end{Bmatrix}=\begin{bmatrix}\\ \mathrm{T}\\ \\ \\ \\ \\ \end{bmatrix}^{\mathrm{T}}\begin{bmatrix}\\ \mathbb{E}\\ \\ \\ \\ \\ \end{bmatrix}\begin{bmatrix}\\ \mathrm{T}\\ \\ \\ \\ \\ \end{bmatrix}\begin{Bmatrix}\varepsilon_x\\ \varepsilon_y\\ \gamma_{xy}\\ \gamma_{xz}\\ \gamma_{yz}\end{Bmatrix} \qquad \textbf{\textit{…(3.5)}}$$

where

$$T = \begin{bmatrix} c^2 & s^2 & sc & 0 & 0 \\ s^2 & c^2 & -sc & 0 & 0 \\ -2sc & 2sc & c^2 - s^2 & 0 & 0 \\ 0 & 0 & 0 & c & -s \\ 0 & 0 & 0 & s & c \end{bmatrix} \qquad \textbf{…(3.6)}$$

in which, $\boldsymbol{c = \cos\theta}$ and $\boldsymbol{s = \sin\theta}$.

Using the above transformations, the stress–strain relations for arbitrary lamina orientation can be written as:

$$\begin{Bmatrix} \sigma_x \\ \sigma_y \\ \tau_{xy} \\ \tau_{xz} \\ \tau_{yz} \end{Bmatrix} = \begin{bmatrix} Q_{11} & Q_{12} & Q_{16} & 0 & 0 \\ Q_{12} & Q_{22} & Q_{26} & 0 & 0 \\ Q_{16} & Q_{26} & Q_{66} & 0 & 0 \\ 0 & 0 & 0 & Q_{55} & Q_{45} \\ 0 & 0 & 0 & Q_{45} & Q_{44} \end{bmatrix} \begin{Bmatrix} \varepsilon_x \\ \varepsilon_y \\ \gamma_{xy} \\ \gamma_{xz} \\ \gamma_{yz} \end{Bmatrix} \qquad \textbf{…(3.7)}$$

A special orthotropic composite lamina is that in which the principal material axes are aligned with the structural axes. For example:

$$\begin{bmatrix} Q_{11} & Q_{12} & Q_{16} & 0 & 0 \\ Q_{12} & Q_{22} & Q_{26} & 0 & 0 \\ Q_{16} & Q_{26} & Q_{66} & 0 & 0 \\ 0 & 0 & 0 & Q_{55} & Q_{45} \\ 0 & 0 & 0 & Q_{45} & Q_{44} \end{bmatrix} = \begin{bmatrix} Q_{11} & Q_{12} & 0 & 0 & 0 \\ Q_{12} & Q_{22} & 0 & 0 & 0 \\ 0 & 0 & Q_{66} & 0 & 0 \\ 0 & 0 & 0 & Q_{55} & 0 \\ 0 & 0 & 0 & 0 & Q_{44} \end{bmatrix} \qquad \textbf{…(3.8)}$$

Finally, a generally orthortropic composite lamina is an orthotropic lamina in which the principal material axes are not aligned with the structural axes and the constitutive matrix (**Q)** is as defined above in Equation (3.7). All the coefficients of the constitutive matrix are listed in **Appendix (A).**

3.3 Laminated plate theories

A laminate plate is a series of laminae bonded together to act as an integral structural element. Thus, a laminate is a structural element with essential features of both material properties and geometry.

The stiffness and strength of such a composite material structural configuration are obtained from the properties of the constituent laminae, and the macromechanical behavior of a laminate is the main topic of this section. Figure (3.3) shows the individual layers with arbitrary orientations.

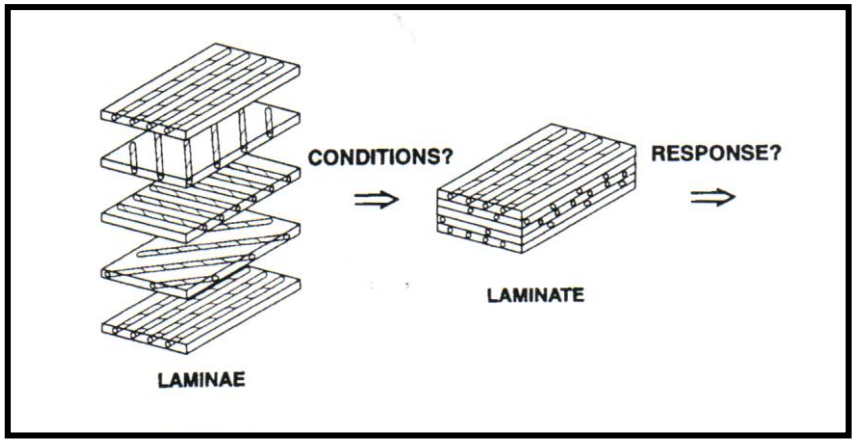

Figure (3.3): Laminated plate with several laminae orientations [14].

As mentioned previously that in the analysis of the laminated plates, there are two categories of theories, equivalent single layer and three-dimensional elasticity theories. In the first category, the material properties of the constituent layers are smeared to form a hypothetical single layer whose properties are equivalent to through thickness integrated sum of its constituents, and this category contains classical lamination theory, first order theory and higher order theory as subclasses.

In the classical laminated plate theory [also called ‘‘classical lamination theory (CLT) ’’], which is based on **Krichhoff-Love** hypothesis for plates and shells, one of its assumptions is that the normals to the midsurface before deformation remain straight and normal to the midsurface after deformation. In other words, the through-thickness shear deformation effects are negligible. In general, layered composite plates exhibit coupling between the inplane displacements, transverse displacement and shear rotations. However, due to the low transverse shear modulus relative to the inplane **Young's** modulus of each lamina, the transverse shear deformation effects are more pronounced in composite than isotropic plates. Hence, several types of shear deformation theories have been introduced.

Timoshenko beam theory, which includes transverse shear deformation and rotary inertia effects, has been extended to isotropic plates by **Reissner** and **Mindlin,** and to laminate anisotropic plates by **Yang**, **Norris** and **Stavsky**. **Yang et al.** Theory, also called " First order shear deformation theory (FSDT) ", takes into account the effect of transverse shear deformation and assumes it constant through the plate thickness. Thus a shear correction factor is used.

The higher order shear deformation theories are more efficient to represent the transverse shear deformation, through-thickness displacements and strains, natural frequency and dynamic response of composite plates, and it contains the first order theory as a special case. Hence, it is adopted in the present study to develop the governing equations of laminated plates. Figure (3.4) shows, briefly, the basic difference between the classical and first order theories with the higher order theories.

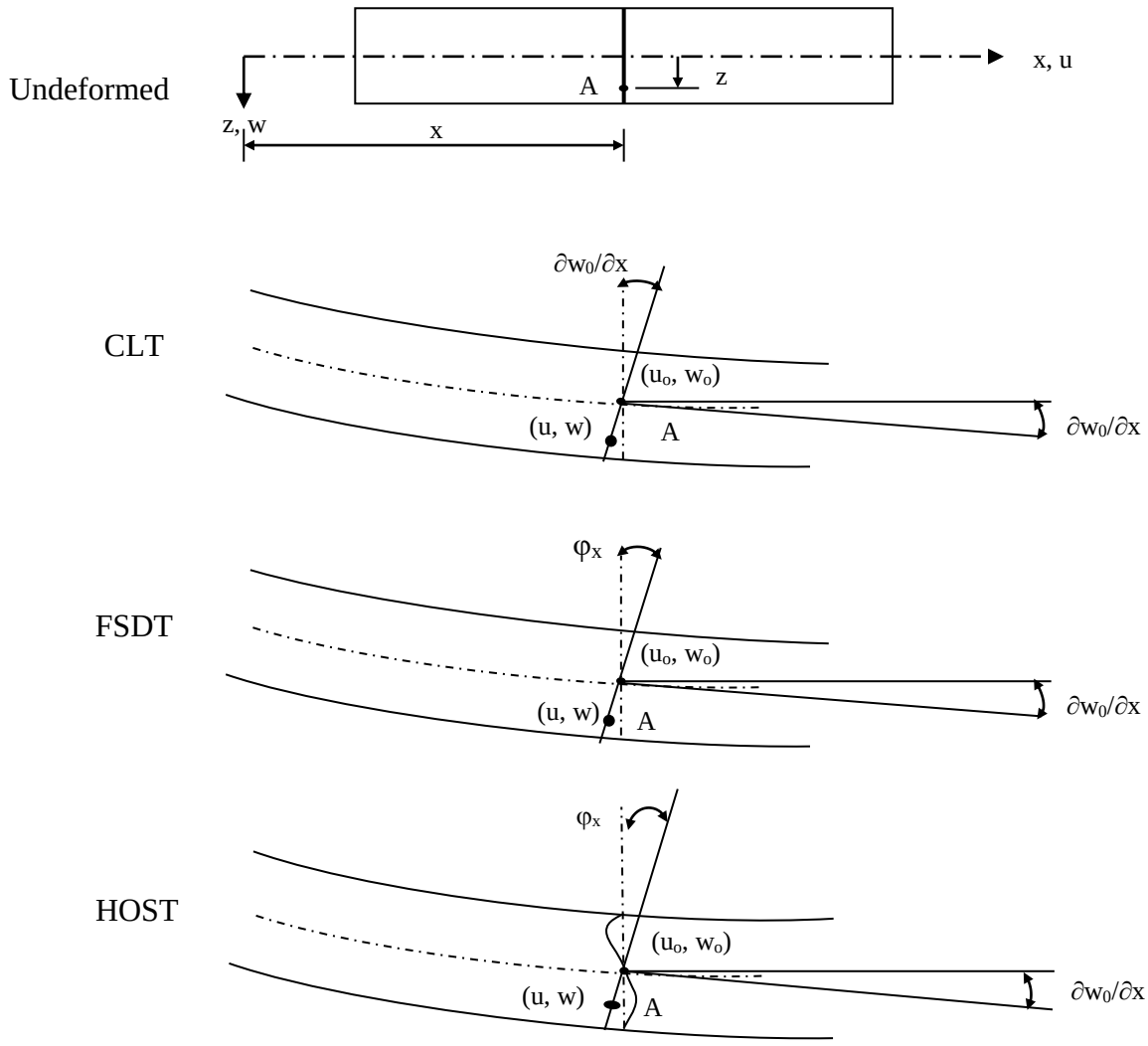

Figure (3.4): Kinematics of deformation of a plate in various plate theories.

3.4 Higher order shear deformation theories

The assumptions of a higher order plate theory can also be used within equivalent single layer formulation ***(Stegmann*** and ***Lund, 2001)*** [14]**:**

1. The plate may be moderately thick.
2. The inplane displacement u (x, y, z, t) and v (x, y, z, t) are cubic functions of z.
3. The transverse shear stress τ_{xz}, τ_{yz} are parabolic in z.
4. The inplane stresses σ_x, σ_y and τ_{xy} are cubic functions of z.

5. The normals to the mid-surface before deformation are straight, but not necessarily remaining normal to the mid-surface after deformation.
6. The transverse normal strain ε_z is negligible.

In the general higher order shear deformation theory for laminated plates, the displacement model of a generic point in a laminate are assumed to be of the form ***(Kommineni*** and ***Kant, 1993)*** [20]**:**

$$\begin{aligned} u(x, y, z, t) &= u_o(x, y, t) + z\theta_x(x, y, t) + z^2 u_o^*(x, y, t) + z^3 \theta_x^*(x, y, t) \\ v(x, y, z, t) &= v_o(x, y, t) + z\theta_y(x, y, t) + z^2 v_o^*(x, y, t) + z^3 \theta_y^*(x, y, t) \\ w(x, y, z, t) &= w_o(x, y, t) \end{aligned} \qquad \textbf{…(3.9)}$$

in which **t** denotes the time, $\mathbf{u_o}$, $\mathbf{v_o}$, and $\mathbf{w_o}$ are the components of midplane displacements of a generic point having displacements **u**, **v** and **w** in **x, y** and **z** directions, respectively. The parameters θ_x and θ_y are rotations of transverse normals in the **xz** and **yz** planes, respectively. The parameters $\mathbf{u^*_o}$, $\mathbf{v^*_o}$, θ^*_x and θ^*_y are corresponding higher order terms in Taylor's series expansion and they are also defined at the midplane. The above higher order shear deformation displacement model is for elements of nine degrees of freedom per node **(HOST9),** and a number of special cases can be derived from it. One of them is called higher order shear deformation theory with seven degrees of freedom per node **(HOST7),** in which the second–order terms are neglected (i. e., $\mathbf{u^*_o} = \mathbf{v^*_o} = 0$).

In this study, the complete formulations for strains, stresses and stress resultants expressions based on prescribed theories are presented in order to represent the displacements of the plate-bending element.

3.4.1 Higher order theory with seven degrees of freedom per node

The displacement representation for this theory is as follows [***Kant*** and ***Mallikarjuna*** [16] ***(1989), Reddy*** [33] ***(1999)***]:

$$\begin{aligned} u(x, y, z, t) &= u_o(x, y, t) + z\theta_x(x, y, t) + z^3\theta_x^*(x, y, t) \\ v(x, y, z, t) &= v_o(x, y, t) + z\theta_y(x, y, t) + z^3\theta_y^*(x, y, t) \\ w(x, y, z, t) &= w_o(x, y, t) \end{aligned} \qquad \textbf{…(3.10)}$$

in which all parameters are defined previously.

The strain-displacement relations are:

$$\begin{aligned} \varepsilon_x &= \varepsilon_x^o + z\kappa_x + z^3\kappa_x^* \\ \varepsilon_y &= \varepsilon_y^o + z\kappa_y + z^3\kappa_y^* \\ \varepsilon_z &= 0 \end{aligned} \qquad \textbf{…(3.11)}$$

$$\gamma_{xy} = \gamma_{xy}^o + z\kappa_{xy} + z^3\kappa_{xy}^*$$
$$\gamma_{xz} = \varphi_x + z^2\varphi_x^*$$
$$\gamma_{yz} = \varphi_y + z^2\varphi_y^*$$

where

$$\varepsilon_x^o = \frac{\partial u_o}{\partial x}, \qquad \varepsilon_y^o = \frac{\partial v_o}{\partial y}, \qquad \gamma_{xy}^o = \frac{\partial u_o}{\partial y} + \frac{\partial v_o}{\partial x}$$

$$\kappa_x = \frac{\partial \theta_x}{\partial x}, \qquad \kappa_y = \frac{\partial \theta_y}{\partial y}, \qquad \kappa_{xy} = \frac{\partial \theta_x}{\partial y} + \frac{\partial \theta_y}{\partial x} \qquad \textbf{…(3.12)}$$

$$\kappa_x^* = \frac{\partial \theta^*_x}{\partial x}, \qquad \kappa_y^* = \frac{\partial \theta^*_y}{\partial y}, \qquad \kappa_{xy}^* = \frac{\partial \theta^*_x}{\partial y} + \frac{\partial \theta^*_y}{\partial x}$$

$$\varphi_x = \theta_x + \frac{\partial w_o}{\partial x}, \qquad \varphi_y = \theta_y + \frac{\partial w_o}{\partial y}$$
$$\varphi^*_x = 3\theta_x^*, \qquad \varphi_y^* = 3\theta_y^*$$

all above strains are defined in the middle–plane of the laminate.

By substitution from Equation (3.11) into the stress–strain relations given by Equation (3.7), the stress– strain relations for the L^{th} lamina are as follows:

$$\begin{Bmatrix}\sigma_x\\ \sigma_y\\ \tau_{xy}\end{Bmatrix}^L = \begin{bmatrix}Q_{11}\,Q_{12}\,Q_{16}\\ Q_{12}\,Q_{22}\,Q_{26}\\ Q_{16}\,Q_{26}\,Q_{66}\end{bmatrix}^L \left(\begin{Bmatrix}\varepsilon_x^o\\ \varepsilon_y^o\\ \gamma_{xy}^o\end{Bmatrix} + z\begin{Bmatrix}\kappa_x\\ \kappa_y\\ \kappa_{xy}\end{Bmatrix} + z^3\begin{Bmatrix}\kappa_x^*\\ \kappa_y^*\\ \kappa_{xy}^*\end{Bmatrix} \right) \qquad \textbf{…(3.13)}$$

$$\begin{Bmatrix}\tau_{xz}\\ \tau_{yz}\end{Bmatrix}^L = \begin{bmatrix}Q_{55}\,Q_{45}\\ Q_{45}\,Q_{44}\end{bmatrix}^L \left(\begin{Bmatrix}\theta_x + \dfrac{\partial w_o}{\partial x}\\ \theta_y + \dfrac{\partial w_o}{\partial y}\end{Bmatrix} + 3z^2\begin{Bmatrix}\theta_x^*\\ \theta_y^*\end{Bmatrix} \right) \qquad \textbf{…(3.14)}$$

The stress, moment and shear resultants of NL–layer laminate are:

$$\begin{Bmatrix}N_x\\ N_y\\ N_{xy}\end{Bmatrix} = \int_{-h/2}^{h/2}\begin{Bmatrix}\sigma_x\\ \sigma_y\\ \tau_{xy}\end{Bmatrix} dz = \sum_{L=1}^{NL}\begin{bmatrix}Q_{11}\,Q_{12}\,Q_{16}\\ Q_{12}\,Q_{22}\,Q_{26}\\ Q_{16}\,Q_{26}\,Q_{66}\end{bmatrix}^L \left\{ \int_{h_{L-1}}^{h_L} \left(\begin{Bmatrix}\varepsilon_x^o\\ \varepsilon_y^o\\ \gamma_{xy}^o\end{Bmatrix} + z\begin{Bmatrix}\kappa_x\\ \kappa_y\\ \kappa_{xy}\end{Bmatrix} + z^3\begin{Bmatrix}\kappa_x^*\\ \kappa_y^*\\ \kappa_{xy}^*\end{Bmatrix} \right) dz \right\} \qquad \textbf{…(3.15)}$$

$$\begin{Bmatrix}M_x\\ M_y\\ M_{xy}\end{Bmatrix} = \int_{-h/2}^{h/2}\begin{Bmatrix}\sigma_x\\ \sigma_y\\ \tau_{xy}\end{Bmatrix} z\,dz = \sum_{L=1}^{NL}\begin{bmatrix}Q_{11}\,Q_{12}\,Q_{16}\\ Q_{12}\,Q_{22}\,Q_{26}\\ Q_{16}\,Q_{26}\,Q_{66}\end{bmatrix}^L \left\{ \int_{h_{L-1}}^{h_L} \left(z\begin{Bmatrix}\varepsilon_x^o\\ \varepsilon_y^o\\ \gamma_{xy}^o\end{Bmatrix} + z^2\begin{Bmatrix}\kappa_x\\ \kappa_y\\ \kappa_{xy}\end{Bmatrix} + z^4\begin{Bmatrix}\kappa_x^*\\ \kappa_y^*\\ \kappa_{xy}^*\end{Bmatrix} \right) dz \right\} \qquad \textbf{…(3.16)}$$

$$\begin{Bmatrix}M^*_x\\ M^*_y\\ M^*_{xy}\end{Bmatrix} = \int_{-h/2}^{h/2}\begin{Bmatrix}\sigma_x\\ \sigma_y\\ \tau_{xy}\end{Bmatrix} z^3 dz = \sum_{L=1}^{NL}\begin{bmatrix}Q_{11}\,Q_{12}\,Q_{16}\\ Q_{12}\,Q_{22}\,Q_{26}\\ Q_{16}\,Q_{26}\,Q_{66}\end{bmatrix}^L \left\{ \int_{h_{L-1}}^{h_L} \left(z^3\begin{Bmatrix}\varepsilon_x^o\\ \varepsilon_y^o\\ \gamma_{xy}^o\end{Bmatrix} + z^4\begin{Bmatrix}\kappa_x\\ \kappa_y\\ \kappa_{xy}\end{Bmatrix} + z^6\begin{Bmatrix}\kappa_x^*\\ \kappa_y^*\\ \kappa_{xy}^*\end{Bmatrix} \right) dz \right\} \qquad \textbf{…(3.17)}$$

$$\begin{Bmatrix}Q_x\\ Q_y\end{Bmatrix} = \int_{-h/2}^{h/2}\begin{Bmatrix}\tau_{xz}\\ \tau_{yz}\end{Bmatrix} dz = \sum_{L=1}^{NL}\begin{bmatrix}Q_{55}\,Q_{45}\\ Q_{45}\,Q_{44}\end{bmatrix}^L \left\{ \int_{h_{L-1}}^{h_L} \left(\begin{Bmatrix}\theta_x + \dfrac{\partial w_o}{\partial x}\\ \theta_y + \dfrac{\partial w_o}{\partial y}\end{Bmatrix} + 3z^2\begin{Bmatrix}\theta_x^*\\ \theta_y^*\end{Bmatrix} \right) dz \right\} \qquad \textbf{…(3.18)}$$

$$\begin{Bmatrix} Q^*_x \\ Q^*_y \end{Bmatrix} = \int_{-h/2}^{h/2} \begin{Bmatrix} \tau_{xz} \\ \tau_{yz} \end{Bmatrix} z^2 dz = \sum_{L=1}^{NL} \begin{bmatrix} Q_{55} & Q_{45} \\ Q_{45} & Q_{44} \end{bmatrix}^L \left\{ \int_{h_{L-1}}^{h_L} \left(z^2 \begin{Bmatrix} \theta_x + \frac{\partial w_o}{\partial x} \\ \theta_y + \frac{\partial w_o}{\partial y} \end{Bmatrix} + 3z^4 \begin{Bmatrix} \theta^*_x \\ \theta^*_y \end{Bmatrix} \right) dz \right\} \quad \textbf{…(3.19)}$$

After the integration, the above expressions are re-written in a matrix form which defines the stress–resultant / strain relations of the laminate as follows:

$$\begin{Bmatrix} N_x \\ N_y \\ N_{xy} \end{Bmatrix} = \begin{bmatrix} A_{11} & A_{12} & A_{16} \\ A_{12} & A_{22} & A_{26} \\ A_{16} & A_{26} & A_{66} \end{bmatrix} \begin{Bmatrix} \varepsilon^o_x \\ \varepsilon^o_y \\ \gamma^o_{xy} \end{Bmatrix} + \begin{bmatrix} B_{11} & B_{12} & B_{16} \\ B_{12} & B_{22} & B_{26} \\ B_{16} & B_{26} & B_{66} \end{bmatrix} \begin{Bmatrix} \kappa_x \\ \kappa_y \\ \kappa_{xy} \end{Bmatrix} + \begin{bmatrix} E_{11} & E_{12} & E_{16} \\ E_{12} & E_{22} & E_{26} \\ E_{16} & E_{26} & E_{66} \end{bmatrix} \begin{Bmatrix} \kappa^*_x \\ \kappa^*_y \\ \kappa^*_{xy} \end{Bmatrix} \quad \textbf{…(3.20)}$$

$$\begin{Bmatrix} M_x \\ M_y \\ M_{xy} \end{Bmatrix} = \begin{bmatrix} B_{11} & B_{12} & B_{16} \\ B_{12} & B_{22} & B_{26} \\ B_{16} & B_{26} & B_{66} \end{bmatrix} \begin{Bmatrix} \varepsilon^o_x \\ \varepsilon^o_y \\ \gamma^o_{xy} \end{Bmatrix} + \begin{bmatrix} D_{11} & D_{12} & D_{16} \\ D_{12} & D_{22} & D_{26} \\ D_{16} & D_{26} & D_{66} \end{bmatrix} \begin{Bmatrix} \kappa_x \\ \kappa_y \\ \kappa_{xy} \end{Bmatrix} + \begin{bmatrix} F_{11} & F_{12} & F_{16} \\ F_{12} & F_{22} & F_{26} \\ F_{16} & F_{26} & F_{66} \end{bmatrix} \begin{Bmatrix} \kappa^*_x \\ \kappa^*_y \\ \kappa^*_{xy} \end{Bmatrix} \quad \textbf{…(3.21)}$$

$$\begin{Bmatrix} M^*_x \\ M^*_y \\ M^*_{xy} \end{Bmatrix} = \begin{bmatrix} E_{11} & E_{12} & E_{16} \\ E_{12} & E_{22} & E_{26} \\ E_{16} & E_{26} & E_{66} \end{bmatrix} \begin{Bmatrix} \varepsilon^o_x \\ \varepsilon^o_y \\ \gamma^o_{xy} \end{Bmatrix} + \begin{bmatrix} F_{11} & F_{12} & F_{16} \\ F_{12} & F_{22} & F_{26} \\ F_{16} & F_{26} & F_{66} \end{bmatrix} \begin{Bmatrix} \kappa_x \\ \kappa_y \\ \kappa_{xy} \end{Bmatrix} + \begin{bmatrix} H_{11} & H_{12} & H_{16} \\ H_{12} & H_{22} & H_{26} \\ H_{16} & H_{26} & H_{66} \end{bmatrix} \begin{Bmatrix} \kappa^*_x \\ \kappa^*_y \\ \kappa^*_{xy} \end{Bmatrix} \quad \textbf{…(3.22)}$$

$$\begin{Bmatrix} Q_x \\ Q_y \end{Bmatrix} = \begin{bmatrix} A_{55} & A_{45} \\ A_{45} & A_{44} \end{bmatrix} \begin{Bmatrix} \theta_x + \frac{\partial w_o}{\partial x} \\ \theta_y + \frac{\partial w_o}{\partial y} \end{Bmatrix} + \begin{bmatrix} D_{55} & D_{45} \\ D_{45} & D_{44} \end{bmatrix} \begin{Bmatrix} \theta^*_x \\ \theta^*_y \end{Bmatrix} \quad \textbf{…(3.23)}$$

$$\begin{Bmatrix} Q^*_x \\ Q^*_y \end{Bmatrix} = \begin{bmatrix} D_{55} & D_{45} \\ D_{45} & D_{44} \end{bmatrix} \begin{Bmatrix} \theta_x + \frac{\partial w_o}{\partial x} \\ \theta_y + \frac{\partial w_o}{\partial y} \end{Bmatrix} + \begin{bmatrix} F_{55} & F_{45} \\ F_{45} & F_{44} \end{bmatrix} \begin{Bmatrix} \theta^*_x \\ \theta^*_y \end{Bmatrix} \quad \textbf{…(3.24)}$$

All the coefficients in A, B, D, E, F and H groups will be defined later.

3.4.2 Higher order theory with nine degrees of freedom per node

The strain expressions derived from the displacement field of Equation (3.9) are:

$$\begin{aligned}
&\varepsilon_x = \varepsilon_x^o + z\kappa_x + z^2\varepsilon_x^{o*} + z^3\kappa_x^* \\
&\varepsilon_y = \varepsilon_y^o + z\kappa_y + z^2\varepsilon_y^{o*} + z^3\kappa_y^* \\
&\varepsilon_z = 0 \\
&\gamma_{xy} = \gamma_{xy}^o + z\kappa_{xy} + z^2\gamma_{xy}^{o*} + z^3\kappa_{xy}^* \\
&\gamma_{xz} = \varphi_x + z\ \gamma_{xz}^o + z^2\varphi_x^* \\
&\gamma_{yz} = \varphi_y + z\ \gamma_{yz}^o + z^2\ \varphi^*{}_y
\end{aligned} \qquad \textbf{…(3.25)}$$

where

$$\varepsilon_x^o = \frac{\partial u_o}{\partial x}\ , \qquad \varepsilon_y^o = \frac{\partial v_o}{\partial y}\ , \qquad \gamma_{xy}^o = \frac{\partial u_o}{\partial y} + \frac{\partial v_o}{\partial x}$$

$$\kappa_x = \frac{\partial \theta_x}{\partial x}\ , \qquad \kappa_y = \frac{\partial \theta_y}{\partial y}\ , \qquad \kappa_{xy} = \frac{\partial \theta_x}{\partial y} + \frac{\partial \theta_y}{\partial x}$$

$$\kappa_x^* = \frac{\partial \theta^*{}_x}{\partial x}, \qquad \kappa_y^* = \frac{\partial \theta^*{}_y}{\partial y}\ , \qquad \kappa_{xy}^* = \frac{\partial \theta^*{}_x}{\partial y} + \frac{\partial \theta^*{}_y}{\partial x} \qquad \textbf{…(3.26)}$$

$$\varepsilon_x^{o*} = \frac{\partial u^*{}_o}{\partial x}, \qquad \varepsilon_y^{o*} = \frac{\partial v^*{}_o}{\partial y}, \qquad \gamma_{xy}^{o\ *} = \frac{\partial u^*{}_o}{\partial y} + \frac{\partial v^*{}_o}{\partial x}$$

$$\varphi_x = \theta_x + \frac{\partial w_o}{\partial x}, \qquad \varphi_y = \theta_y + \frac{\partial w_o}{\partial y}$$

$$\gamma^o{}_{xz} = 2\,u_o^*\,, \qquad \gamma^o{}_{yz} = 2\,v_o^*\,, \qquad \varphi_x^* = 3\theta_x^*, \qquad \varphi_y^* = 3\theta_y^*$$

all above strains are defined in the middle–plane of the laminate.

By substituting Equation (3.25) into the stress–strain relations given by Equation (3.7), the stress–strain relations for the L^{th} lamina are as follows:

$$\begin{Bmatrix}\sigma_x\\ \sigma_y\\ \tau_{xy}\end{Bmatrix}^L = \begin{bmatrix}Q_{11} & Q_{12} & Q_{16}\\ Q_{12} & Q_{22} & Q_{26}\\ Q_{16} & Q_{26} & Q_{66}\end{bmatrix}^L \left(\begin{Bmatrix}\varepsilon_x^o\\ \varepsilon_y^o\\ \gamma_{xy}^o\end{Bmatrix} + z\begin{Bmatrix}\kappa_x\\ \kappa_y\\ \kappa_{xy}\end{Bmatrix} + z^2\begin{Bmatrix}\varepsilon_x^{o*}\\ \varepsilon_y^{o*}\\ \gamma_{xy}^{o*}\end{Bmatrix} + z^3\begin{Bmatrix}\kappa_x^*\\ \kappa_y^*\\ \kappa_{xy}^*\end{Bmatrix} \right) \qquad \textbf{…(3.27)}$$

$$\begin{Bmatrix}\tau_{xz}\\ \tau_{yz}\end{Bmatrix}^{L}=\begin{bmatrix}Q_{55}\,Q_{45}\\ Q_{45}\,Q_{44}\end{bmatrix}^{L}\left(\begin{Bmatrix}\theta_x+\dfrac{\partial w_o}{\partial x}\\ \theta_y+\dfrac{\partial w_o}{\partial y}\end{Bmatrix}+2z\begin{Bmatrix}u_o^*\\ v_o^*\end{Bmatrix}+3z^2\begin{Bmatrix}\theta_x^*\\ \theta_y^*\end{Bmatrix}\right) \qquad \textbf{…(3.28)}$$

The stress, moment and shear resultants acting on N-layered laminate are:

$$\begin{Bmatrix}N_x & N^*_x\\ N_y & N^*_y\\ N_{xy} & N^*_{xy}\end{Bmatrix}=\int_{-h/2}^{h/2}\begin{Bmatrix}\sigma_x\\ \sigma_y\\ \tau_{xy}\end{Bmatrix}\begin{bmatrix}1 & z & z^2\end{bmatrix}dz$$

$$\begin{Bmatrix}M_x & M^*_x\\ M_y & M^*_y\\ M_{xy} & M^*_{xy}\end{Bmatrix}=\int_{-h/2}^{h/2}\begin{Bmatrix}\sigma_x\\ \sigma_y\\ \tau_{xy}\end{Bmatrix}\begin{bmatrix}z & z^3\end{bmatrix}dz \qquad \textbf{…(3.29)}$$

$$\begin{Bmatrix}Q_x & S_x & Q^*_x\\ Q_y & S_y & Q^*_y\end{Bmatrix}=\int_{-h/2}^{h/2}\begin{Bmatrix}\tau_{xz}\\ \tau_{yz}\end{Bmatrix}\begin{bmatrix}1 & z & z^2\end{bmatrix}dz$$

by substituting Equations (3.27) and (3.28) of the stresses in Equation (3.29), the following expressions for the stress resultants of NL– layer laminate will be obtained:

$$\begin{Bmatrix}N_x\\ N_y\\ N_{xy}\end{Bmatrix}=\sum_{L=1}^{NL}\begin{bmatrix}Q_{11}\,Q_{12}\,Q_{16}\\ Q_{12}\,Q_{22}\,Q_{26}\\ Q_{16}\,Q_{26}\,Q_{66}\end{bmatrix}^{L}\left\{\int_{h_{L-1}}^{h_L}\left(\begin{Bmatrix}\varepsilon_x^o\\ \varepsilon_y^o\\ \gamma_{xy}^o\end{Bmatrix}+z\begin{Bmatrix}\kappa_x\\ \kappa_y\\ \kappa_{xy}\end{Bmatrix}+z^2\begin{Bmatrix}\varepsilon_x^{o*}\\ \varepsilon_y^{o*}\\ \gamma_{xy}^{o*}\end{Bmatrix}+z^3\begin{Bmatrix}\kappa_x^*\\ \kappa_y^*\\ \kappa_{xy}^*\end{Bmatrix}\right)dz\right\} \qquad \textbf{…(3.30)}$$

$$\begin{Bmatrix}N^*_x\\ N^*_y\\ N^*_{xy}\end{Bmatrix}=\sum_{L=1}^{NL}\begin{bmatrix}Q_{11}\,Q_{12}\,Q_{16}\\ Q_{12}\,Q_{22}\,Q_{26}\\ Q_{16}\,Q_{26}\,Q_{66}\end{bmatrix}^{L}\left\{\int_{h_{L-1}}^{h_L}\left(z^2\begin{Bmatrix}\varepsilon_x^o\\ \varepsilon_y^o\\ \gamma_{xy}^o\end{Bmatrix}+z^3\begin{Bmatrix}\kappa_x\\ \kappa_y\\ \kappa_{xy}\end{Bmatrix}+z^4\begin{Bmatrix}\varepsilon_x^{o*}\\ \varepsilon_y^{o*}\\ \gamma_{xy}^{o*}\end{Bmatrix}+z^5\begin{Bmatrix}\kappa_x^*\\ \kappa_y^*\\ \kappa_{xy}^*\end{Bmatrix}\right)dz\right\} \qquad \textbf{…(3.31)}$$

$$\begin{Bmatrix} M_x \\ M_y \\ M_{xy} \end{Bmatrix} = \sum_{L=1}^{NL} \begin{bmatrix} Q_{11}\, Q_{12}\, Q_{16} \\ Q_{12}\, Q_{22}\, Q_{26} \\ Q_{16}\, Q_{26}\, Q_{66} \end{bmatrix}^{L} \left\{ \int_{h_{L-1}}^{h_L} \left(z \begin{Bmatrix} \varepsilon_x^o \\ \varepsilon_y^o \\ \gamma_{xy}^o \end{Bmatrix} + z^2 \begin{Bmatrix} \kappa_x \\ \kappa_y \\ \kappa_{xy} \end{Bmatrix} + z^3 \begin{Bmatrix} \varepsilon_x^{o*} \\ \varepsilon_y^{o*} \\ \gamma_{xy}^{o*} \end{Bmatrix} + z^4 \begin{Bmatrix} \kappa_x^* \\ \kappa_y^* \\ \kappa_{xy}^* \end{Bmatrix} \right) dz \right\} \quad \textbf{…(3.32)}$$

$$\begin{Bmatrix} M^*_x \\ M^*_y \\ M^*_{xy} \end{Bmatrix} = \sum_{L=1}^{NL} \begin{bmatrix} Q_{11}\, Q_{12}\, Q_{16} \\ Q_{12}\, Q_{22}\, Q_{26} \\ Q_{16}\, Q_{26}\, Q_{66} \end{bmatrix}^{L} \left\{ \int_{h_{L-1}}^{h_L} \left(z^3 \begin{Bmatrix} \varepsilon_x^o \\ \varepsilon_y^o \\ \gamma_{xy}^o \end{Bmatrix} + z^4 \begin{Bmatrix} \kappa_x \\ \kappa_y \\ \kappa_{xy} \end{Bmatrix} + z^5 \begin{Bmatrix} \varepsilon_x^{o*} \\ \varepsilon_y^{o*} \\ \gamma_{xy}^{o*} \end{Bmatrix} + z^6 \begin{Bmatrix} \kappa_x^* \\ \kappa_y^* \\ \kappa_{xy}^* \end{Bmatrix} \right) dz \right\} \quad \textbf{…(3.33)}$$

$$\begin{Bmatrix} Q_x \\ Q_y \end{Bmatrix} = \sum_{L=1}^{NL} \begin{bmatrix} Q_{55}\, Q_{45} \\ Q_{45}\, Q_{44} \end{bmatrix}^{L} \left\{ \int_{h_{L-1}}^{h_L} \left(\begin{Bmatrix} \theta_x + \dfrac{\partial w_o}{\partial x} \\ \theta_y + \dfrac{\partial w_o}{\partial y} \end{Bmatrix} + 2z \begin{Bmatrix} u_O^* \\ v_O^* \end{Bmatrix} + 3z^2 \begin{Bmatrix} \theta_x^* \\ \theta_y^* \end{Bmatrix} \right) dz \right\} \quad \textbf{…(3.34)}$$

$$\begin{Bmatrix} S_x \\ S_y \end{Bmatrix} = \sum_{L=1}^{NL} \begin{bmatrix} Q_{55}\, Q_{45} \\ Q_{45}\, Q_{44} \end{bmatrix}^{L} \left\{ \int_{h_{L-1}}^{h_L} \left(z \begin{Bmatrix} \theta_x + \dfrac{\partial w_o}{\partial x} \\ \theta_y + \dfrac{\partial w_o}{\partial y} \end{Bmatrix} + 2z^2 \begin{Bmatrix} u_O^* \\ v_O^* \end{Bmatrix} + 3z^3 \begin{Bmatrix} \theta_x^* \\ \theta_y^* \end{Bmatrix} \right) dz \right\} \quad \textbf{…(3.35)}$$

$$\begin{Bmatrix} Q^*_x \\ Q^*_y \end{Bmatrix} = \sum_{L=1}^{NL} \begin{bmatrix} Q_{55}\, Q_{45} \\ Q_{45}\, Q_{44} \end{bmatrix}^{L} \left\{ \int_{h_{L-1}}^{h_L} \left(z^2 \begin{Bmatrix} \theta_x + \dfrac{\partial w_o}{\partial x} \\ \theta_y + \dfrac{\partial w_o}{\partial y} \end{Bmatrix} + 2z^3 \begin{Bmatrix} u_O^* \\ v_O^* \end{Bmatrix} + 3z^4 \begin{Bmatrix} \theta_x^* \\ \theta_y^* \end{Bmatrix} \right) dz \right\} \quad \textbf{…(3.36)}$$

After integration through the thickness, Equations (3.30) to (3.36) can be re-written as follows:

$$\begin{Bmatrix} N_x \\ N_y \\ N_{xy} \end{Bmatrix} = \begin{bmatrix} A_{11}\, A_{12}\, A_{16} \\ A_{12}\, A_{22}\, A_{26} \\ A_{16}\, A_{26}\, A_{66} \end{bmatrix} \begin{Bmatrix} \varepsilon_x^o \\ \varepsilon_y^o \\ \gamma_{xy}^o \end{Bmatrix} + \begin{bmatrix} B_{11}\, B_{12}\, B_{16} \\ B_{12}\, B_{22}\, B_{26} \\ B_{16}\, B_{26}\, B_{66} \end{bmatrix} \begin{Bmatrix} \kappa_x \\ \kappa_y \\ \kappa_{xy} \end{Bmatrix} + \begin{bmatrix} D_{11}\, D_{12}\, D_{16} \\ D_{12}\, D_{22}\, D_{26} \\ D_{16}\, D_{26}\, D_{66} \end{bmatrix} \begin{Bmatrix} \varepsilon_x^{o*} \\ \varepsilon_y^{o*} \\ \gamma_{xy}^{o*} \end{Bmatrix} + \begin{bmatrix} E_{11}\, E_{12}\, E_{16} \\ E_{12}\, E_{22}\, E_{26} \\ E_{16}\, E_{26}\, E_{66} \end{bmatrix} \begin{Bmatrix} \kappa_x^* \\ \kappa_y^* \\ \kappa_{xy}^* \end{Bmatrix} \quad \textbf{…(3.37)}$$

$$\begin{Bmatrix} N^*_x \\ N^*_y \\ N^*_{xy} \end{Bmatrix} = \begin{bmatrix} D_{11}\, D_{12}\, D_{16} \\ D_{12}\, D_{22}\, D_{26} \\ D_{16}\, D_{26}\, D_{66} \end{bmatrix} \begin{Bmatrix} \varepsilon_x^o \\ \varepsilon_y^o \\ \gamma_{xy}^o \end{Bmatrix} + \begin{bmatrix} E_{11}\, E_{12}\, E_{16} \\ E_{12}\, E_{22}\, E_{26} \\ E_{16}\, E_{26}\, E_{66} \end{bmatrix} \begin{Bmatrix} \kappa_x \\ \kappa_y \\ \kappa_{xy} \end{Bmatrix} + \begin{bmatrix} F_{11}\, F_{12}\, F_{16} \\ F_{12}\, F_{22}\, F_{26} \\ F_{16}\, F_{26}\, F_{66} \end{bmatrix} \begin{Bmatrix} \varepsilon_x^{o*} \\ \varepsilon_y^{o*} \\ \gamma_{xy}^{o*} \end{Bmatrix} + \begin{bmatrix} G_{11}\, G_{12}\, G_{16} \\ G_{12}\, G_{22}\, G_{26} \\ G_{16}\, G_{26}\, G_{66} \end{bmatrix} \begin{Bmatrix} \kappa_x^* \\ \kappa_y^* \\ \kappa_{xy}^* \end{Bmatrix} \quad \textbf{…(3.38)}$$

$$\begin{Bmatrix} M_x \\ M_y \\ M_{xy} \end{Bmatrix} = \begin{bmatrix} B_{11}\, B_{12}\, B_{16} \\ B_{12}\, B_{22}\, B_{26} \\ B_{16}\, B_{26}\, B_{66} \end{bmatrix} \begin{Bmatrix} \varepsilon_x^o \\ \varepsilon_y^o \\ \gamma_{xy}^o \end{Bmatrix} + \begin{bmatrix} D_{11}\, D_{12}\, D_{16} \\ D_{12}\, D_{22}\, D_{26} \\ D_{16}\, D_{26}\, D_{66} \end{bmatrix} \begin{Bmatrix} \kappa_x \\ \kappa_y \\ \kappa_{xy} \end{Bmatrix} + \begin{bmatrix} E_{11}\, E_{12}\, E_{16} \\ E_{12}\, E_{22}\, E_{26} \\ E_{16}\, E_{26}\, E_{66} \end{bmatrix} \begin{Bmatrix} \varepsilon_x^{o*} \\ \varepsilon_y^{o*} \\ \gamma_{xy}^{o*} \end{Bmatrix} + \begin{bmatrix} F_{11}\, F_{12}\, F_{16} \\ F_{12}\, F_{22}\, F_{26} \\ F_{16}\, F_{26}\, F_{66} \end{bmatrix} \begin{Bmatrix} \kappa_x^* \\ \kappa_y^* \\ \kappa_{xy}^* \end{Bmatrix} \quad \textbf{…(3.39)}$$

$$\begin{Bmatrix} M^*_x \\ M^*_y \\ M^*_{xy} \end{Bmatrix} = \begin{bmatrix} E_{11}\, E_{12}\, E_{16} \\ E_{12}\, E_{22}\, E_{26} \\ E_{16}\, E_{26}\, E_{66} \end{bmatrix} \begin{Bmatrix} \varepsilon_x^o \\ \varepsilon_y^o \\ \gamma_{xy}^o \end{Bmatrix} + \begin{bmatrix} F_{11}\, F_{12}\, F_{16} \\ F_{12}\, F_{22}\, F_{26} \\ F_{16}\, F_{26}\, F_{66} \end{bmatrix} \begin{Bmatrix} \kappa_x \\ \kappa_y \\ \kappa_{xy} \end{Bmatrix} + \begin{bmatrix} G_{11}\, G_{12}\, G_{16} \\ G_{12}\, G_{22}\, G_{26} \\ G_{16}\, G_{26}\, G_{66} \end{bmatrix} \begin{Bmatrix} \varepsilon_x^{o*} \\ \varepsilon_y^{o*} \\ \gamma_{xy}^{o*} \end{Bmatrix} + \begin{bmatrix} H_{11}\, H_{12}\, H_{16} \\ H_{12}\, H_{22}\, H_{26} \\ H_{16}\, H_{26}\, H_{66} \end{bmatrix} \begin{Bmatrix} \kappa_x^* \\ \kappa_y^* \\ \kappa_{xy}^* \end{Bmatrix} \quad \textbf{…(3.40)}$$

$$\begin{Bmatrix} Q_x \\ Q_y \end{Bmatrix} = \begin{bmatrix} A_{55}\ A_{45} \\ A_{45}\ A_{44} \end{bmatrix} \begin{Bmatrix} \theta_x + \dfrac{\partial w_o}{\partial x} \\ \theta_y + \dfrac{\partial w_o}{\partial y} \end{Bmatrix} + \begin{bmatrix} B_{55}\ B_{45} \\ B_{45}\ B_{44} \end{bmatrix} \begin{Bmatrix} u_o^* \\ v_o^* \end{Bmatrix} + \begin{bmatrix} D_{55}\ D_{45} \\ D_{45}\ D_{44} \end{bmatrix} \begin{Bmatrix} \theta_x^* \\ \theta_y^* \end{Bmatrix} \qquad \textbf{…(3.41)}$$

$$\begin{Bmatrix} S_x \\ S_y \end{Bmatrix} = \begin{bmatrix} B_{55}\ B_{45} \\ B_{45}\ B_{44} \end{bmatrix} \begin{Bmatrix} \theta_x + \dfrac{\partial w_o}{\partial x} \\ \theta_y + \dfrac{\partial w_o}{\partial y} \end{Bmatrix} + \begin{bmatrix} D_{55}\ D_{45} \\ D_{45}\ D_{44} \end{bmatrix} \begin{Bmatrix} u_o^* \\ v_o^* \end{Bmatrix} + \begin{bmatrix} E_{55}\ E_{45} \\ E_{45}\ E_{44} \end{bmatrix} \begin{Bmatrix} \theta_x^* \\ \theta_y^* \end{Bmatrix} \qquad \textbf{…(3.42)}$$

$$\begin{Bmatrix} Q^*_x \\ Q^*_y \end{Bmatrix} = \begin{bmatrix} D_{55}\ D_{45} \\ D_{45}\ D_{44} \end{bmatrix} \begin{Bmatrix} \theta_x + \dfrac{\partial w_o}{\partial x} \\ \theta_y + \dfrac{\partial w_o}{\partial y} \end{Bmatrix} + \begin{bmatrix} E_{55}\ E_{45} \\ E_{45}\ E_{44} \end{bmatrix} \begin{Bmatrix} u_o^* \\ v_o^* \end{Bmatrix} + \begin{bmatrix} F_{55}\ F_{45} \\ F_{45}\ F_{44} \end{bmatrix} \begin{Bmatrix} \theta_x^* \\ \theta_y^* \end{Bmatrix} \qquad \textbf{…(3.43)}$$

All coefficients in A, B, D, E, F, G, and H groups are defined as follows:

$$A_{ij} = \sum_{L=1}^{NL} (Q_{ij})_L (h_L - h_{L-1}), \qquad i,j = 1,2,6 \quad or \quad ij = 4,5 \qquad \textbf{…(3.44 a)}$$

$$B_{ij} = (1/2) \sum_{L=1}^{NL} (Q_{ij})_L \left(h^2{}_L - h^2{}_{L-1}\right), \qquad i,j = 1,2,6 \quad or \quad ij = 4,5 \qquad \textbf{…(3.44 b)}$$

$$D_{ij} = (1/3) \sum_{L=1}^{NL} (Q_{ij})_L \left(h^3{}_L - h^3{}_{L-1}\right), \qquad i,j = 1,2,6 \quad or \quad ij = 4,5 \qquad \textbf{…(3.44 c)}$$

$$E_{ij} = (1/4) \sum_{L=1}^{NL} (Q_{ij})_L \left(h^4{}_L - h^4{}_{L-1}\right), \qquad i,j = 1,2,6 \quad or \quad ij = 4,5 \qquad \textbf{…(3.44 d)}$$

$$F_{ij} = (1/5) \sum_{L=1}^{NL} (Q_{ij})_L \left(h^5{}_L - h^5{}_{L-1}\right), \qquad i,j = 1,2,6 \quad or \quad ij = 4,5 \qquad \textbf{…(3.44 e)}$$

$$G_{ij} = (1/6) \sum_{L=1}^{NL} (Q_{ij})_L \left(h^6{}_L - h^6{}_{L-1}\right), \qquad i,j = 1,2,6 \qquad \textbf{…(3.44 f)}$$

$$H_{ij} = (1/7)\sum_{L=1}^{NL}(Q_{ij})_L \left(h^7{}_L - h^7{}_{L-1}\right), \quad i,j = 1,2,6 \qquad \textbf{\textit{…(3.44 g)}}$$

3.5 Classification of laminated plates

The mathematical models which is derived in the previous section can be applied to analyze two main useful types of laminated plates, and these types can be illustrated as follows:

3.5.1 Symmetric laminated plates

This type of lamination is symmetric in both geometry and material properties about the plate middle surface of plate. In practice, and because of the symmetry of $(\mathbf{Q_{ij}})_k$ and thickness ($\mathbf{h_k}$) of layers, all the coupling stiffnesses ,[B, E and G, group in Equations (3.37) to (3.43)], can be shown to be zero. The symmetric lamination includes two configurations as follows:

1. Cross-ply lamination

Symmetric cross-ply laminated plates consist of an odd or even number of orthotropic layers that have principal material directions aligned with the plate axes. The orthotropic layers are laminated symmetrically about the plate middle surface. For example ($0^o/90^o/0^o$) as shown in Figure (3.5). The configuration of the stress resultants equations for this type of lamination is presented in **Appendix (B)** ***(Jones, 1975)*** [15].

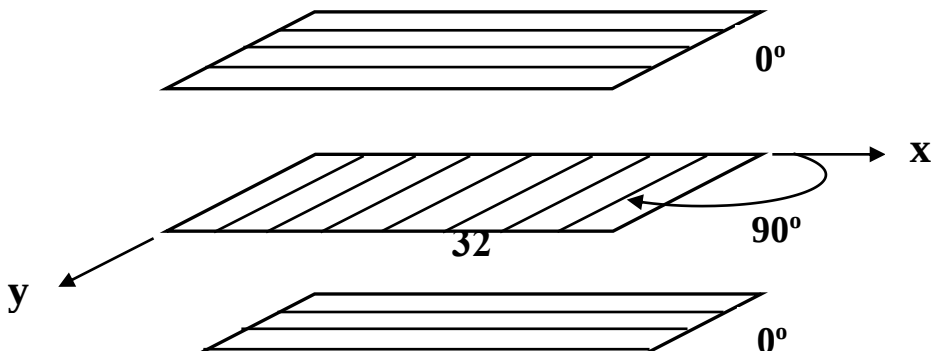

Figure (3.5): Symmetric cross-ply lamination of composite plates.

2. Angle-ply lamination

Symmetric angle-ply laminated plates include an odd or even number of orthotropic layers that are symmetrically disposed about the middle surface of the plate. The principal material directions are not aligned with the plate axes. For example ($30^o/75^o/30^o$) as shown in Figure (3.6). The configuration of the stress resultants equations for this type of lamination is presented in **Appendix (B)** ***(Jones, 1975)*** [15] .

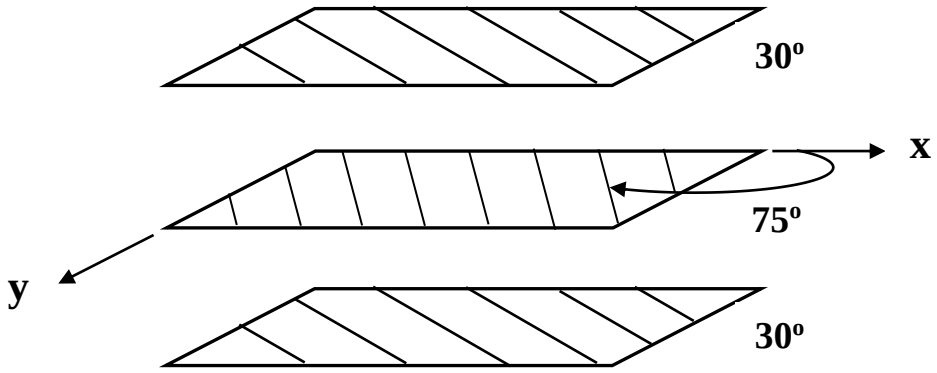

Figure (3.6): Symmetric angle-ply lamination of composite plates.

3.5.2 Antisymmtric laminated plates

This type of lamination is very important in practical application of laminated plates. Material properties are not symmetric about the middle surface of the plate. The antisymmtric lamination has bending-extension coupling [B, E and G

groups in Equations (3.37) to (3.40)] and bend-twist coupling [D_{16}, D_{26}, F_{16}, F_{26}, H_{16} and H_{26} in Equations (3.39) and (3.40)].

The bending-extension coupling effects are illustrated by an antisymmetric laminated plates after curing .The laminate is flat before curing but thermally induced residual stresses causes the laminate to become highly curved, as shown in Figure (3.7) ***(Stegmann*** and ***Lund, 2001)*** [14].

Figure (3.7): An antisymmetric laminated plate after curing [14].

The effect of bend-twist coupling on plate bending can be shown in Figure (3.8). Utilization from this coupling in advanced design can be illustrated in the design of forward-swept wings subjected to aerodynamic loads which tend to twist the wing about an axis that is along the wing and off perpendicular to the fuselage. The wings are designed using composite laminates at various angles to the wing axis which result in bend-twist coupling that cause the wing to twist in the opposite sense to the aerodynamic wing-twisting effect, as shown in Figure (3.9) ***(Stegmann*** and ***Lund, 2001)*** [14].

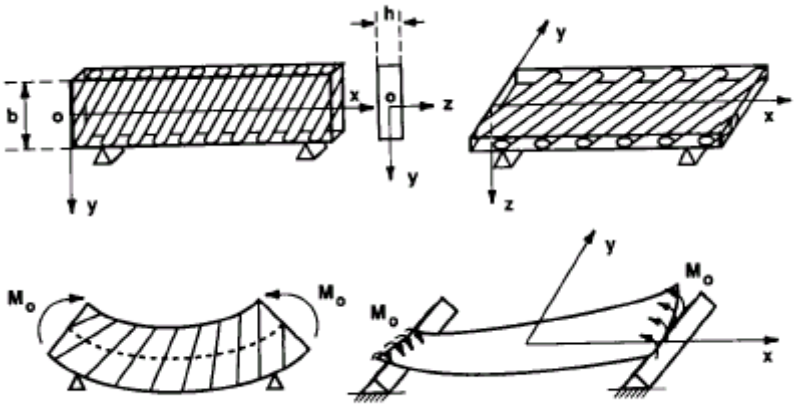

Figure (3.8): Effect of bending-twist coupling on plate [14].

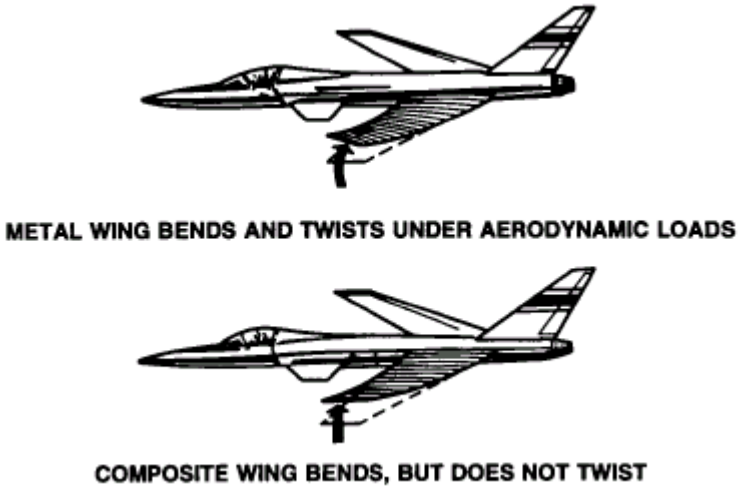

Figure (3.9): Aerodynamic response of metal and composite wings [14].

Similarly to symmetric lamination, antisymmetric lamination includes two configurations as follows:

1. Cross-ply lamination

Antisymmetric cross-ply laminated plates consist of an even number of orthotropic layers laid on each other with principal material directions alternating at 0^o and 90^o to the plate axes. For example ($0^o/90^o/0^o/90^o$) as shown in Figure (3.10). The configuration of the stress resultants equations for this type of lamination is presented in **Appendix (B)** ***(Jones, 1975)*** [15].

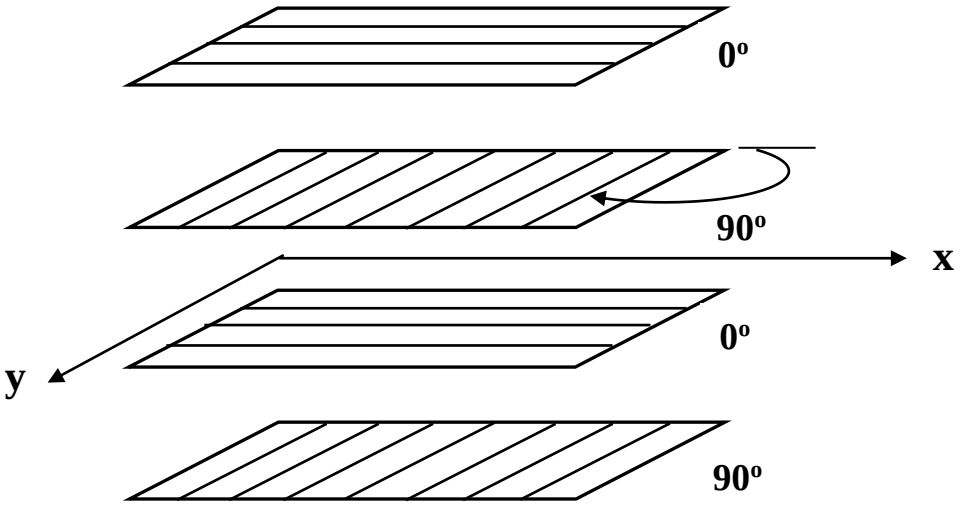

Figure (3.10): Antisymmetric cross-ply lamination of composite plates.

2.Angle-ply lamination

This is the most general configuration type of laminated plates. It contains even number of orthotropic layers laid on each other with principal material directions not aligned with the plate axes. For example ($60^o/30^o/60^o/30^o$) as shown in Figure (3.11). The configuration of the stress resultants equations for this type of lamination is presented in **Appendix (B)** ***(Jones, 1975)*** [15].

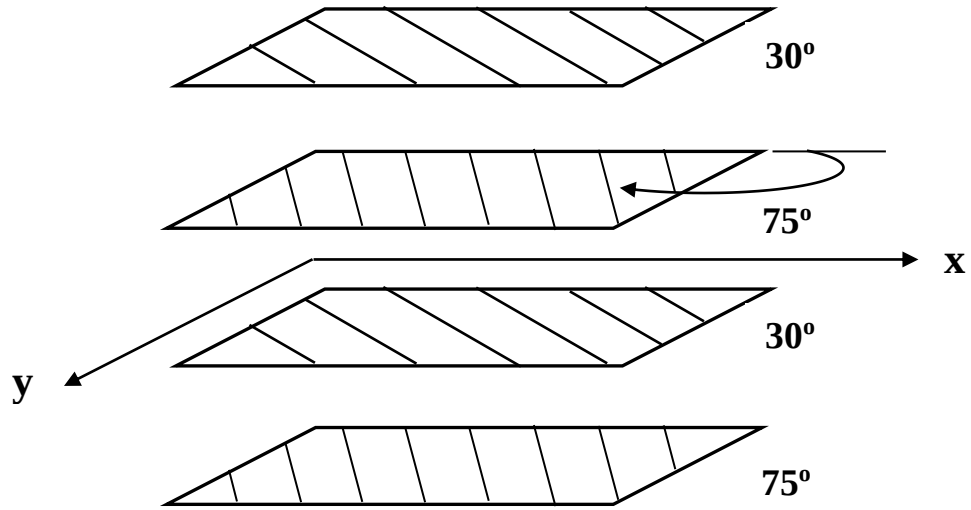

Figure (3.10): Antisymmetric angle-ply lamination of composite plates.

CHAPTER FOUR

FINITE

ELEMENT FORMULATION

AND NUMERICAL SOLUTIONS

4.1 Introduction

The development of suitable methods, more accurately, for analyzing various engineering structures are needed in order to investigate their behavior under different loading conditions. At present, the finite element method is the most powerful numerical technique, which offers approximate solution to realistic types of structures such as plates. However, the term "finite elements" was first used by **Clough** in **1960** (mentioned by ***Reddy, 1984***) [35]. This method has become useful in many areas such as heat conduction, seepage flow, electric and magnetic fields, biological and geological regions.

In the present study, the 9–noded **Lagrangian** isoparametric quadrilateral element is used for discretization of layered plates. The derivation of the strain–displacement matrix [$\mathbb{B}$], the elasticity matrix [$\mathbb{E}$] and, as a result, the stiffness matrix of layered plates is presented. Also, the formulation of element mass matrix [**M**] and damping matrix [**C**] of layered plates are introduced.

Finally, the numerical solutions which are used to solve the basic dynamic equilibrium equation and the eigenvalue problem are presented.

4.2 Nine–noded Lagrangian element

The 9–noded Lagrangian element shown in Figure (4.1) is adopted. This element contains four nodes at the corners, four nodes at the mid–side of the element boundaries and one at the center of the element.

The topology is ordered counter clockwise in the sequence from 1 to 8. The degrees of freedom u, v, w, θ_x, θ_y, u^*, v^*, θ^*_x and θ^*_y are exist at every node from 1 to 9.

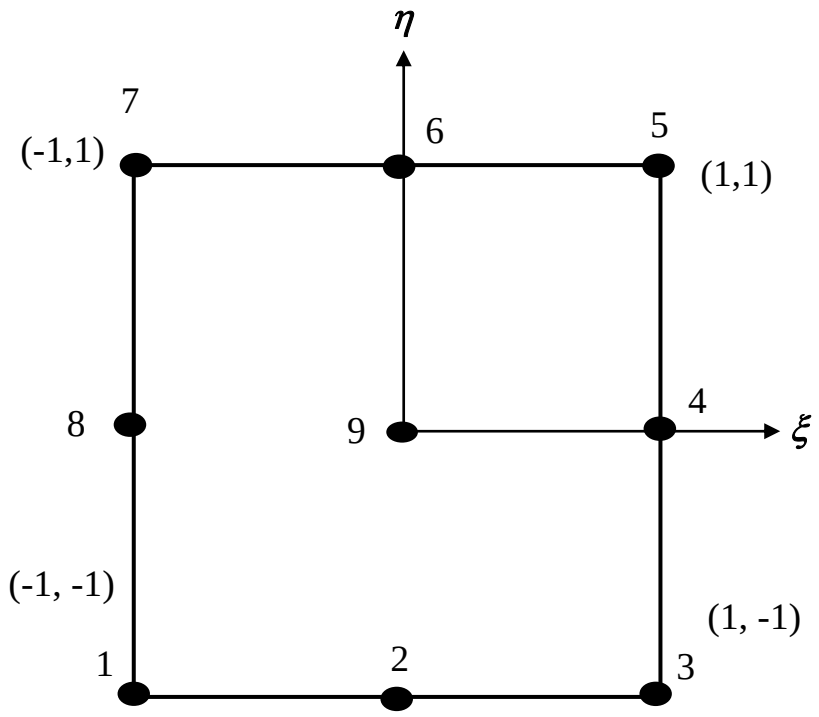

Figure (4.1): Nine–noded quadrilateral isoparametric element.

The shape function, N_i (ξ,η), at the i–th node of this element and its derivatives are given in Table (4.1).

Table (4.1): Shape functions and their derivatives (Bathe, 1996) [4].

Location	N_i	N_i , ξ	N_i , η
Corner Nodes (1, 3, 5, 7)	$(1/4)(1+\xi_o)(1+\eta_o)(\xi_o+\eta_o-1)$	$(\xi_i/4)(1+\eta_o)(2\xi_o+\eta_o)$	$(\eta_i/4)(1+\xi_o)(2\eta_o+\xi_o)$
Mid-side Nodes (2, 6)	$(1/2)(1-\xi^2)(1+\eta_o)$	$-\xi(1+\eta_o)$	$(\eta_i/2)(1-\xi^2)$
Mid-side Nodes (4, 8)	$(1/2)(1-\eta^2)(1+\xi_o)$	$(\xi_i/2)(1-\eta^2)$	$-\eta(1-\xi_o)$
Center Node (9)	$(1-\xi^2)(1-\eta^2)$	$-2\xi(1-\eta^2)$	$-2\eta(1-\xi^2)$

where $\xi_o=\xi\xi_i$, $\eta_o= \eta\eta_i$,

ξ_i and η_i are the natural coordinates of node(i).

4.3 Derivation of strain–displacement matrix

The geometrical nonlinearity is not considered in the present work, and hence the engineering components of strain can be expressed in terms of the first partial derivatives of the displacement components. Therefore, the linear strain–

displacement matrix, [$\mathbb{B}$] at any point within an element, and for seven degrees of freedom per node can be written as:

$$\{\varepsilon\}=\begin{Bmatrix}\varepsilon^{o}_{x}\\ \varepsilon^{o}_{y}\\ \gamma^{o}_{xy}\\ \kappa_{x}\\ \kappa_{y}\\ \kappa_{xy}\\ \kappa^{*}_{x}\\ \kappa^{*}_{y}\\ \kappa^{*}_{xy}\\ \varphi_{x}\\ \varphi_{y}\\ \varphi^{*}_{x}\\ \varphi^{*}_{y}\end{Bmatrix}=\begin{Bmatrix}\frac{\partial u_o}{\partial x}\\ \frac{\partial v_o}{\partial y}\\ \frac{\partial u_o}{\partial y}+\frac{\partial v_o}{\partial x}\\ \frac{\partial \theta_x}{\partial x}\\ \frac{\partial \theta_y}{\partial y}\\ \frac{\partial \theta_x}{\partial y}+\frac{\partial \theta_y}{\partial x}\\ \frac{\partial \theta^*_x}{\partial x}\\ \frac{\partial \theta^*_y}{\partial y}\\ \frac{\partial \theta^*_x}{\partial y}+\frac{\partial \theta^*_y}{\partial x}\\ \theta_x+\frac{\partial w_o}{\partial x}\\ \theta_y+\frac{\partial w_o}{\partial y}\\ 3\theta^*_x\\ 3\theta^*_y\end{Bmatrix}=\sum_{i=1}^{9}\underbrace{\left[\begin{array}{ccccccc}\frac{\partial N_i}{\partial x}&0&0&0&0&0&0\\ 0&\frac{\partial N_i}{\partial y}&0&0&0&0&0\\ \frac{\partial N_i}{\partial y}&\frac{\partial N_i}{\partial x}&0&0&0&0&0\\ 0&0&0&\frac{\partial N_i}{\partial x}&0&0&0\\ 0&0&0&0&\frac{\partial N_i}{\partial y}&0&0\\ 0&0&0&\frac{\partial N_i}{\partial y}&\frac{\partial N_i}{\partial x}&0&0\\ 0&0&0&0&0&\frac{\partial N_i}{\partial x}&0\\ 0&0&0&0&0&0&\frac{\partial N_i}{\partial y}\\ 0&0&0&0&0&\frac{\partial N_i}{\partial y}&\frac{\partial N_i}{\partial x}\\ \hline 0&0&\frac{\partial N_i}{\partial x}&N_i&0&0&0\\ 0&0&\frac{\partial N_i}{\partial y}&0&N_i&0&0\\ 0&0&0&0&0&3N_i&0\\ 0&0&0&0&0&0&3N_i\end{array}\right]}_{\begin{pmatrix}\mathbb{B}_{m,\,c,\,b}\\ \hline \mathbb{B}_{s}\end{pmatrix}}\underbrace{\begin{Bmatrix}u_oi\\ v_oi\\ w_oi\\ \theta_xi\\ \theta_yi\\ \theta^*_xi\\ \theta^*_yi\end{Bmatrix}}_{\{a\}^e}$$ ***…(4.1)***

Also, the strain–displacement matrix at any point within an element and for nine degrees of freedom per node is:

$$\{\varepsilon\}=\begin{Bmatrix}\varepsilon^{o}_{x}\\ \varepsilon^{o}_{y}\\ \gamma^{o}_{xy}\\ \varepsilon^{o*}_{x}\\ \varepsilon^{o*}_{y}\\ \gamma^{o*}_{xy}\\ \kappa_{x}\\ \kappa_{y}\\ \kappa_{xy}\\ \kappa^{*}_{x}\\ \kappa^{*}_{y}\\ \kappa^{*}_{xy}\\ \varphi_{x}\\ \varphi_{y}\\ \gamma^{o}_{xz}\\ \gamma^{o}_{yz}\\ \varphi^{*}_{x}\\ \varphi^{*}_{y}\end{Bmatrix}=\begin{Bmatrix}\frac{\partial u_o}{\partial x}\\ \frac{\partial v_o}{\partial y}\\ \frac{\partial u_o}{\partial y}+\frac{\partial v_o}{\partial x}\\ \frac{\partial u^{*}_{o}}{\partial x}\\ \frac{\partial v^{*}_{o}}{\partial y}\\ \frac{\partial u^{*}_{o}}{\partial y}+\frac{\partial v^{*}_{o}}{\partial x}\\ \frac{\partial \theta_x}{\partial x}\\ \frac{\partial \theta_y}{\partial y}\\ \frac{\partial \theta_x}{\partial y}+\frac{\partial \theta_y}{\partial x}\\ \frac{\partial \theta^{*}_{x}}{\partial x}\\ \frac{\partial \theta^{*}_{y}}{\partial y}\\ \frac{\partial \theta^{*}_{x}}{\partial y}+\frac{\partial \theta^{*}_{y}}{\partial x}\\ \theta_x+\frac{\partial w_o}{\partial x}\\ \theta_y+\frac{\partial w_o}{\partial y}\\ 2u^{*}_{o}\\ 2v^{*}_{o}\\ 3\theta^{*}_{x}\\ 3\theta^{*}_{y}\end{Bmatrix}=\sum_{i=1}^{9}\underbrace{\left[\begin{array}{ccccccccc}\frac{\partial N_i}{\partial x}&0&0&0&0&0&0&0&0\\ 0&\frac{\partial N_i}{\partial y}&0&0&0&0&0&0&0\\ \frac{\partial N_i}{\partial y}&\frac{\partial N_i}{\partial x}&0&0&0&0&0&0&0\\ 0&0&0&0&0&\frac{\partial N_i}{\partial x}&0&0&0\\ 0&0&0&0&0&0&\frac{\partial N_i}{\partial y}&0&0\\ 0&0&0&0&0&\frac{\partial N_i}{\partial y}&\frac{\partial N_i}{\partial x}&0&0\\ 0&0&0&\frac{\partial N_i}{\partial x}&0&0&0&0&0\\ 0&0&0&0&\frac{\partial N_i}{\partial y}&0&0&0&0\\ 0&0&0&\frac{\partial N_i}{\partial y}&\frac{\partial N_i}{\partial x}&0&0&0&0\\ 0&0&0&0&0&0&0&\frac{\partial N_i}{\partial x}&0\\ 0&0&0&0&0&0&0&0&\frac{\partial N_i}{\partial y}\\ 0&0&0&0&0&0&0&\frac{\partial N_i}{\partial y}&\frac{\partial N_i}{\partial x}\\ \hline 0&0&\frac{\partial N_i}{\partial x}&N_i&0&0&0&0&0\\ 0&0&\frac{\partial N_i}{\partial y}&0&N_i&0&0&0&0\\ 0&0&0&0&0&2N_i&0&0&0\\ 0&0&0&0&0&0&2N_i&0&0\\ 0&0&0&0&0&0&0&3N_i&0\\ 0&0&0&0&0&0&0&0&3N_i\end{array}\right]}_{\left[\begin{array}{c}\mathbf{B_{m,c,b}}\\ \hline \mathbf{B_s}\end{array}\right]}\underbrace{\begin{Bmatrix}u_oi\\ v_oi\\ w_oi\\ \theta_xi\\ \theta_yi\\ u^{*}_{o}i\\ v^{*}_{o}i\\ \theta^{*}_{x}i\\ \theta^{*}_{y}i\end{Bmatrix}}_{\{a\}^e} \qquad \textbf{…(4.2)}$$

Since the shape functions $\mathbf{N_i}$ are functions of the local coordinates rather than Cartesian coordinates, a relationship needs to be established between the derivatives in the two coordinates systems. By using the chain rule, the partial differential relation can be expressed in matrix form as:

$$\begin{bmatrix} \frac{\partial N_i}{\partial \xi} \\ \frac{\partial N_i}{\partial \eta} \end{bmatrix} = \underbrace{\begin{bmatrix} \frac{\partial x}{\partial \xi} & \frac{\partial y}{\partial \xi} \\ \frac{\partial x}{\partial \eta} & \frac{\partial y}{\partial \eta} \end{bmatrix}}_{[J]} \begin{bmatrix} \frac{\partial N_i}{\partial x} \\ \frac{\partial N_i}{\partial y} \end{bmatrix} \qquad \textbf{…(4.3)}$$

where [J] is the **Jacobian** matrix and the elements of this matrix can be obtained by differentiating the following equations:

$$\begin{aligned} x(\xi,\eta) &= \sum_{i=1}^{4} N_i(\xi,\eta)\ x_i \\ y(\xi,\eta) &= \sum_{i=1}^{4} N_i(\xi,\eta)\ y_i \end{aligned} \qquad \textbf{…(4.4)}$$

Hence, the **Jacobian** matrix can be expressed as:

$$[J] = \begin{bmatrix} \sum_{i=1}^{9} \frac{\partial N_i}{\partial \xi} \mathrm{x_i} & \sum_{i=1}^{9} \frac{\partial N_i}{\partial \xi} y_i \\ \sum_{i=1}^{9} \frac{\partial N_i}{\partial \eta} \mathrm{x_i} & \sum_{i=1}^{9} \frac{\partial N_i}{\partial \eta} y_i \end{bmatrix} \qquad \textbf{…(4.5)}$$

Then, the derivatives of the shape functions with respect to Cartesian coordinates can be given as:

$$\begin{bmatrix} \frac{\partial N_i}{\partial x} \\ \frac{\partial N_i}{\partial y} \end{bmatrix} = [J]^{-1} \begin{bmatrix} \frac{\partial N_i}{\partial \xi} \\ \frac{\partial N_i}{\partial \eta} \end{bmatrix} \qquad \textbf{…(4.6)}$$

where $[J]^{-1}$ is the inverse of **Jacobian** matrix given as:

$$[J]^{-1} = \begin{bmatrix} \frac{\partial \xi}{\partial x} & \frac{\partial \eta}{\partial x} \\ \frac{\partial \xi}{\partial y} & \frac{\partial \eta}{\partial y} \end{bmatrix} \qquad \textbf{\textit{...(4.7)}}$$

4.4 Derivation of elasticity matrix

The total potential energy π of a plate of mid–plane area **A** and volume **V**, loaded with an equivalent load vector {P} corresponding to seven degrees of freedom per node for a point on the mid–plane can be represented as:

$$\pi = \frac{1}{2}\int_{v} \varepsilon^t \sigma \, dV - \int d^t q \, dA \qquad \textbf{\textit{...(4.8)}}$$

where, $\{\sigma\} = \{\sigma_x, \sigma_y, \tau_{xy}, \tau_{xz}, \tau_{yz}\}^t$ and $\{\varepsilon\} = \{\varepsilon_x, \varepsilon_y, \gamma_{xy}, \gamma_{xz}, \gamma_{yz}\}^t$ are the stress and linear strain columns with respect to the laminate axes as shown in Figure (4.2), $\{d\} = \{u_o, v_o, w_o, \theta_x, \theta_y, \theta^*_x, \theta^*_y\}^t$, and $\{P\} = \{\mathbf{0\ 0\ q\ 0\ 0\ 0\ 0}\}^t$.

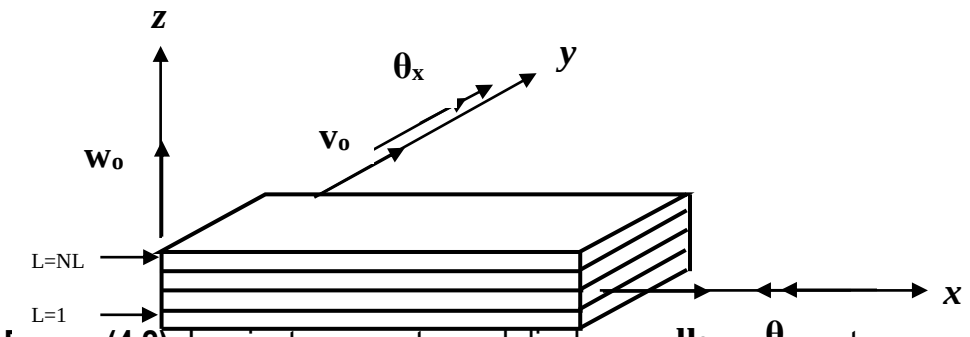

Figure (4.2): Laminate geometry and displacements.

The expressions for the strain components given by Equation (3.11) are substituted in the energy expression, Equation (4.8), and then minimized, while

carrying out explicit integration through the plate thickness. This leads to the following stress resultants for the NL–layered plates:

symbolically, $[\bar{\sigma}] = [\mathbb{E}]\,[\bar{\varepsilon}_o]$ ***…(4.9a)***

$$\begin{Bmatrix} N_x \\ N_y \\ N_{xy} \\ M_x \\ M_y \\ M_{xy} \\ M^*_x \\ M^*_y \\ M^*_{xy} \end{Bmatrix} = \underbrace{\sum_{L=1}^{NL} \begin{bmatrix} [A] & [B] & [E] \\ [B] & [D] & [F] \\ [E] & [F] & [A] \end{bmatrix}}_{[\mathbb{E}]_{\mathbf{m,\,c,\,b}}} \begin{Bmatrix} \dfrac{\partial u_o}{\partial x} \\ \dfrac{\partial v_o}{\partial y} \\ \dfrac{\partial u_o}{\partial y} + \dfrac{\partial v_o}{\partial x} \\ \dfrac{\partial \theta_x}{\partial x} \\ \dfrac{\partial \theta_y}{\partial y} \\ \dfrac{\partial \theta_x}{\partial y} + \dfrac{\partial \theta_y}{\partial x} \\ \dfrac{\partial \theta^*_x}{\partial x} \\ \dfrac{\partial \theta^*_y}{\partial y} \\ \dfrac{\partial \theta^*_x}{\partial y} + \dfrac{\partial \theta^*_y}{\partial x} \end{Bmatrix} \qquad \textit{…(4.9b)}$$

$$\begin{Bmatrix} Q_x \\ Q_y \\ Q^*x \\ Q^*y \end{Bmatrix} = \underbrace{\sum_{L=1}^{NL} \begin{bmatrix} [\bar{A}] & [\bar{D}] \\ [\bar{D}] & [\bar{F}] \end{bmatrix}}_{[\mathbb{E}]_{\mathbf{s}}} \begin{Bmatrix} \theta_x + \dfrac{\partial w_o}{\partial x} \\ \theta_y + \dfrac{\partial w_o}{\partial y} \\ 3\theta^*_x \\ 3\theta^*_y \end{Bmatrix} \qquad \textit{…(4.9c)}$$

Also, by the same manner but for nine degrees of freedom per node:

$$\pi = \frac{1}{2}\int_v \varepsilon^t \sigma \, dV - \int d^t q \, dA \qquad \textit{…(4.10)}$$

in which,

$\{d\} = \{u_o, v_o, w_o, \theta_x, \theta_y, u^*_o, v^*_o, \theta^*_x, \theta^*_y\}^t$

$\{P\} = \{\mathbf{0\ 0\ q\ 0\ 0\ 0\ 0\ 0\ 0}\}^t$

By substituting Equation (3.25) in Equation (4.10), and minimizing $\boldsymbol{\pi}$, while carrying out explicit integration through the plate thickness, one can get the following expression for the stress resultants for NL–layered plates:

symbolically, $[\overline{\sigma}]=[\mathbb{E}][\overline{\varepsilon}_o]$ ***…(4.11a)***

$$\begin{Bmatrix} N_x \\ N_y \\ N_{xy} \\ N^*_x \\ N^*_y \\ N^*_{xy} \\ M_x \\ M_y \\ M_{xy} \\ M^*_x \\ M^*_y \\ M^*_{xy} \end{Bmatrix} = \sum_{i=1}^{NL} \underbrace{\begin{bmatrix} [A][D][B][E] \\ [D][F][E][G] \\ [B][E][D][F] \\ [E][G][F][H] \end{bmatrix}}_{[\mathbb{E}]_{\mathbf{m,\,c,\,b}}} \begin{Bmatrix} \frac{\partial u_o}{\partial x} \\ \frac{\partial v_o}{\partial y} \\ \frac{\partial u_o}{\partial y} + \frac{\partial v_o}{\partial x} \\ \frac{\partial u^*_o}{\partial x} \\ \frac{\partial v^*_o}{\partial y} \\ \frac{\partial u^*_o}{\partial y} + \frac{\partial v^*_o}{\partial x} \\ \frac{\partial \theta_x}{\partial x} \\ \frac{\partial \theta_y}{\partial y} \\ \frac{\partial \theta_x}{\partial y} + \frac{\partial \theta_y}{\partial x} \\ \frac{\partial \theta^*_x}{\partial x} \\ \frac{\partial \theta^*_y}{\partial y} \\ \frac{\partial \theta^*_x}{\partial y} + \frac{\partial \theta^*_y}{\partial x} \end{Bmatrix} \qquad \textit{…(4.11b)}$$

$$\begin{Bmatrix} Q_x \\ Q_y \\ S_x \\ S_y \\ Q^*_x \\ Q^*_y \end{Bmatrix} = \sum_{L=1}^{NL} \underbrace{\begin{bmatrix} [\bar{A}][\bar{B}][\bar{D}] \\ [\bar{B}][\bar{D}][\bar{E}] \\ [\bar{D}][\bar{E}][\bar{F}] \end{bmatrix}}_{[\mathbb{E}]_s} \begin{Bmatrix} \theta_x + \dfrac{\partial w_o}{\partial x} \\ \theta_y + \dfrac{\partial w_o}{\partial y} \\ 2u^*_o \\ 2v^*_o \\ 3\theta^*_x \\ 3\theta^*_y \end{Bmatrix} \qquad \textbf{…(4.11c)}$$

where,

$$[A] = \begin{bmatrix} Q_{11}H_1 & Q_{12}H_1 & Q_{16}H_1 \\ Q_{12}H_1 & Q_{22}H_1 & Q_{26}H_1 \\ Q_{16}H_1 & Q_{26}H_1 & Q_{66}H_1 \end{bmatrix} \qquad \textbf{…(4.12)}$$

and,

$$[\bar{A}] = \begin{bmatrix} Q_{55}H_1 & Q_{45}H_1 \\ Q_{45}H_1 & Q_{44}H_1 \end{bmatrix} \qquad \textbf{…(4.13)}$$

The elements of the matrix [B] can be obtained by replacing H_1 in the matrix [A] by H_2, and the elements of D, E, F, G and H matrices can be obtained by replacing H_1 by H_3, H_4, H_5, H_6 and H_7, respectively. The elements of the $[\bar{B}]$ matrix can be obtained by replacing H_1 in the matrix $[\bar{A}]$ by H_2, and the elements of $\bar{D}$, $\bar{E}$, and $\bar{F}$ matrices can be obtained by replacing H_1 by H_3, H_4 and H_5, respectively. In all the above sub–matrices, the $\mathbf{Q_{ij}}$ coefficients are defined in **Appendix (A)** as mentioned previously, and

$$H_i = (1 / i)\ (h_L{}^i - h_{L-1}{}^i),\ i = 1,2,3,\ldots,\ 7 \qquad \textbf{…(4.14)}$$

Also, the suffices **m**, **c**, **b** and **s** refer to membrane, coupling, bending and shear terms.

4.5 Formulation of element stiffness matrix

The basic concept of the finite elements method is to discretize the continuum into arbitrary numbers of small elements connected together at their common nodes. For a finite element (**e)**, of the discrete model, the displacement vector at any point is:

$$\{u\}^e = [N]\{a\}^e \qquad \textbf{…(4.15)}$$

where **[N]** is a matrix containing the interpolation functions which relate the element displacement $\{u\}^e$ to the nodal displacements $\{a\}^e$.

By differentiation of the displacements, the corresponding strains $\{\varepsilon\}^e$ are obtained such that:

$$\{\varepsilon\}^e = [A]\{u\}^e \qquad \textbf{…(4.16)}$$

where **[A]** is the differential operators matrix.

The substitution of Equation (4.15) into Equation (4.16) yields:

$$\{\varepsilon\}^e = [A][N]\{a\}^e \qquad \textbf{…(4.17)}$$

or

$$\{\varepsilon\}^e = [B]\{a\}^e \qquad \textbf{…(4.18)}$$

Also, the total solution domain is discretized into a number of elements **(NE)** [sub–domain] such that:

$$\pi(a) = \sum_{e=1}^{NE} \pi^e(a) \qquad \textbf{…(4.19)}$$

where $\boldsymbol{\pi}$ and $\boldsymbol{\pi^e}$ are the potential energy of the total solution domain and the sub–domain, respectively. The potential energy for an element, **e**, can be expressed in terms of the internal strain energy, **SE**, and external work done, **WF**, such that:

$$\pi^e (a) = SE - WF \qquad \textbf{\textit{…(4.20)}}$$

in which **(a)** is the vector of nodal degrees of freedom of an element.

The internal strain energy of an elastic body is given by:

$$SE = \frac{1}{2}\int_A \varepsilon^T \bar{\sigma}\ \mathrm{dA} \qquad \textbf{\textit{…(4.21)}}$$

By substitution of Equations (4.11a) and (4.18) into Equation (4.21), then:

$$SE = \frac{1}{2}\{a\}^{eT}\int_A [\mathbb{B}]^T [\mathbb{E}][\mathbb{B}]\ dA\ \{a\} \qquad \textbf{\textit{…(4.22)}}$$

The external work done by uniformly distributed load is given by:

$$W_f = \int_A \{a\}\lfloor P \rfloor\ dA \qquad \textbf{\textit{…(4.23)}}$$

But, the displacement vector **{a}** can also be defined as:

$$\{a\} = [N]\{a\}^e \qquad \textbf{\textit{…(4.24)}}$$

Also, by substitution Equation (4.24) in Equation (4.23) then:

$$W_f = \int_A \{a\}^{eT}[N]^{\mathrm{T}}\lfloor \mathrm{P} \rfloor \mathrm{dA} \qquad \textbf{\textit{…(4.25)}}$$

$$\pi^{e}(a) = \frac{1}{2}\{a\}^{eT}\int_A [\mathbb{B}]^T [\mathbb{E}][\mathbb{B}]\ dA\ \{a\}^e - \int_A \{a\}^{eT}[N]^T \lfloor P \rfloor\ dA \qquad \textbf{\textit{…(4.26)}}$$

To obtain the Equilibrium State of the plate element, the potential energy must be minimized with respect to nodal displacements as follows:

$$\{\frac{\partial \pi}{\partial a^e}\} = \{0\} \qquad \textbf{…(4.27)}$$

By substitution of Equation (4.26) in Equation (4.27) and carrying out the partial differentiation, then:

$$\{\frac{\partial \pi}{\partial a^e}\} = \int_A [\mathbb{B}]^T [\mathbb{E}][\mathbb{B}]\, dA\ \{a\}^e - \int_A [N]^T \lfloor P \rfloor\, dA = \{0\} \qquad \textbf{…(4.28)}$$

or

$$[k]^e \{a\}^e - [F]^e = \{0\} \qquad \textbf{…(4.29)}$$

where,

$$[k]^e = \int_A [\mathbb{B}]^T [\mathbb{E}][\mathbb{B}]\, dA = \int_{-1}^{1}\int_{-1}^{1} [\mathbb{B}]^T [\mathbb{E}][\mathbb{B}] |J|\, d\xi\, d\eta \qquad \textbf{…(4.30)}$$

$$[F]^e = \int_A [N]^T \lfloor P \rfloor\, dA = \int_{-1}^{1}\int_{-1}^{1} [N]^T \lfloor P \rfloor |J|\, d\xi\, d\eta \qquad \textbf{…(4.31)}$$

in which,

$[K]^e$: is the element stiffness matrix,

$[F]^e$: is the element external applied force vector,

$|J|$: is the determinant of the **Jacobian** matrix.

For layered plates, the element stiffness matrix can be written as:

$$[k]^e = \sum_{L=1}^{NL} [k]^L \qquad \textbf{…(4.32)}$$

In general, it is not possible to evaluate the element stiffness matrix explicitly. Thus, numerical integration has to be used based on **Gauss–quadrature** rules, and the selective integration, **3x3** for membrane, coupling and inertia terms, while **2x2** for shear terms are employed ***(Zienkiewicz et al., 1971)*** [(50)].

4.6 Dynamic analysis

The dynamic equilibrium equation and the derivatives of mass and damping matrices will be presented in this section.

4.6.1 Dynamic equilibrium equation

The dynamic equation for a system can be formulated by directly expressing the equilibrium of all forces acting on the mass. In general, four types of forces will be involved; the externally applied load and three forces namely, inertia, damping and the elastic forces. Thus, the dynamic equation may be expressed in a matrix form as follows ***(Clough*** and ***Penzien, 1982)*** [(7)]**:**

$$\{F_I\}+\{F_D\}+\{F_S\}=\{F(t)\} \qquad \textbf{…(4.33)}$$

in which,

$$\{F_I\}=[M]\{\ddot{X}\} \qquad \textbf{…(4.34)}$$

$$\{F_D\}=[C]\{\dot{X}\} \qquad \textbf{…(3.35)}$$

$$\{F_S\}=[K]\{X\} \qquad \textbf{…(3.36)}$$

where [M], [C] and [K] are mass, damping and stiffness matrices respectively, also $\{\ddot{X}\}$, $\{\dot{X}\}$ and {X} are acceleration, velocity and displacement vectors of the nodal points of the system, respectively.

Substituting Equations (4.34) to (4.36) into Equation (4.33) gives the dynamic equilibrium equation for a multi–degree of freedom system:

$$[M]\{\ddot{X}\}+[C]\{\dot{X}\}+[K]\{X\}=\{F(t)\} \qquad \textbf{…(4.37)}$$

4.6.2 Formulation of element mass matrix

When the shape functions used for the derivation of the mass matrix are identical to those used in formulating the element stiffness matrix; matrix **[M]** is called the consistent mass matrix. This matrix was first derived by **Archer** in **1963** ***(Hyder, 2000)***[13].

To derive the consistent mass matrix, one can consider the kinetic energy of the total solution domain discretized into number of elements **(NE**) such that:

$$TI(\dot{a})=\sum_{e=1}^{NE} TI^{e}(\dot{a}) \qquad \textbf{…(4.38)}$$

where **TI** and **TI^{e}** are the kinetic energy of the total solution domain and the sub–domain respectively. The kinetic energy of the element (**e**) can be expressed as follows:

$$TI^{e}=\frac{1}{2}\int_{A}\{\dot{a}\}^{T}[m]\{\dot{a}\}dA \qquad \textbf{…(4.39)}$$

The velocity vector within an element is discretized such that:

$$\{\dot{a}\}=\sum_{i=1}^{NN} N_i\{\dot{a}_i\}, \qquad \text{NN (number of nodes)} \qquad \textbf{…(4.40)}$$

By substituting Equation (4.40) into Equation (4.39), then:

$$TI^{e}=\frac{1}{2}\sum_{i=1}^{NN}\{\dot{a}_i\}^{T}\left(\int_{A} N_i^{T}[m]\,N_i\,dA\right)\{\dot{a}_i\} \qquad \textbf{…(4.41)}$$

or in a matrix form:

$$TI^e = \frac{1}{2}\{\dot{a}\}^T \int_A [N]^T [m][N] dA \{\dot{a}\} = \frac{1}{2}\{\dot{a}\}^T [M]^e \{\dot{a}\} \qquad \textbf{…(4.42)}$$

thus,

$$[M]^e = \int_A [N]^T [m][N] dA = \int_{-1}^{1}\int_{-1}^{1} [N]^T [m][N] |J| \, d\xi \, d\eta \qquad \textbf{…(4.43)}$$

where

$$[N] = [N_1, N_2, N_3, \ldots, N_{nn}] \qquad \textbf{…(4.44)}$$

$$[m] = \begin{bmatrix} I_1 & & & & & & 0 \\ & I_1 & & & & & \\ & & I_1 & & & & \\ & & & I_2 & & & \\ & & & & I_2 & & \\ & & & & & I_3 & \\ 0 & & & & & & I_3 \end{bmatrix} \qquad \textbf{…(4.45 a)}$$

and for nine degrees of freedom per node, one can get:

$$[m] = \begin{bmatrix} I_1 & & & & & & & & 0 \\ & I_1 & & & & & & & \\ & & I_1 & & & & & & \\ & & & I_2 & & & & & \\ & & & & I_2 & & & & \\ & & & & & I_3 & & & \\ & & & & & & I_3 & & \\ & & & & & & & I_4 & \\ 0 & & & & & & & & I_4 \end{bmatrix} \qquad \textbf{…(4.45 b)}$$

For layered plates, the element mass matrix can be written as follows:

$$[M]^e = \sum_{L=1}^{NL} [M]^L \qquad \textbf{…(4.46)}$$

where in above two Equations (4.45a) and (4.45b), I_1, I_2, I_3, and I_4 are translation inertia, rotary inertia and respectively higher order inertia terms, and these are given by:

$$(I_1, I_2, I_3, I_4) = \sum_{L=1}^{NL} \int_{h_{L-1}}^{h_L} (1, h^2, h^4, h^6) \rho^L dz \qquad \textbf{...(4.47)}$$

where ρ^L is material density of L–th layer.

4.6.3 Formulation of damping properties

In the analysis of dynamic problems, it is assumed that the amplitude of free vibration remains constant with time, but experience shows that the amplitude diminishes with time and that the vibrations are gradually damped out.

To bring the vibration analysis into better agreement with reality, the equation of motion for a discretized body or structure, often, must include a term to account for energy dissipation, i.e. damping forces. These forces may arise from several causes, such as friction, air or fluid resistance, internal friction due to imperfect elasticity of materials, and so on. Among all of these sources of energy dissipation, the case where the damping force is proportional to velocity is called viscous damping, and this is the simplest to deal with mathematically. For this reason resisting forces of a complicated nature are usually replaced, for purpose of analysis, by equivalent viscous damping ***(Timoshenko et al. ,1974)***[43]**.**

4.6.3.1 Effect of damping

In most cases the effect of damping on the response of a vibratory system is minor and thus, it can be ignored. However, for vibratory system with a periodic excitation and a frequency at or near the natural frequency, i.e. the resonance

phenomena, damping will be of primary importance and must be taken into account ***(Timoshenko et al. ,1974)*** [43]**.**

Figure (4.3) shows the relationship between the magnification factor (**β**) which represents the ratio of dynamic response to static response (function of dynamic response of the system), and the ratio (**Ω/ω**) which represents the ratio of the angular frequency (**Ω**) of a simple harmonic force function (**PsinΩt** or **PcosΩt**) to the natural frequency of the system, **ω**, plotted for various levels of damping ratios (**γ)**. As for undamped case, the value of (**β)** is approximately unity for small values of (**Ω/ω**), and approaches zero for large values of (**Ω/ω**). However, as the value of **Ω** approaches **ω** (i.e. (**Ω/ω**) approaches unity), the magnification factor grows rapidly. Furthermore, the value of **β** at or near resonance is very sensitive to the amount of damping. Thus, while the damping has only a minor effect when the system is remote from resonance, it has a dramatic effect at or near resonance. In structural dynamics the influence of damping is critical for this case and represents its most important application ***(Weaver*** and ***Johnston, 1987)*** [46]**.**

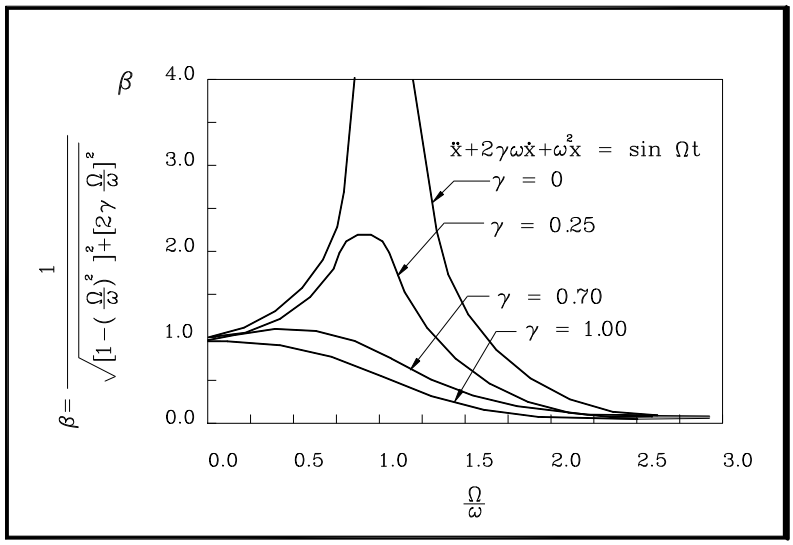

Figure (4.3): Effect of damping on the magnification factor [13].

4.6.3.2 Damping matrix

With the present understanding of damping in structures, it is not possible to formulate an explicit damping matrix for distributed damping throughout a structure, in a manner similar to that followed for the stiffness **[K]** and mass **[M]** matrices **(Pytet, 1990)** [31]. In practice, damping is usually expressed in terms of damping ratios for each of the natural frequency modes. These ratios are established from experiments on similar structures. A number of alternative methods for generating the damping matrix **[C]**, however, exist and include discrete viscous damping and structural damping ***(Wheeler*** and ***Hancock, 1985)*** [47]**.**

The most common form of representation of the damping matrix **[C]** is the so-called **Rayleigh-**type damping ***(Timoshenko et al. ,1974)*** [43] which was given as:

$$[C] = a_o [M] + a_1 [K] \qquad \textbf{…(4.48)}$$

in which $\mathbf{(a_o)}$ and $\mathbf{(a_1)}$ are arbitrary proportionality factors, which make the damping matrix satisfy the orthogonality condition with respect to the modal matrix **[ϕ]** in the same way of the orthogonality conditions for the mass and stiffness matrices that is ***(Bathe, 1996)*** [4]:

$$[\phi]^T [M] [\phi] = [I] \qquad \textbf{…(4.49)}$$

$$[\phi]^T [K] [\phi] = [\Lambda] \qquad \textbf{…(4.50)}$$

$$[\phi]^T [C] [\phi] = 2 [\gamma] [\Lambda]^{1/2} \qquad \textbf{…(4.51)}$$

where:

[ϕ] = the modal matrix whose columns represent the natural modal shapes and the superscript (**T)** denotes transpose,

[I] = Identity matrix,

$[\Lambda]$ = Spectral matrix, which is diagonal with elements representing the squares of the natural frequencies (ω_i^2) and

$[\gamma]$ = Modal damping matrix which is also diagonal with elements representing the damping ratios for the system modes (γ_i).

Premultiplying Equation (4.48) by $[\phi]^T$ and postmultiplying it by $[\phi]$ yields:

$$[\phi]^T [C] [\phi] = a_o [\phi]^T [M] [\phi] + a_1 [\phi]^T [K] [\phi] \quad \textbf{…(4.52)}$$

Substituting Equations (4.49) to (4.51) into Equation (4.52) gives:

$$2 [\gamma] [\Lambda]^{1/2} = a_o [I] + a_1 [\Lambda] \quad \textbf{…(4.53)}$$

The two factors, $\mathbf{a_o}$ and $\mathbf{a_1}$, can be determined by specifying damping ratios for two modes, for example **1** and **2**, and substituting into Equation (4.53) as ***(Pytet, 1990)*** [31]:

$$2 \gamma_1 \omega_1 = a_o + \omega_1^2 a_1 \quad \textbf{…(4.54)}$$

$$2 \gamma_2 \omega_2 = a_o + \omega_2^2 a_1 \quad \textbf{…(4.55)}$$

where ω_1 and ω_2 are the natural frequencies for modes **1** and **2** respectively.

Solving the above two equations one can get:

$$a_o = \frac{2\omega_1\omega_2(\omega_2\gamma_1 - \omega_1\gamma_2)}{(\omega_2^2 - \omega_1^2)} \quad \textbf{…(4.56)}$$

$$a_1 = \frac{2(\omega_2\gamma_2 - \omega_1\gamma_1)}{(\omega_2^2 - \omega_1^2)} \quad \textbf{…(4.57)}$$

Then, the values of $\mathbf{a_o}$ and $\mathbf{a_1}$ are substituted into Equation (4.48) to get the required damping matrix.

Natural frequencies (ω_i) which are used in the above equations can be obtained from the solution of the eigenvalue problem for the undamped case ***(Timoshenko et al. ,1974)*** [43]. As will be shown later, the corresponding damping ratios (γ_i) can be obtained by finding the damping ratio γ_1 , related to the first mode of vibration, using field testing of a structure or from previous experience or even by assuming it within an acceptable range according to the type of the structure. With the value γ_1 on hand, other values of γ_i can be extrapolated using the approximate formula ***(Weaver*** and ***Johnston, 1987)*** [46]:

$$\gamma_i \approx \gamma_1 \left(\frac{\omega_i}{\omega_1} \right)^{el} \quad ; (0.5 \le el \le 0.7) \qquad \textbf{\textit{…(4.58)}}$$

Rewriting Equation (4.53) for an arbitrary mode (**i)** gives:

$$2\,\gamma_i\,\omega_i = a_o + a_1\,\omega_1^2 \qquad \textbf{\textit{…(4.59)}}$$

from which the damping ratio (γ_i) can be defined as:

$$\gamma_i = \frac{a_o + a_1 \omega_i^2}{2\omega_i} \qquad \textbf{\textit{…(4.60)}}$$

The relationship of Equation (4.60) between the natural frequency(ω_i) and the damping ratio(γ_i) is illustrated in Figure (4.4) ***(Pytet, 1990)*** [31]**.**

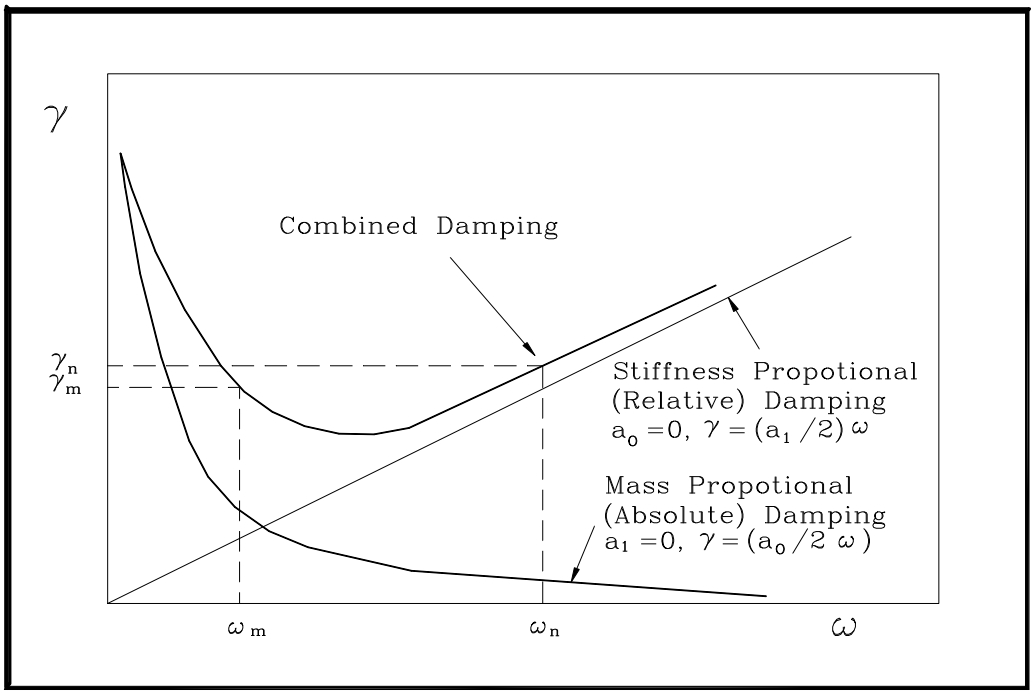

Figure(4.4): Relationship between damping ratio and frequency for Rayleigh damping [13].

4.7 Numerical methods for the dynamic analysis

The dynamic equilibrium equation, Equation (4.37), represents a system of linear differential equations of second order and, in principle, the solution of the equations can be obtained by standard procedures for the solution of differential equations with constant coefficients. However, the procedures proposed for the solution of general system of differential equations become very expensive if the order of the matrices is large. In practical finite element analysis, there are few effective methods. These are mainly, direct time–integration and mode superposition. In the present work, the direct integration method is used.

In direct integration methods the dynamic equilibrium equations are integrated using a numerical step–by–step procedure. The term "direct" meaning that prior to the numerical integration, no transformation of the equation into different form is carried out.

In essence, direct numerical integration is based on two ideas. First, Equation (4.37) is satisfied at discrete time intervals (**Δt**) apart. The second idea is that a variation of displacements, velocities and accelerations within each time interval (**Δt**) is assumed. The available direct procedures can be further sub–divided into implicit and explicit methods.

The implicit algorithms are more effective for structural dynamic problems, in which the response is controlled by a relatively small number of low frequency modes, while explicit algorithms are very efficient for wave propagation problems, in which the contribution of intermediate and high frequency structural modes to the response is important (***Subbaraj*** and ***Dokainish***, ***1989***) [(41)].

In the present study, only implicit methods will be considered because of their properties discussed above. The most conventional implicit time–integration procedures are **Newmark–β**, **Wilson–θ, Hilber–α** and **Houbolt** methods ***(Bathe, 1996)*** [(4)]**,** from which the commonly used is **Newmark– β** method.

4.7.1 The Newmark family of methods

Newmark method is based on using the equilibrium conditions given by Equation (4.37) at time **t+Δt** in order to calculate the displacements at this time. This method is based on the following assumptions:

$$\dot{X}_{t+\Delta t} = \dot{X}_t + \Delta t[(1-\gamma)\ddot{X}_t + \gamma\ddot{X}_{t+\Delta t}] \qquad \textbf{\textit{…(4.61a)}}$$

and,

$$X_{t+\Delta t} = X_t + \Delta t\dot{X}_t + (\Delta t)^2[(\frac{1}{2}-\beta)\ddot{X}_t + \beta\ddot{X}_{t+\Delta t}] \qquad \textbf{\textit{…(4.61b)}}$$

where the parameters β and γ determine the stability and accuracy of the algorithm.

Assuming different values for γ and β, gives different formulas within the **Newmark** family of methods. This method is unconditionally stable if $\gamma \geq 1/2$ and $\beta \geq (2\gamma+1)^2/16$.

Unless γ is taken to be **0.5,** the method introduces artificial damping which can be negative when **γ < 0.5 (*Pytet, 1990*)** [31]. Therefore, as remarked by **Newmark**, all schemes for which

$$\gamma \geq 1/2 \text{ , } \beta \geq 1/4 \qquad \textbf{\textit{…(4.62)}}$$

are unconditionally stable and indeed show no artificial damping, (***Zienkiewicz, 1977***) [49].

In the present study, values of γ and β are (**0.5** and **0.25),** respectively. **Newmark** method with these values of γ and β is called **constant –average-acceleration method**. This method is generally used in structural dynamics because it has been shown to have high degree of numerical stability, (***Al-Sarraf et al., 2003***) [2]. The complete algorithm of the present method is given in (***Subbaraj*** and ***Dokainish***, ***1989***) [41].

4.8 Calculation of natural frequencies

In the dynamic analysis, the natural frequency, ω, of the vibration is important to give an idea about the oscillation of the system with time, and to determine the natural period (**T**) of the vibration which represents the time for which the vibration repeats itself, as:

$$T = 2\pi/\omega \qquad \textbf{\textit{…(4.63)}}$$

in addition, the natural frequencies for more than one mode of vibration are used in constructing the damping matrix **[C]** as shown previously.

To determine the natural frequencies of a structure, a free vibration problem (no external applied loads) for the undamped case is assumed ***(Weaver*** and ***Johnston, 1987)*** [46]:

$$[M]\{\ddot{X}\}+[K]\{X\}=0 \qquad \textbf{\textit{…(4.64)}}$$

Assuming harmonic motion, that is:

$$\{X_i\}=\{\phi_i\}\sin\omega_i t \quad ; \quad i=1,2,..n \qquad \textbf{\textit{…(4.65)}}$$

where:

n = the number of D.O.F. of the system

$\{\phi_i\}$ = the mode shape vector for the **ith** mode of vibration, and

ω_i = the angular frequency of mode **i**.

Differentiating Equation (4.65) twice with respect to time yields:

$$\{\ddot{X}_i\}=-\omega_i^2\{\phi_i\}\sin\omega_i t \qquad \textbf{\textit{…(4.66)}}$$

Then, substituting Equations (4.65) and (4.66) into Equation (4.64) yields, after canceling the term (**sin ω_it**):

$$([K]-\omega_i^2[M])\{\phi_i\}\{\phi_i\}^T=0 \qquad \textbf{\textit{…(4.67)}}$$

Equation (4.67) has the form of the algebraic eigenvalue problem (**Kϕ=λMϕ**). From the theory of homogeneous equations, nontrivial solutions exist only if the determinant of the coefficient matrix is equal to zero. Thus:

$$\left|[K]-\omega_i^2[M]\right|=0 \qquad \textbf{…(4.68)}$$

Expansion of the determinant yields a polynomial of order **n** called characteristic equation. The **n** roots of this polynomial **(ω_i^2)** are the characteristic values or the eigenvalues.

The cyclic natural frequencies (**f_i**) is then obtained from:

$$f_i = \omega_i / 2\pi \qquad \textbf{…(4.69)}$$

substitution of these roots (one at each time) into the homogeneous equation, Equation (4.67), produces the characteristic vectors or the eigenvectors **{ϕ_i}** within arbitrary constants.

A number of solution algorithms have been developed for the solution of the eigenvalue problem. However, only two techniques which are the most important will be presented here, namely the inverse iteration method and the matrix deflation method.

4.8.1 Inverse iteration method

This technique is very effective in calculating the smallest eigenvalue and the corresponding eigenvector, which are the most important eigenpair in structural dynamics.

The basic steps for solving the eigenvalue problem of the form (**D ϕ= λ I ϕ**) using the inverse iteration method are ***(Husain et al., 2002)*** [12]:

1. Computing the dynamic matrix **[D]** as following :

$$[D]= [M]^{-1}[K] \qquad \textbf{…(4.70)}$$

2. Assuming initial trial vector **{ϕ_1}** almost with all terms equal **1.0**.

3. Substituting the vector, **{ϕ_1}**, in the following equation:

$$([D] - (1/\lambda) [I]) \{ \phi^{(1)} \} = 0 \qquad \textbf{…(4.71)}$$

4. Approximate value of **($1/\lambda$)** is obtained by dividing the first element of the column matrix **[D]** {$\phi^{(1)}$} by $\phi_1^{(1)}$, that is:

$$\lambda^1 = \frac{(\textit{first row of } D) \times \left\{ \phi^{1\,(1)} \right\}}{\phi^{(1)}_1} \qquad \textbf{…(4.72)}$$

where $\phi^{(1)}{}_1$ is the first element of the matrix {$\phi^{(1)}$}.

5. The second approximate value of the characteristic vector {$\phi^{(2)}$} is obtained by:

$$\left\{ \phi_{\,appr.} \right\} = \frac{[D] \left\{ \phi^{(1)} \right\}}{(1/\lambda)} \qquad \textbf{…(4.73)}$$

These steps can be continued until the errors become sufficiently small where the used error criterion is the absolute differences, such that:

$$\varepsilon_r = \sum |\phi_i - \phi_{i-1}| \qquad \textbf{…(4.74)}$$

4.8.2 Matrix deflation method

This method is used to determine any desired number of eigenpairs. Its technique is based on matrix deflation, that is, after finding the first eigenpair, λ_1 and {$\phi^{(1)}$}, by inverse or any other iteration method, a new matrix has to be constructed from the original matrix by a deflation process in such a way that it contains only the remaining unknown eigenvalues of the original matrix.

To solve a generalized eigenvalue problem ($\mathbf{D\phi=\lambda\phi}$) by this method it must first construct the deflation matrix $\mathbf{[B_{22}]}$ of order $\mathbf{n-1}$ from the original matrix **[D]** of order **n**. The following steps show the complete procedure of the present method ***(Wang, 1966)*** [45]:

1. Forming the matrix **[B]** such that

$$[B]=[T]\,[D]\,[T]^{-1} \qquad \textbf{…(4.75)}$$

2. Partitioning **[B]** matrix into

$$[B]=\left[\begin{array}{c|c} b_{11} & B_{12} \\ \hline 0 & B_{22} \end{array}\right] \qquad \textbf{…(4.76)}$$

3. Then the first eigenvalue of the matrix

$$[C]=[B_{22}] \qquad \textbf{…(4.77)}$$

is the second eigenvalue (λ_2 **)** of matrix **[D].**

In above equations, **[B]** is a matrix that has the same eigenvalue as **[D],** $\mathbf{b_{11}}$ is a single element equal to λ_1 , and $[\mathbf{B_{12}}]$ is a row identical with the first row of matrix **[D]** excluding the first element, while $\mathbf{[B_{22}]}$ matrix possesses the eigenvalues $\lambda_2, \lambda_3, \ldots, \lambda_n$ **.** Also matrix **[T]** that satisfies the requirement of Equation (4.74) is found to be

$$[T]=\begin{bmatrix} 1 & 0 & . & . & . & 0 & 0 \\ \phi^{(1)}{}_2 & 1 & . & . & . & 0 & 0 \\ \phi^{(1)}{}_3 & 0 & . & . & . & . & 0 \\ . & . & . & . & . & . & . \\ . & . & . & . & . & . & . \\ . & . & . & . & . & 1 & . \\ \phi^{(1)}{}_n & 0 & . & . & . & . & 1 \end{bmatrix} \qquad \textbf{…(4.78)}$$

where the first column of **[T]** matrix is the characteristic vector corresponding to eigenvalue λ_1.

Also, the procedure to find the characteristic vector corresponding to λ_2 is as follows:

1. Computing the characteristic vector $\{Y_2\}$ of **[B]** matrix from the relationship

$$[B]\{Y_2\}=\lambda_2\{Y_2\} \qquad \textbf{…(4.79)}$$

or

$$\left[\begin{array}{c|c} \lambda_1 & B_{12} \\ \hline 0 & \mathrm{C} \end{array}\right]\left\{\begin{array}{c} y_{12} \\ \hline Y_2^* \end{array}\right\}=\lambda_2\left\{\begin{array}{c} y_{12} \\ \hline Y_2^* \end{array}\right\} \qquad \textbf{…(4.80)}$$

2. Then, the characteristic vector $\{\phi^{(2)}\}$ of matrix **[D]** can be obtained as

$$\{\phi^{(2)}\}=[\mathrm{T}]\{\mathrm{Y}_2\} \qquad \textbf{…(4.81)}$$

in above equations, $\mathbf{y_{12}}$ is the first element of the characteristic vector $\mathbf{\{Y_2\}}$, and $\mathbf{\{Y_2^*\}}$ is the characteristic vector of matrix **[C]**, because $\mathbf{[C]\{Y_2^*\}=\lambda_2\{Y_2^*\}}$.

From Equation (4.79), one can find that:

$$\lambda_1 y_{12} + B_{12}\{Y_2^*\} = \lambda_2 y_{12}$$

then,

$$y_{12}=-\frac{B_{12}\,Y_2^*}{\lambda_1-\lambda_2} \qquad \textbf{…(4.82)}$$

The succeeding eigenpairs can be obtained in a way similar to the above procedures.

CHAPTER FIVE

COMPUTER PROGRAM TESTING AND DISCUSSION

5.1 Introduction

The co[illegible] Laminated Plates) which is written as a part of this study will be described in this chapter and the results for several examples will be checked with other researches. This program are designed to deal with the static, free vibration and dynamic analysis of laminated composite plates using higher order shear deformation theory and the finite element formulation. All the boundary conditions are defined in **Appendix (C)**.

The input data of the program consists of the overall plate geometry, material properties of each layer, type of the boundary conditions, type of the analysis (static, free vibration or dynamic), and type of loading for static and dynamic analysis.

The output of computer program includes maximum deflection, stress and strain for static analysis. While for free vibration, the outputs are the eigenvalue and the corresponding eigenvector. Also, in the dynamic analysis, the output includes the time history of maximum deflection, stresses, stress resultants and strains in each layer.

Finally, the program is coded in **FORTRAN–77** language by PC Pentium-II at 633 MHz Intel processor compatible computer with 128 MB RAM.

5.2 Properties of the Program

The main properties of the present computer program will be summarized as follows:

1. Analyzing of any type of laminated plates with any number of layers.

2. The layers may have different material properties and thickness.

3. Including damping properties using Rayleigh type damping.

4. Solving the eigenvalue problem by using the inverse iteration and the matrix deflation methods to determine any desired number of the system natural frequencies.

5. In the dynamic analysis, the program can be used with any function of loading i.e. step, ramp, triangle impact or impulse loading.

The structure of the flow chart of the present program is given in Figure (5.1) to outline the main operations in the main routines of the program.

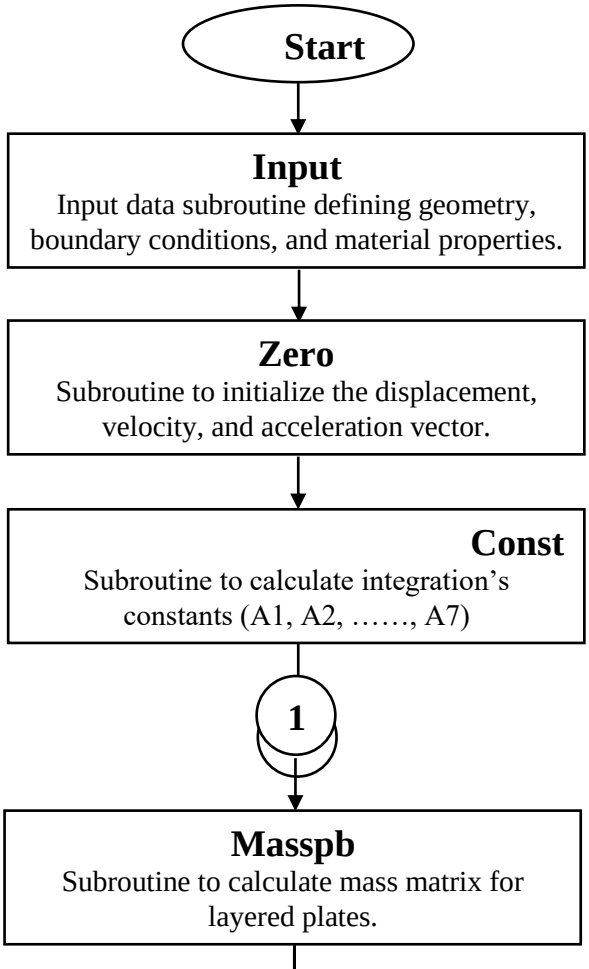

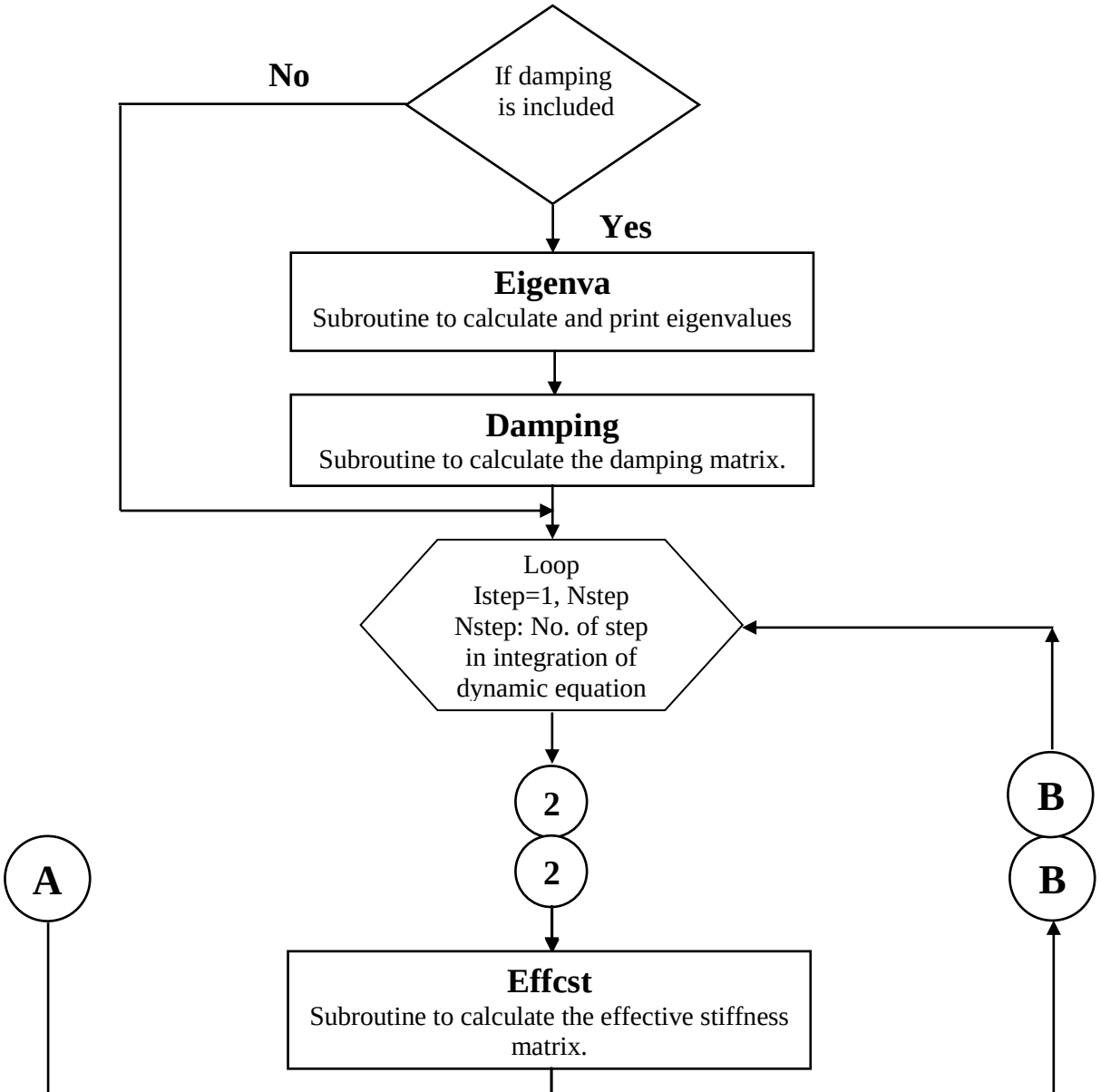
No
If damping is included
Yes
Eigenva
Subroutine to calculate and print eigenvalues
Damping
Subroutine to calculate the damping matrix.
Loop
Istep=1, Nstep
Nstep: No. of step in integration of dynamic equation
2
2
B
B
A
Effcst
Subroutine to calculate the effective stiffness matrix.

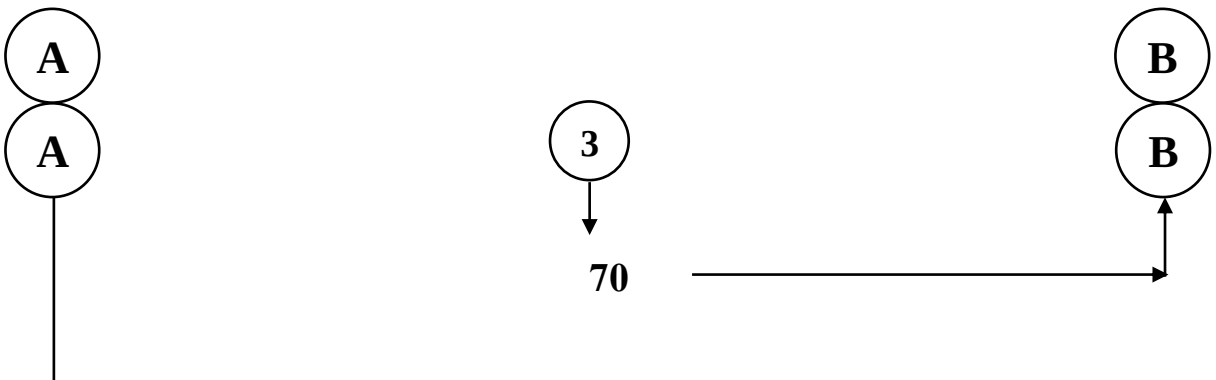
A
A
3
70
B
B

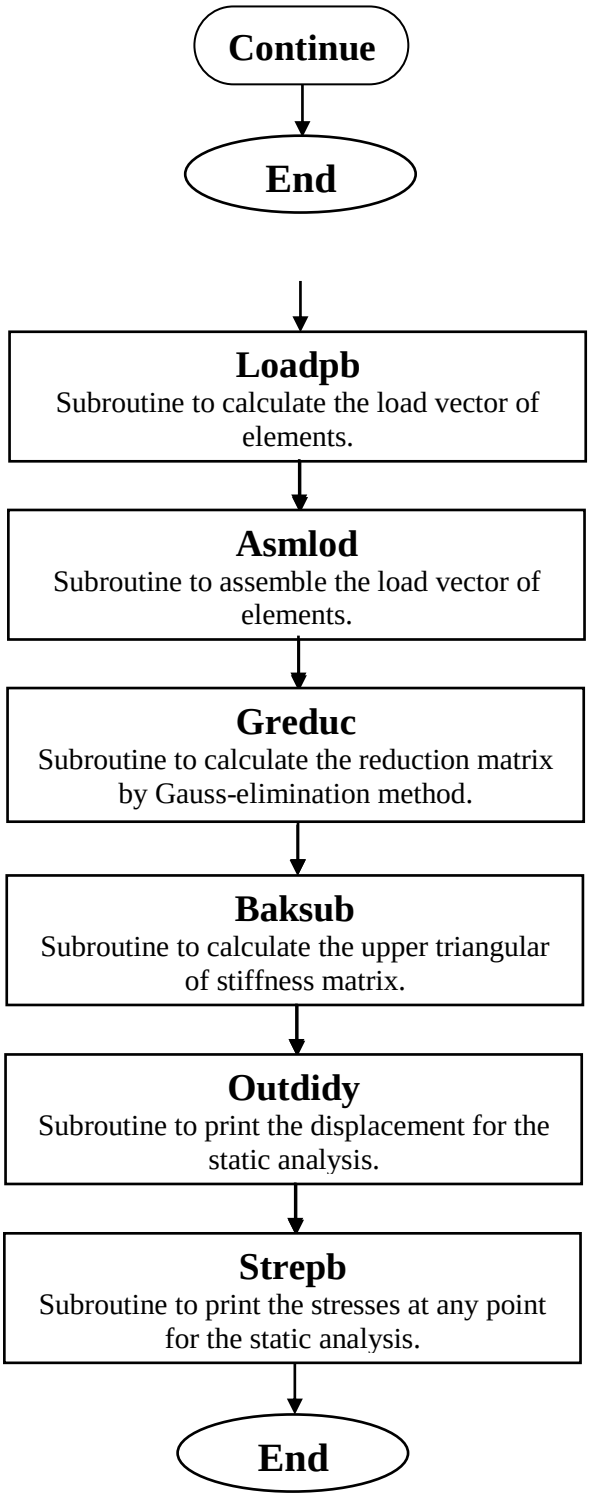

Figure (5.1): The f low-chart of the computer program.

5.3 Numerical Examples

In order to verify the reliability of the computer program, some examples reported in previous researches are considered. These examples are varied among static, free vibration and dynamic analyses.

Example No. 1: (Static Analysis)

To validate the computer program and higher order shear deformation theories, exact three-dimensional elasticity solution is existing for a symmetric laminated composite and sandwich plate consisting of three layers and all edges being simply supported and the plate has uniformly distributed loading. All the details of plate geometry are given in Figure (5.2).

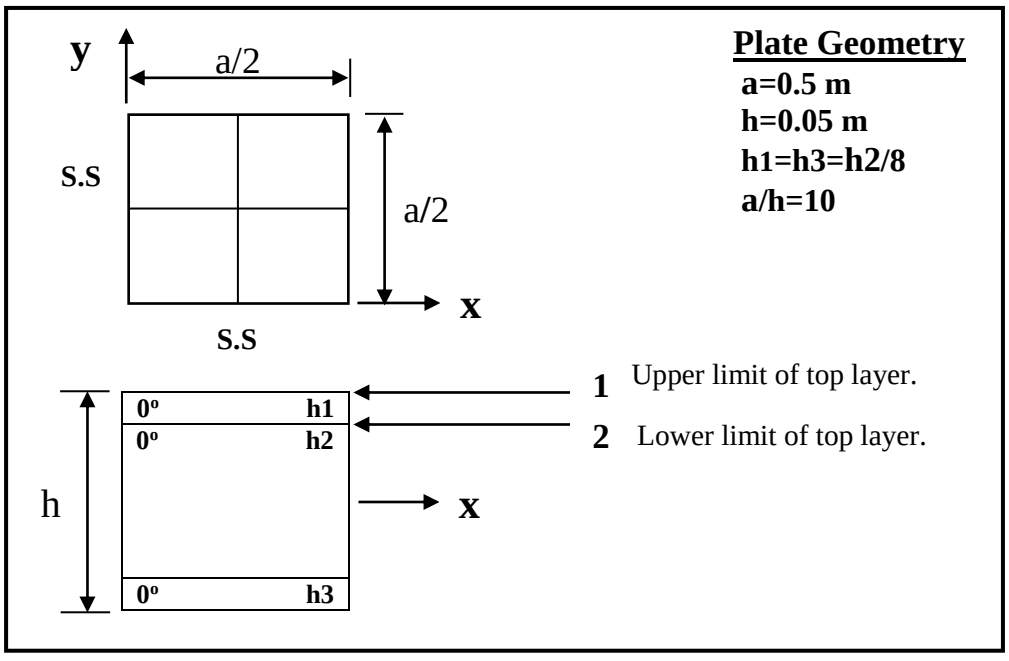

Figure (5. 2): Details of plate geometry and characteristics.

The problem had been solved by **Pandya** and **Kant** [26] in 1988, using a finite element method with the higher order shear deformation theory with five degrees of freedom per node, which are **($w, \theta_x, \theta_y, \theta^*_x,$** and **$\theta^*_y$)**.

They used nine-noded quadrilateral Lagrangian elements in a quarter plate with **2*2** mesh. The material properties for present problem are:

c_{11} = 0.999781, c_{12} = c_{21}=0.231192, c_{22}=0.524886

c_{33}=0.262931, c_{44}=0.26681, c_{55}=0.159914

Also, the symbol (**R** modular ratio) refers to that the stiffness matrix coefficients for top and bottom laminate are some constant multiplier (which is R) times the corresponding stiffness matrix coefficient for middle lamina.

The deflection and stresses as presented are non-dimensional using the following multipliers:

$m_5 = c_{11}(core) / hq$, $m_4 = 1.0 / q$

The three-dimensional exact solution was selected from **Srinivas** and **Rao** in 1970, as mentioned in **Pandya** and **Kant** work [26].

In the present study, only one quarter of the plate is used with **2*2** mesh size. Table (5.1) shows the results of the present higher order shear deformation theories and the percentage errors with respect to the exact solution and the modular ratio **(R)** equal to **5,** while Table (5.2) shows the results for the modular ratio equal to **15.** From these tables, it is noticed that the present higher order theories have a good agreement with the exact solution, and the higher order theory with nine degrees of freedom per node **(HOST 9)** gives more accurate results than the higher order theory with seven degrees of freedom per node **(HOST 7)**. Also, the errors which are between parenthesis for stresses and deflections of first order shear deformation theory **(FSDT)**, classical lamination plate theory **(CLT)** and higher order theory **(HOST5)** with five degrees of freedom per node increase with increasing the modular ratio **(R)**. Therefore, as a result, the results of the present higher order theory with nine degrees of freedom per node are superior to the other results.

Table (5.1): Comparison of results with theoretical studies (Ex. 1, R=5).

Source	$w_o * m_5$ (a/2, a/2, 0)	$\sigma_{x1} * m_4$ (a/2, a/2, h/2)	$\sigma_{y1} * m_4$ (a/2, a/2, h/2)	$\sigma_{x2} * m_4$ (a/2, a/2, 0.4h)	$\sigma_{y2} * m_4$ (a/2, a/2, 0.4h)	$\tau_{xz2} * m_4$ (0, a/2, 0)
Exact	258.97	60.353	38.491	46.623	30.097	4.3641
Present (HOST 7)	257.51 (- 0.56)	60.586 (0.38)	38.697 (0.27)	47.005 (0.82)	30.280 (0.60)	4.520 (3.57)
Present (HOST 9)	257.76 (- 0.46)	60.439 (0.143)	38.572 (0.21)	47.046 (0.90)	30.390 (0.973)	4.532 (3.85)
Kant[26] HOST5	257.78 (- 0.46)	61.03 (1.12)	38.78 (0.75)	47.32 (1.49)	30.42 (1.07)	3.259 (- 25.9)
FSDT[26]	236.10 (- 8.83)	61.87 (2.51)	36.65 (- 4.78)	49.50 (6.17)	29.32 (- 2.58)	3.313 (- 24.1)
CLT [26]	216.94 (-16.23)	61.141 (1.31)	36.622 (- 4.86)	48.913 (4.91)	29.297 (- 2.66)	4.6899 (5.17)

Table (5.2): Comparison of results with theoretical studies (Ex. 1, R=15).

Source	$w_o * m_5$ (a/2, a/2, 0)	$\sigma_{x1} * m_4$ (a/2, a/2, h/2)	$\sigma_{y1} * m_4$ (a/2, a/2, h/2)	$\sigma_{x2} * m_4$ (a/2, a/2, 0.4h)	$\sigma_{y2} * m_4$ (a/2, a/2, 0.4h)	$\tau_{xz2} * m_4$ (0, a/2, 0)
Exact	121.72	66.787	46.424	48.299	34.955	3.9638
Present (HOST 7)	116.94 (- 3.93)	67.428 (0.96)	46.175 (- 0.536)	50.699 (4.97)	35.875 (2.632)	4.103 (3.512)
Present (HOST 9)	119.28 (- 2.0)	68.776 (2.97)	47.097 (1.449)	49.624 (2.74)	35.277 (0.921)	4.057 (2.35)
Kant[26] HOST 5	117.14 (- 3.76)	67.88 (1.64)	46.45 (0.06)	49.94 (3.40)	35.36 (1.16)	2.989 (- 24.59)
FSDT[26]	90.85 (- 25.36)	70.04 (4.87)	41.39 (- 10.84)	56.03 (16.00)	33.11 (- 5.28)	3.091 (- 22.02)
CLT[26]	81.768 (- 32.82)	69.135 (3.52)	41.410 (- 10.80)	55.308 (14.51)	33.128 (- 5.23)	4.2825 (8.04)

$m_5=c_{11}(core)/hq$, $m_4= 1.0/q$

Example No.2: (Free Vibration Analysis)

Three–dimensional elasticity theory solution exists for two layers, simply supported, square and anti-symmetric cross-ply laminated plate in the free vibration field. All the details of the plate geometry are given in Figure (5.3).

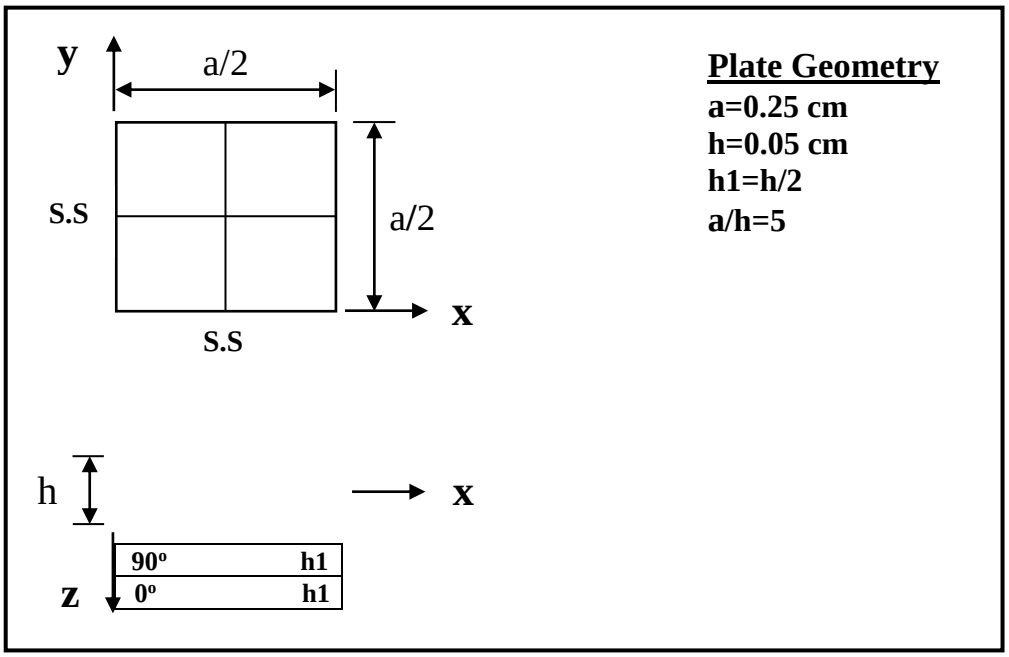

Figure (5.3): Details of plate geometry and dynamic characteristics.

The problem had been solved by **Kant** and **Millikarjuna** [16] in 1989 by using finite element method with the higher order shear deformation theory with seven degrees of freedom per node **(HOST 7)**. They used subspace iteration technique to obtain the eigenvalues and the corresponding eigenvectors. Also, they used nine–noded Lagrangian quadrilateral elements and full plate discretized into **4*4** mesh size.

The material properties used in the analysis are:

Dimensionless material property [typical of graphite (fiber)/epoxy (matrix)]

$E_1/E_2=40$, $G_{12}/E_2=0.6$, $G_{13}=G_{12}$, $G_{23}/E_2=0.5$, $\nu_{12}=\nu_{21}=0.25$, $E_2=1.0$, $\rho=1.0$

The boundary conditions used for the simply supported plate are as follows:

$\mathbf{v_o=w_o=\theta_y, \theta^*_y=0}$ **at x=0,a**

$\mathbf{u_o=w_o=\theta_x, \theta^*_x=0}$ **at y=0,b**

The three–dimensional elasticity theory solution was given by **Noor** in 1973, as mentioned in **Kant** and **Mallikarjuna** work.[16]

In the present study, only one quarter of the plate is used with **2*2** mesh size, utilizing the symmetry. Table (5.3) shows all the results of the present higher order shear deformation theories together with the percentage errors, given between parenthesis with respect to the elasticity solution. From this table, it is noticed that the higher order shear deformation theories have good agreement with the elasticity solution. Also, the higher order theory with nine degrees of freedom per node **(HOST 9)** has more accurate results than the theory with seven degrees of freedom per node **(HOST 7)**. Therefore, this theory can be adopted in future analysis. The error in the classical lamination plate theory **(CLT)** predictions is mainly attributed to neglecting the deformation through plate thickness. Values in Table (5.2) represent (**ω).**

Table (5.2): Comparison of results with theoretical studies (Ex. 2).

Source	Number of layers		
	2	4	6
3-D E.T.*	0.3425	0.42719	0.45091
Present (HOST 7)	0.3600 (5.11)	0.44668 (4.56)	0.46265 (2.60)
Present (HOST 9)	0.3486 (1.78)	0.43360 (1.50)	0.45695 (1.34)
Kant & Mallikarjuna	0.35138 (2.59)	0.43786 (2.49)	0.4609 (2.21)
CLT	0.42884 (25.21)	0.6669 (56.11)	0.70359 (56.03)

* **3-D E.T.: Three-dimensional elasticity theory.**

Example No. 3: (Dynamic Analysis)

A four-layer, simply supported, square and symmetric cross-ply laminated plate is chosen to be analyzed in the present study to assess the validity of the computer program in the dynamic analysis. All the details of the plate geometry and dynamic characteristics are given in Figure (5.4).

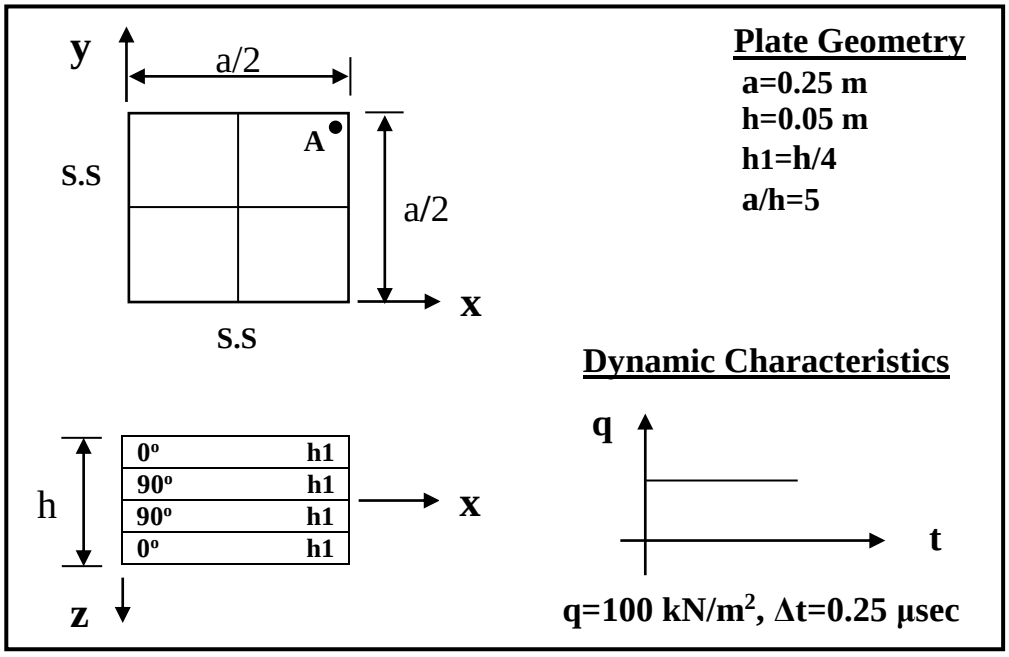

Figure (5.4): Details of plate geometry and dynamic characteristics.

The problem had been solved by **Mallikarjuna** and **Kant** [22] in 1988, using finite element method with the higher order shear deformation theory with seven degrees of freedom per node. They used **Newmark** direct integration method with time step equal to (0.25μsec). Because of symmetry, only one quadrant of the plate was analyzed and 2*2 mesh size was used for this quadrant. The composite material properties in each lamina were:

$E_1/E_2=25$, $E_2=2.1*10^6$ N/cm^2, $G_{12}=G_{13}=G_{23}=0.5\ E_2$, $\nu_{12}=\nu_{21}=0.25$,

$\rho=8*10^{-6}$ Ns^2/cm^4.

In the present study, also one quadrant of the plate is chosen with 2*2 mesh size utilizing symmetry. The time step is also (0.25μsec). Also, the higher order shear deformation theory with seven degrees of freedom is used.

Figures (5.8) and (5.9) show the dynamic response curves of the maximum central deflection and maximum central normal stress **(σ_x),** at point **A,** for the plate under consideration. It can be noticed that the results obtained in the present study by using the higher order shear deformation theory with seven degrees of freedom per node has good agreement with the corresponding results reported by **Mallikarjuna** and **Kant** [22].

Example No. 4: (Dynamic Analysis)

A five-layer, simply supported, square and symmetric angle-ply laminated plate is chosen to be analyzed in the present study as another example to assess the reliability of the dynamic part of the computer program. All the details of the plate geometry and dynamic characteristics are given in Figure (5.5).

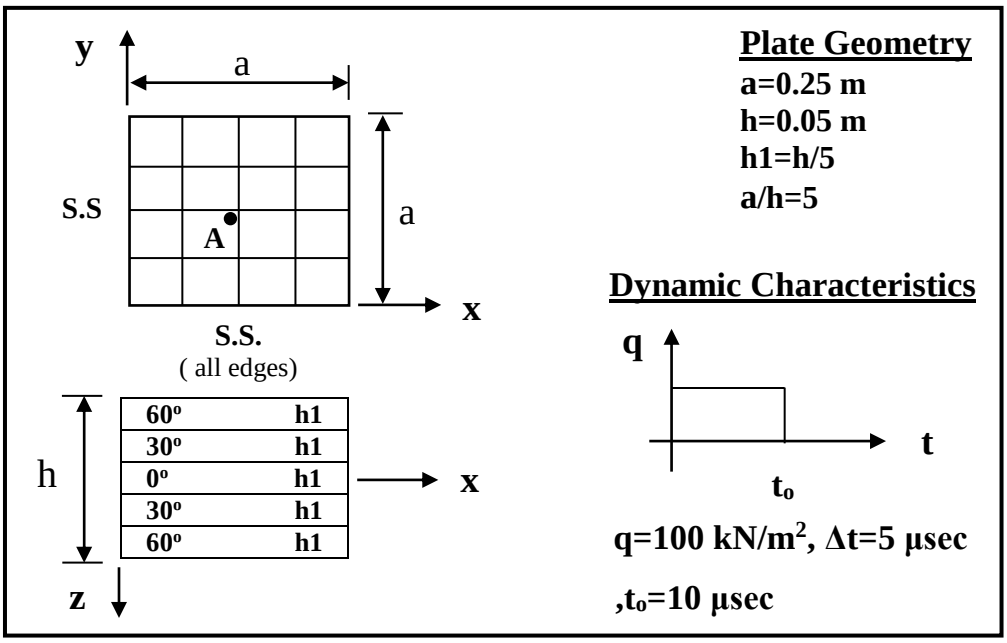

Figure (5.5): Details of plate geometry and dynamic characteristics.

The problem had been solved by **Mallikarjuna** and **Kant** [22] in 1988, using a finite element method with the higher order shear deformation theory with seven degrees of freedom per node. They used **Newmark** direct integration method with time step equal to (0.5μsec) and full plate model with **4*4** mesh size. The composite material properties are the same as in the previous example.

In the present study, the full plate model is also chosen with **4*4** mesh size. The time step is also (0.5μsec). Also, the higher order shear deformation theory with seven degrees of freedom is used.

Figure (5.10) to (5.12) show the time history of central deflection, maximum central normal stresses **(σ_x)** and **(σ_y),** at point **A,** for the present problem. It is noticed that the solution of the present study has good agreement with the pervious solution obtained by **Mallikarjuna** and **Kant** [22]**.**

Example No. 5: (Dynamic Analysis)

A three-layer, clamped edge, square and symmetric cross-ply laminated plate is selected to be solved in the present study as another example. All the details of the plate geometry and dynamic characteristics are given in Figure (5.6).

Reddy [36] in 1983 solved this example using a finite element formulation with the first order shear deformation theory with five degrees of freedom per node. He used **Newmark** method with time step equal to (5μsec), and only one quadrant of the plate with **2*2** mesh was cosidered.

Mallikarjuna and **Kant** [22] in 1988 solved the same example by using the same tools as in example No. (3). The material properties of this example are similar to the example No.(3).

In the present study, the time step is equal to (0.25μsec) and also one quarter of the plate is used with **2*2** mesh. Also, the higher order shear deformation with seven degrees of freedom is used.

Figures (5.13) and (5.14) show the dynamic response curves of the central deflection and the maximum central normal stress **(σ_x),** at point **A,** for the present example. Again, good agreement between the present solution and **Mallikarjuna** and **Kant** [22] solution is noticed. From these figures, it can be shown that the first order shear deformation theory predicts significantly lower values of stresses and that happens because of neglecting the higher order terms which contribute to the cubic variation of in-plane deformations across the plate thickness.

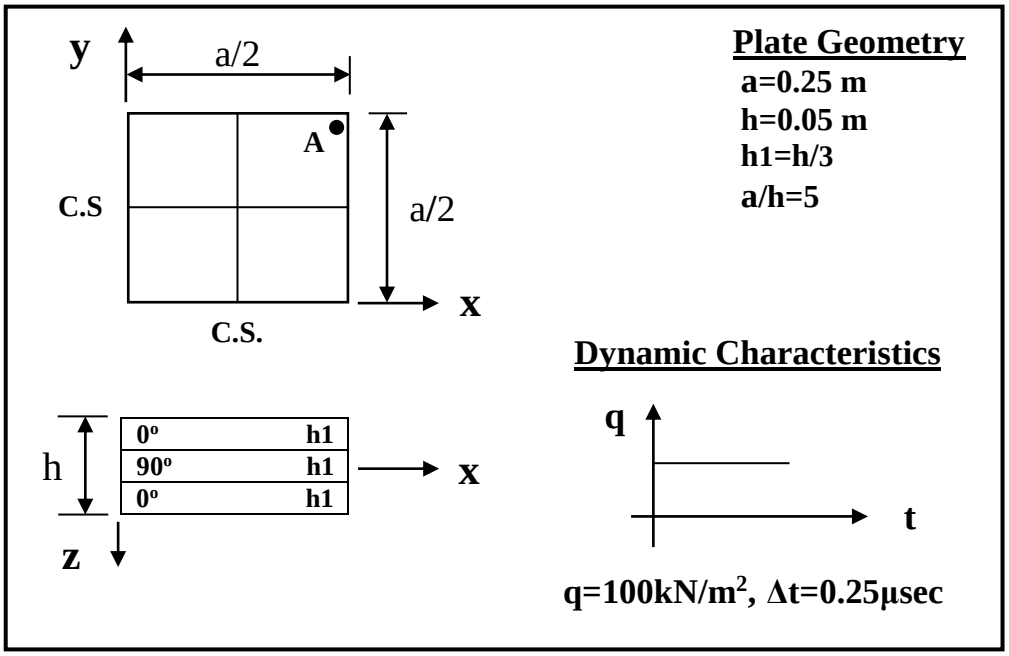

Figure (5.6): Details of plate geometry and dynamic characteristics.

Example No. 6: (Dynamic Analysis)

To validate the computer program and the higher order shear deformation theory with nine degrees of freedom per node, a closed-form higher order solution exists for a three-layer, simply supported, symmetric and sandwich laminated plate under step and triangular impulse loading. All the details of the plate geometry and dynamic characteristics are given in Figure (5.7).

Kommineni and **Kant** [20] in 1993 solved the problem by using finite element formulation with the higher order shear deformation theory with nine degrees of freedom per node. They used explicit central difference integration method with time step equal to (1μsec) and only one quadrant of plate was used. The boundary conditions were:

@ x=0

$$v_o = v^*_o = w_o = \theta_y = \theta^*_y = 0$$

@ x=a/2

$$u_o = u^*_o = \theta_x = \theta^*_x = 0$$

@ y=0

$$u_o = u^*_o = w_o = \theta_x = \theta^*_x = 0$$

@ y=a/2

$$v_o = v^*_o = \theta_y = \theta^*_y = 0$$

Also, the material properties of each layer were as follow:

Middle layer **$E=19.2*10^6$psi; $\nu=0.24$; $G=0.82*10^6$psi; $\rho=0.00013$lb s^2/in^4.**

Outer layers **$E=20.83*10^6$psi; $\nu=0.44$, $G=3.7*10^6$psi; $\rho=0.00013$lb s^2/in^4.**

Nosier and **Reddy** as mentioned by **Kommineni** and **Kant** [20] obtained the closed form solution in 1991.

In the present study, the same problem is solved by tacking one quadrant of the plate and time step equal to (4 μsec). Figures (5.15) and (5.16) show the dynamic response of center deflection, at point **A**, for the present example. From these figures, it can be noticed that the present solution is really conformable with the closed-form solution of **Nosier** and **Reddy**, and with **Kommineni** and **Kant** [20] solution.

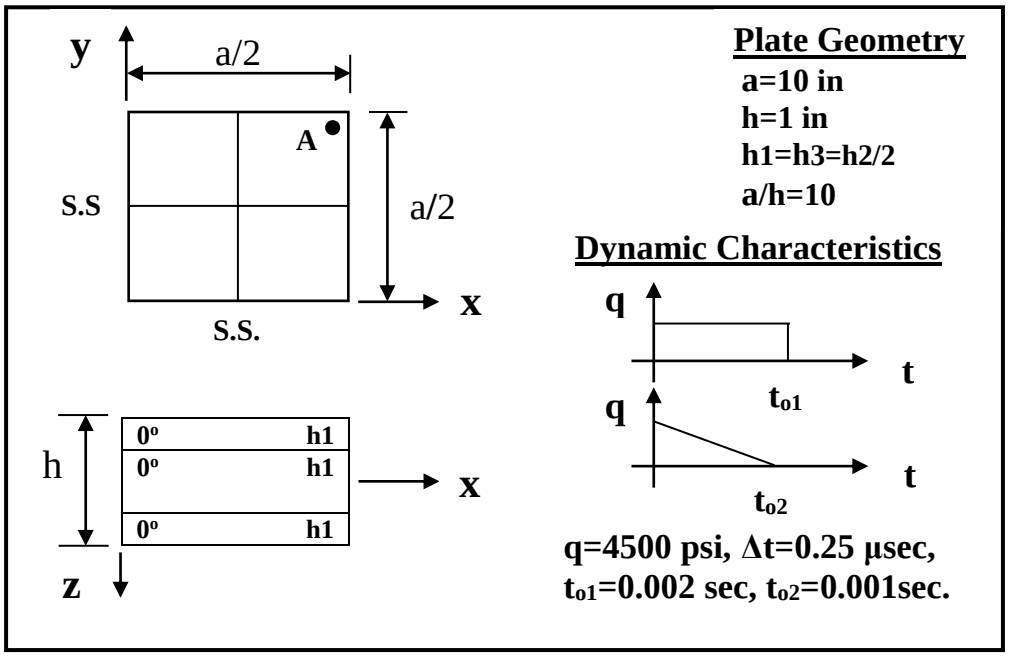

Figure (5.7): Details of plate geometry and dynamic characteristics.

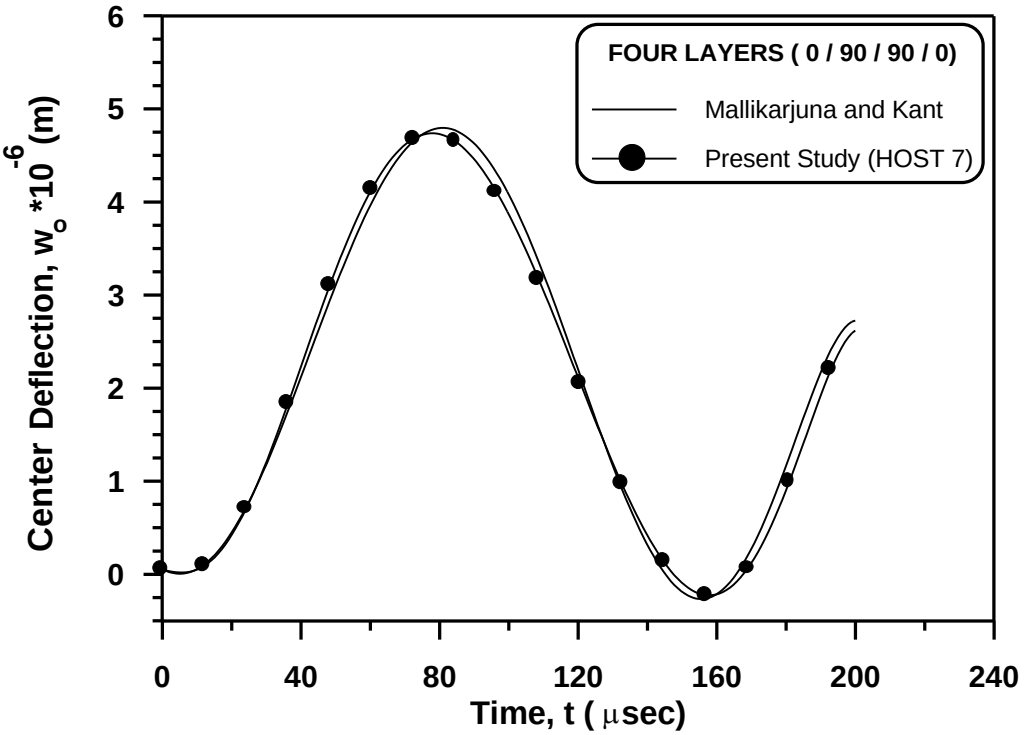

Figure (5.8): Center deflection for a square simply supported laminated plate subjected to suddenly applied pulse loading.

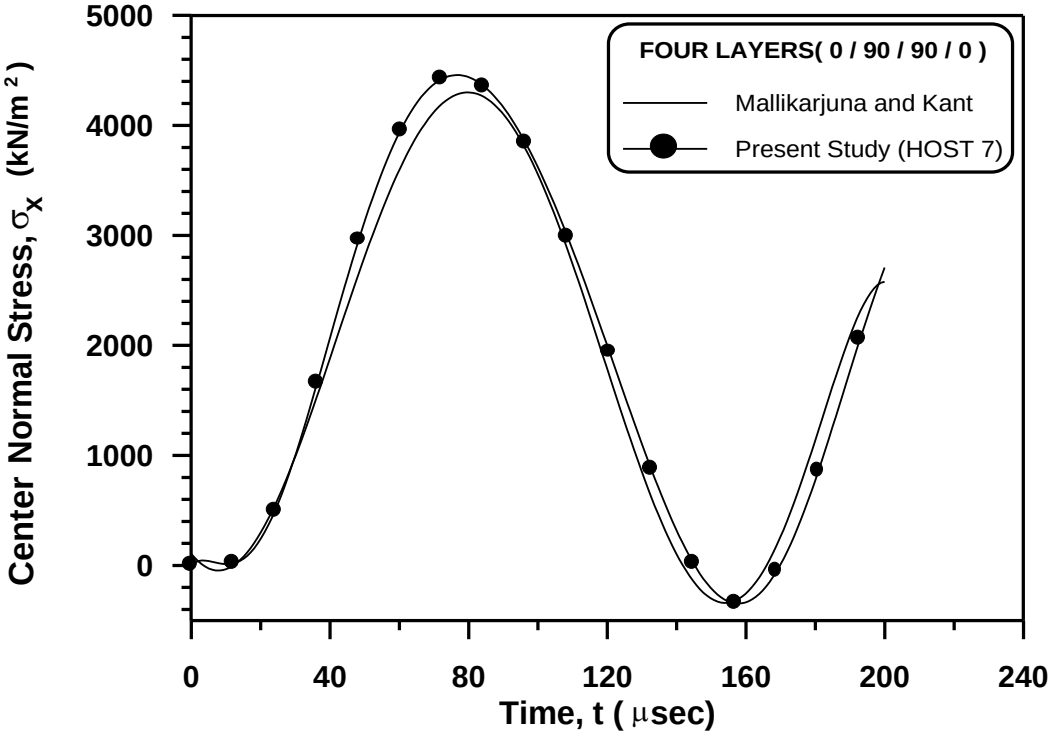

Figure (5.9): Center normal stress (σ_x) for a square simply supported laminated plate subjected to suddenly applied pulse loading.

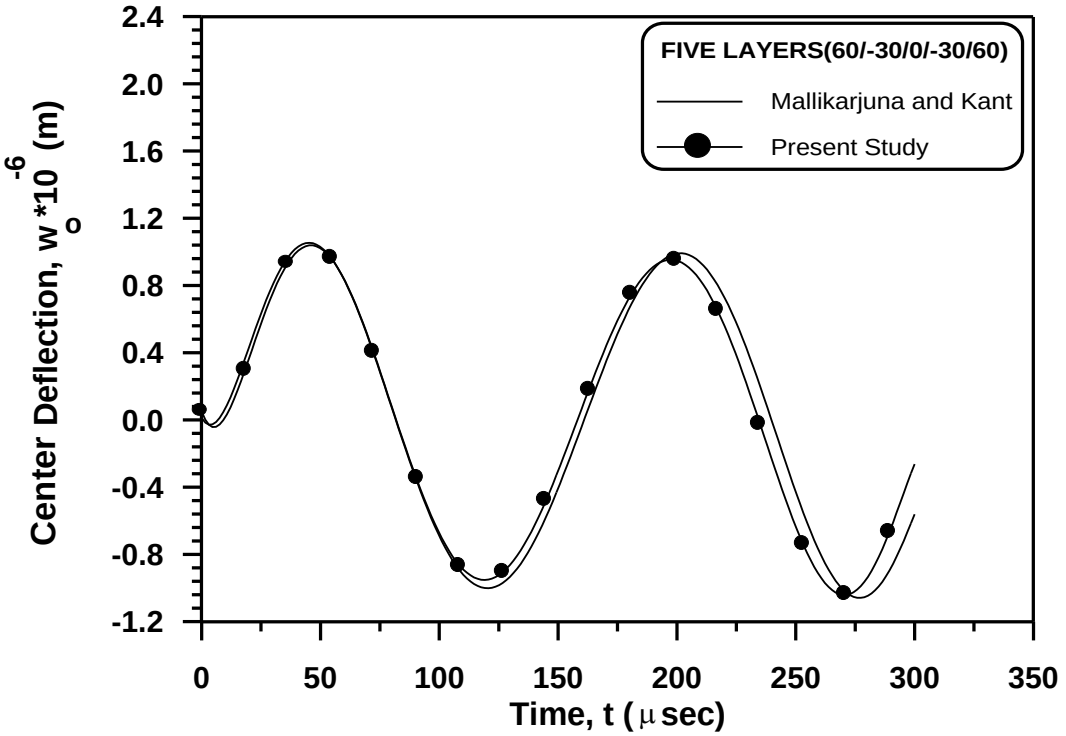

Figure (5.10): Center deflection for a square simply supported laminated plate subjected to suddenly applied impulsive loading.

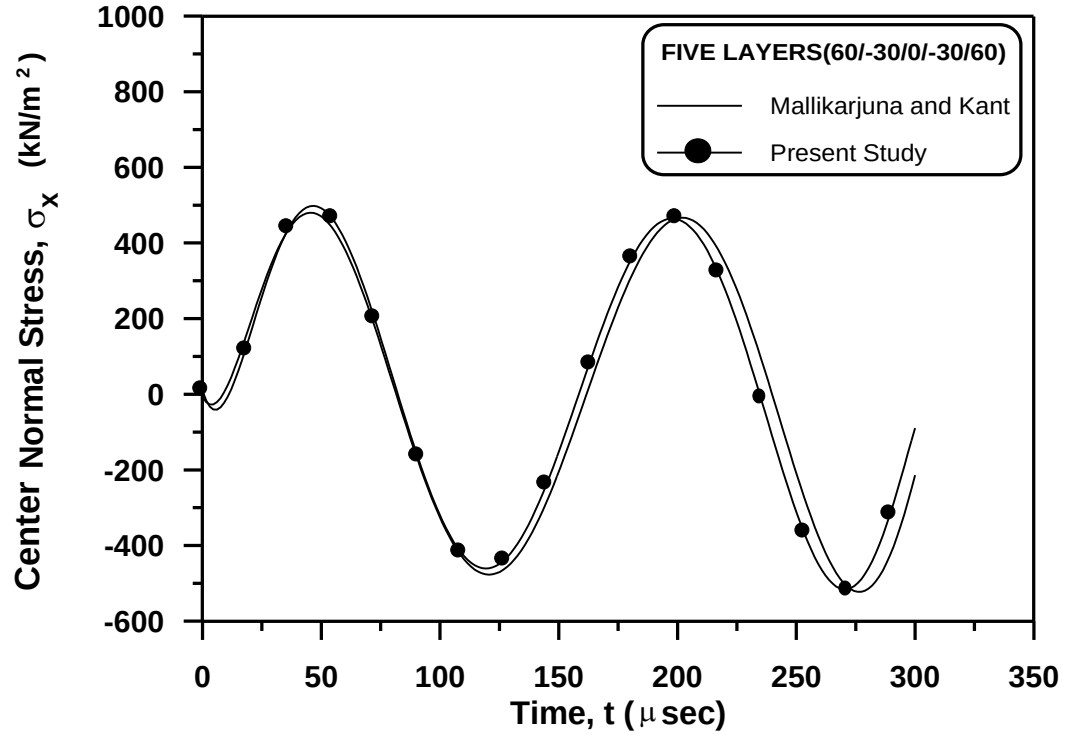

Figure (5.11): Center normal stress (σ_x) for a square simply supported laminated plate subjected to suddenly applied impulsive loading.

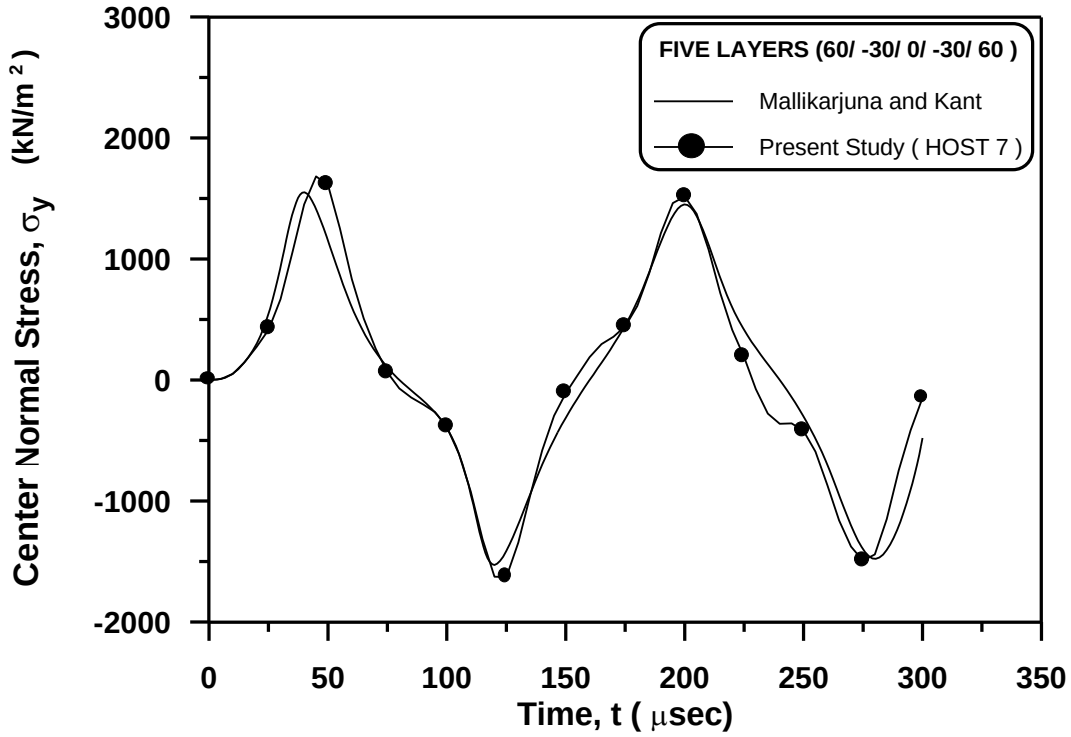

Figure (5.12): Center normal stress (σ_y) for a square simply supported laminated plate subjected to suddenly applied impulsive loading.

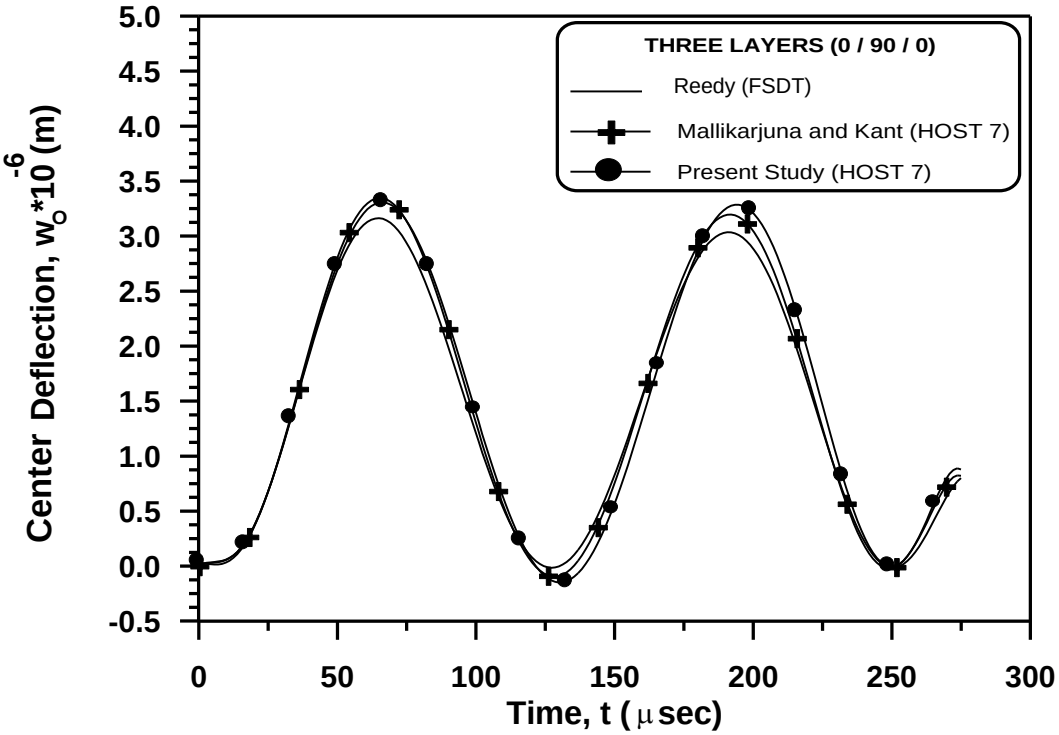

Figure (5.13): Center deflection for a square simply supported laminated plate subjected to suddenly applied pulse loading.

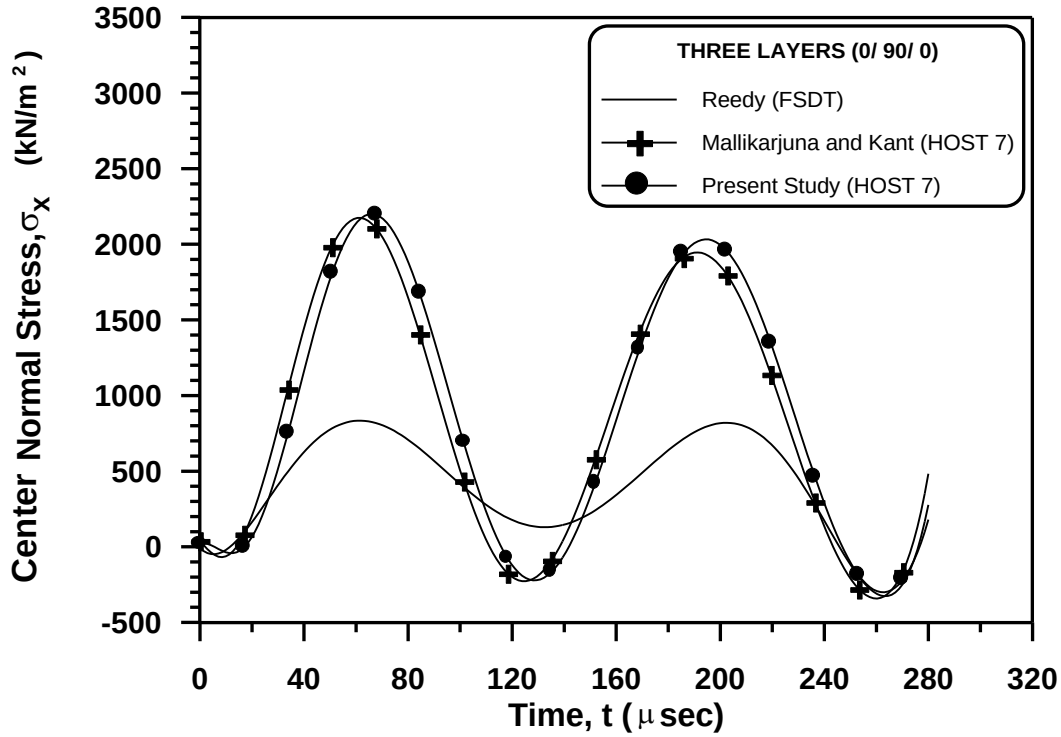

Figure (5.14): Center normal stress (σ_x) for a square clamped supported laminated plate subjected to suddenly applied pulse loading.

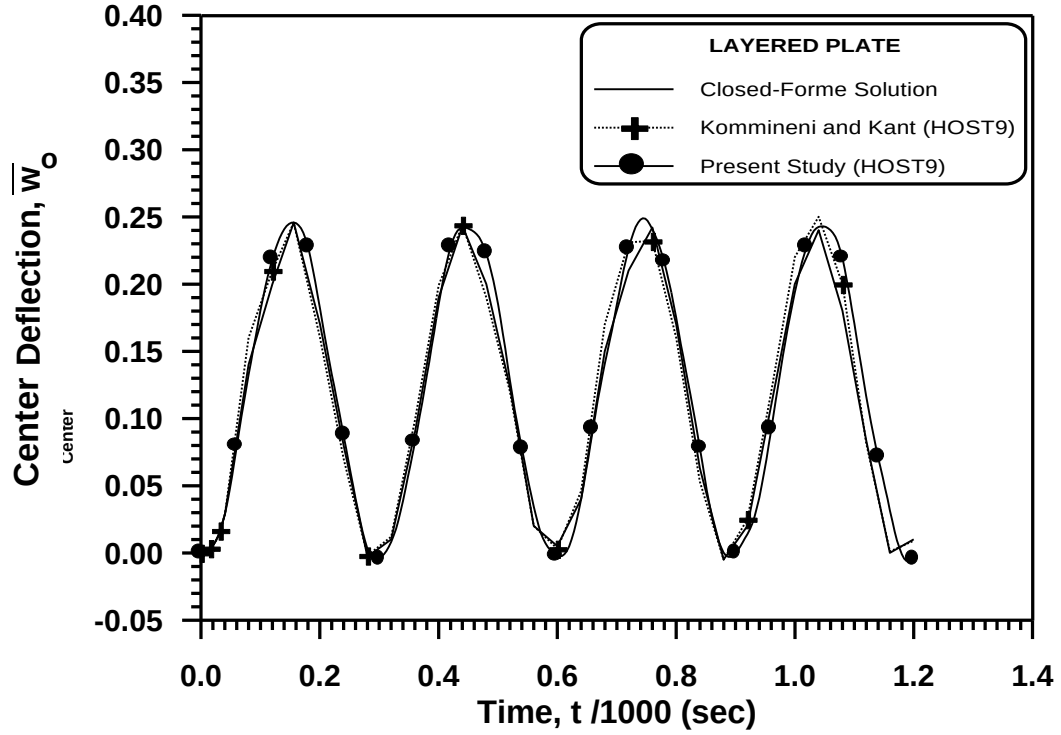

Figure (5.15): Center deflection for a square simply supported layered plate subjected to suddenly step pulse loading.

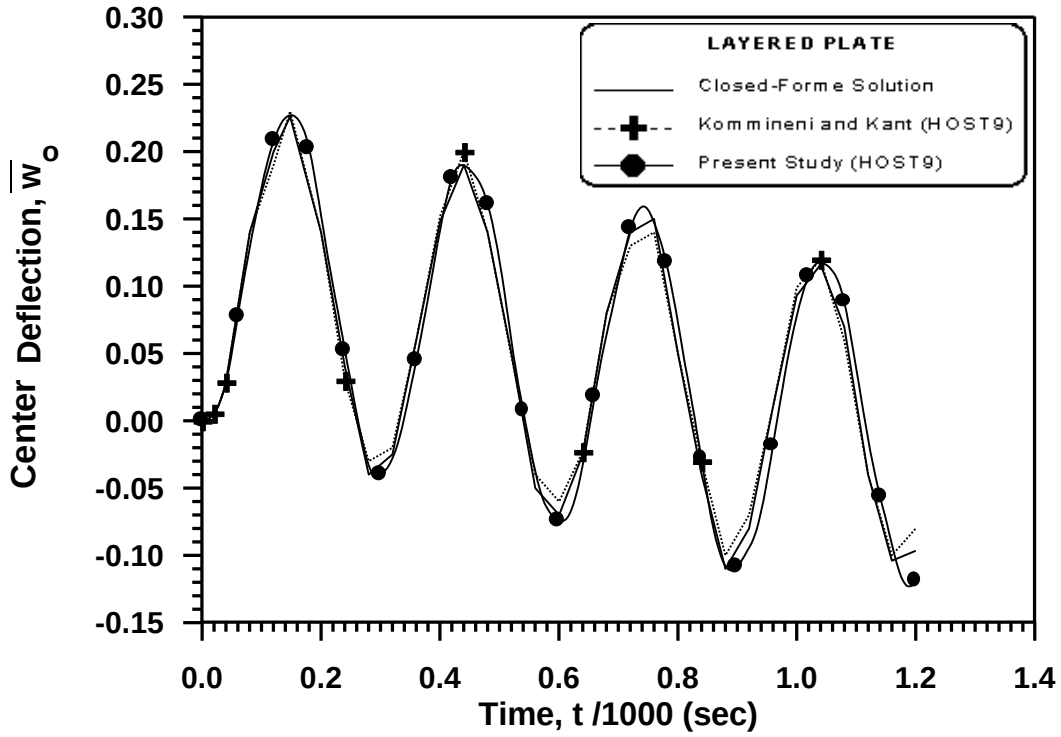

Figure (5.16): Center deflection for a square simply supported layered plate subjected to suddenly triangular pulse loading.

CHAPTER SIX

PARAMETRIC STUDY

6.1 Introduction

A parametric study is performed to assess the influence of several important parameters on the dynamic behavior of laminated plates.

The selected parametric studies in this chapter can be summarized as follows:

1. The effect of degree of orthotropy of individual layers.
2. The effect of fiber's orientation angle.
3. The effect of number of layers.
4. The effect of boundary conditions.
5. The effect of plate aspect ratio.
6. The effect of damping ratio.

Each one of the above parameters was studied individually by analyzing a type of laminated composite plate. In all cases, only one quadrant of the plate was analyzed due to double symmetry about **x** and **y**-axes and **2*2** mesh is used except for the angle-ply plates which were analyzed by considering the full plates with **4*4** mesh size. Also, the composite material in each lamina is graphite (fiber)-epoxy (matrix) lamina with the following properties ***(Parhi et al., 2001)*** [27]:

E_1=172.5GPa, E_2=6.9GPa, G_{12}=G_{13}=3.45GPa, G_{23}=1.38 GPa, v_{12}=v_{21}=0.25, ρ=0.8 kN.s^2/m^4

6.2 The effect of degree of orthotropy of individual layers

To show the effect of degree of orthotropy of individual layers on the dynamic response of the plate structure, four-layer, simply supported, square and symmetric angle-ply laminated plate is analyzed. All the details of plate geometry and dynamic characteristics are given in Figure (6.1).

Figure (6.7) shows that when the material orthotropy ratio **(E1/E2)** increases from **(3)** to **(40)**, the central deflection, at point **A,** will decrease by about **30%,** because of increasing stiffness of the laminated plate with the same volume and number of layers. The degree of orthotropy ratio may be changed by using different types of fibers such as boron, graphite, glass, … etc.

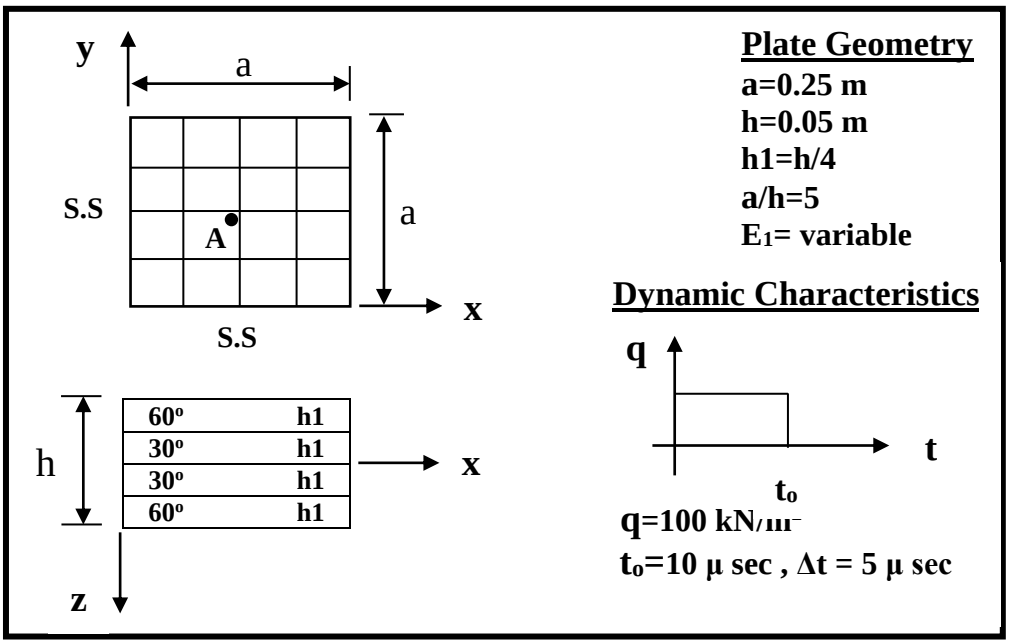

Figure (6.1): Details of plate geometry and dynamic characteristics.

6.3 The effect of fiber's orientation angle

To study the effect of fiber's orientation angle on the dynamic response, two-layer, simply supported, square, antisymmetric cross and angle-ply laminated plate under pulse loading is analyzed. All the details of plate geometry, and dynamic characteristics are given in Figure (6.2).

Figures (6.8) to (6.12) show that the best fiber's orientation angle at which the plate has a maximum stiffness with the same number of layers and plate thickness (i.e. lowest central deflection, at point **A**, lowest summation for central normal stresses **(σ_x** and **σ_y),** and lowest transverse shear stresses occurring in the plate, **(τ_{xz}, τ_{yz})** at points **B** and **C)** is **45º**. Also, it can be noticed that the antisymmetric angle-ply lamination of plates is stiffer than the antisymmetric cross-ply lamination.

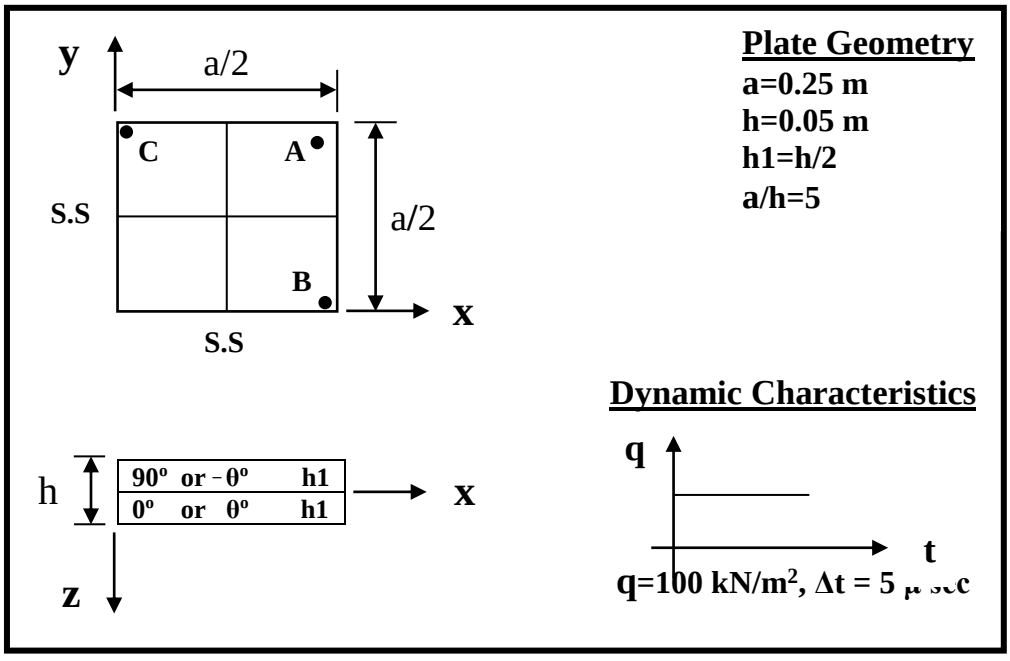

Figure (6.2): Details of plate geometry and dynamic characteristics.

6.4 The effect of number of layers

A simply supported, square, symmetric and cross-ply laminated plate is chosen to assess the effect of the number of layers on the dynamic response of the structure. All the details of plate geometry, and dynamic characteristics are given in Figure (6.3).

Figure (6.13) shows that, for the same volume of the plate, the amplitude of the central deflection, at point **A,** will decrease by about **24%,** and the time period is decreased when the number of layers increase from **(3)** to **(9)** because of increasing of the number of the reinforced layers. Then, extension and bending stiffness will increase; therefore, the amplitude will decrease. Also, increasing the number of layers will give a better distribution of orthogonal stiffness through the depth. It can be noticed that increasing the number of layers more than (**9)** have no further significant effect on increasing the stiffness of the plate.

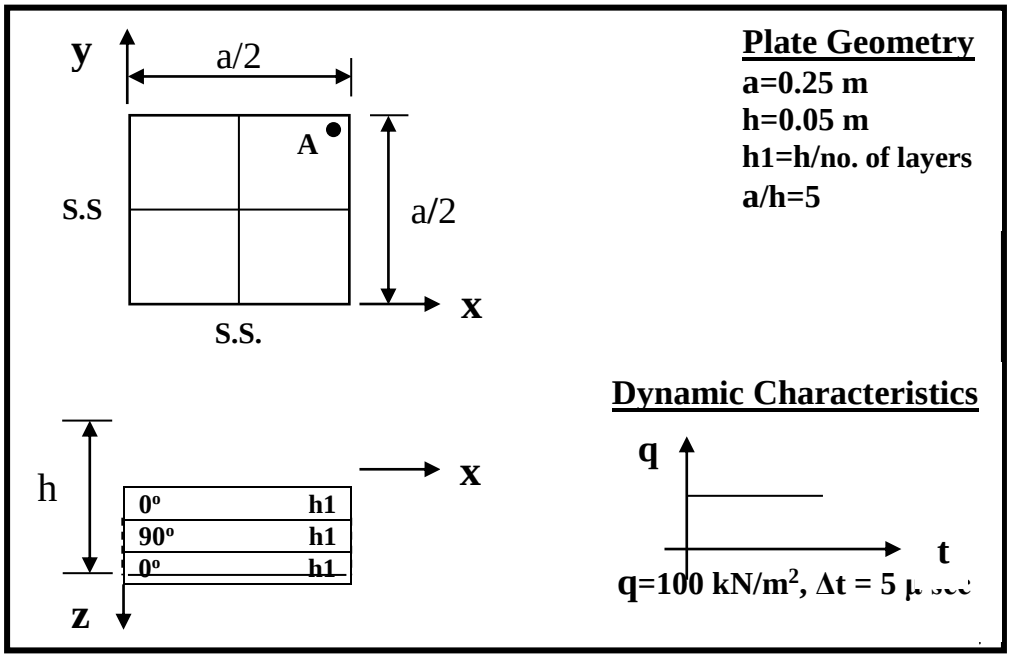

Figure (6.3): Details of plate geometry and dynamic characteristics.

6.5 The effect of boundary conditions

To assess the effect of boundary conditions, three-layer, square, symmetric and cross-ply laminated plate under pulse loading is analyzed. All the details of plate geometry, and dynamic characteristics are given in Figure (6.4)

Figure (6.14) shows that the amplitude of the central deflection, at point **A**, decreases from all edges simply supported to all edges clamped because of added restrains by edges.

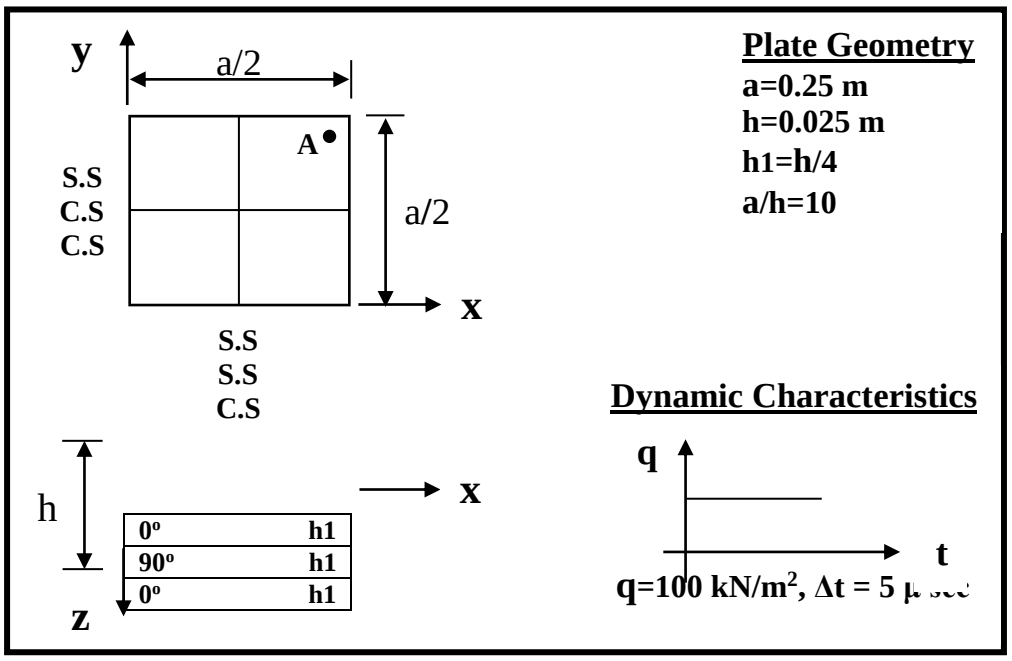

Figure (6.4): Details of plate geometry and dynamic characteristics.

6.6 The effect of plate aspect ratio

To study the effect of plate aspect ratio on dynamic behavior, two-layer, simply supported, antisymmetric and angle-ply laminated plate is analyzed. All the

details of plate geometry, and dynamic characteristics are given in Figure (6.5).

Figure (6.15) shows that, for the same width, the amplitude of the central deflection, at point **A**, increases by about **63%,** and the time period is increased from **(a/b=1)** to **(a/b=6),** and when increasing the plate aspect ratio more than a specified value the increase in amplitude becomes very small.

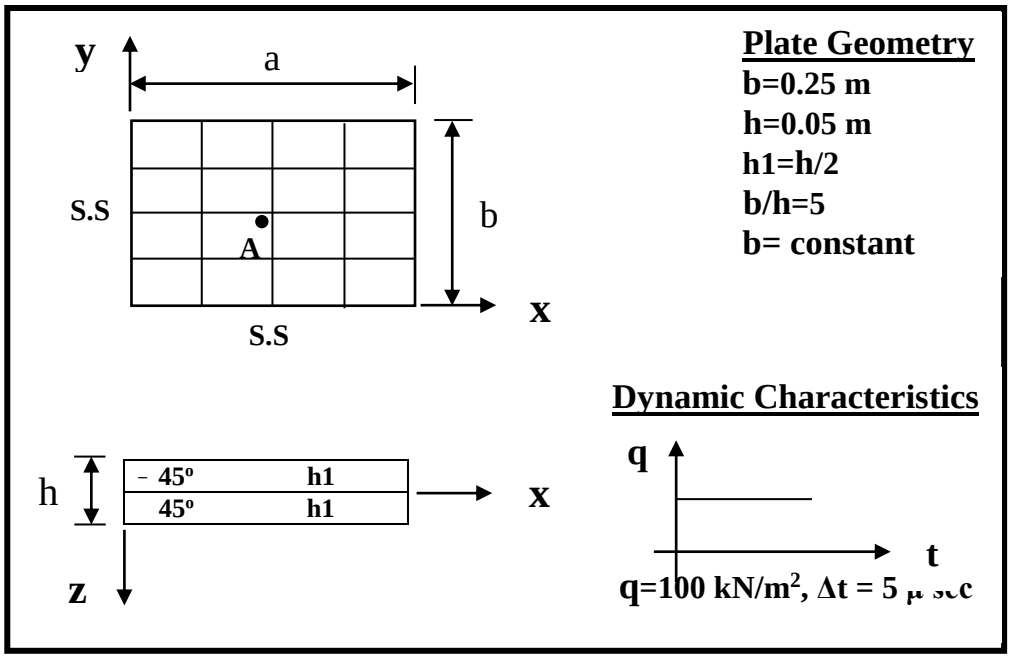

Figure (6.5): Details of plate geometry and dynamic characteristics.

6.7 The effect of damping ratio

To show the effect of damping on the oscillation of the structure, two examples are considered. The first is a square, symmetric and angle-ply laminated plate consisting of four-layer under pulse loading. The second is a square, antisymmetric and angle-ply laminated plate consisting of four layers under pulse loading. All the details of plate geometry, and dynamic characteristics are given in Figure (6.6).

Figures (6.16) and (6.17) show that the amplitude of oscillation, at point **A**, decreases with time due to the effect of viscous damping, and increasing damping ratio results in decreasing the amplitude of the response gradually with time and slowing the oscillation of the structure. When the response of the structure shows no oscillation about the static deflection position, it means that it is under the critical damping ratio. Also, it can be seen that the antisymmetric lamination of plates has a rate of damping faster than the symmetric lamination i.e. it reaches to critical damping case in a shorter time. This lamination can be used in places that need damping.

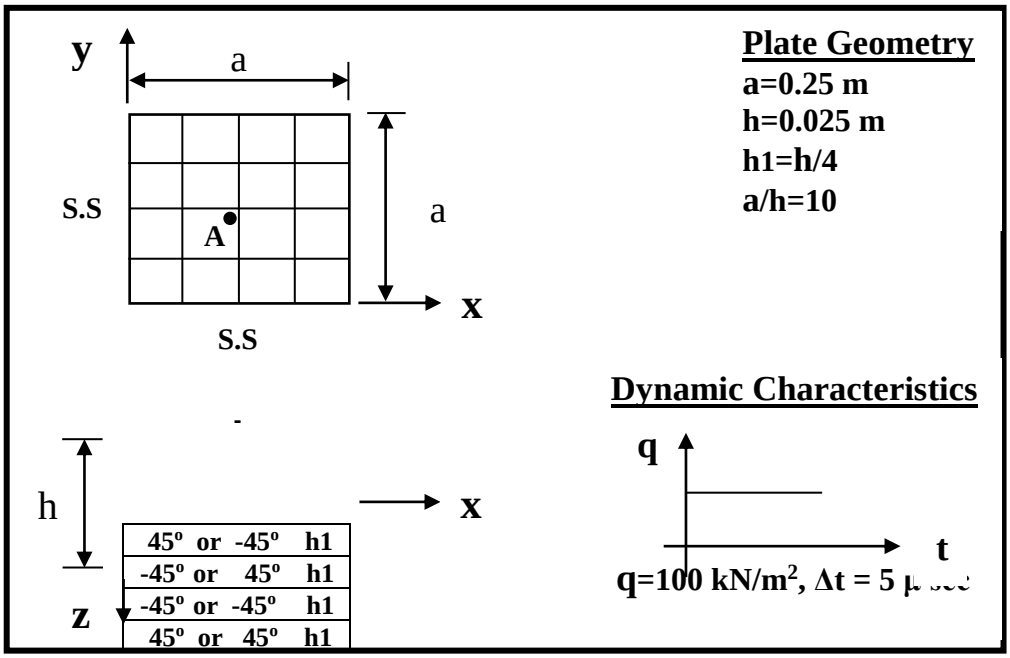

Figure (6.6): Details of plate geometry and dynamic characteristics.

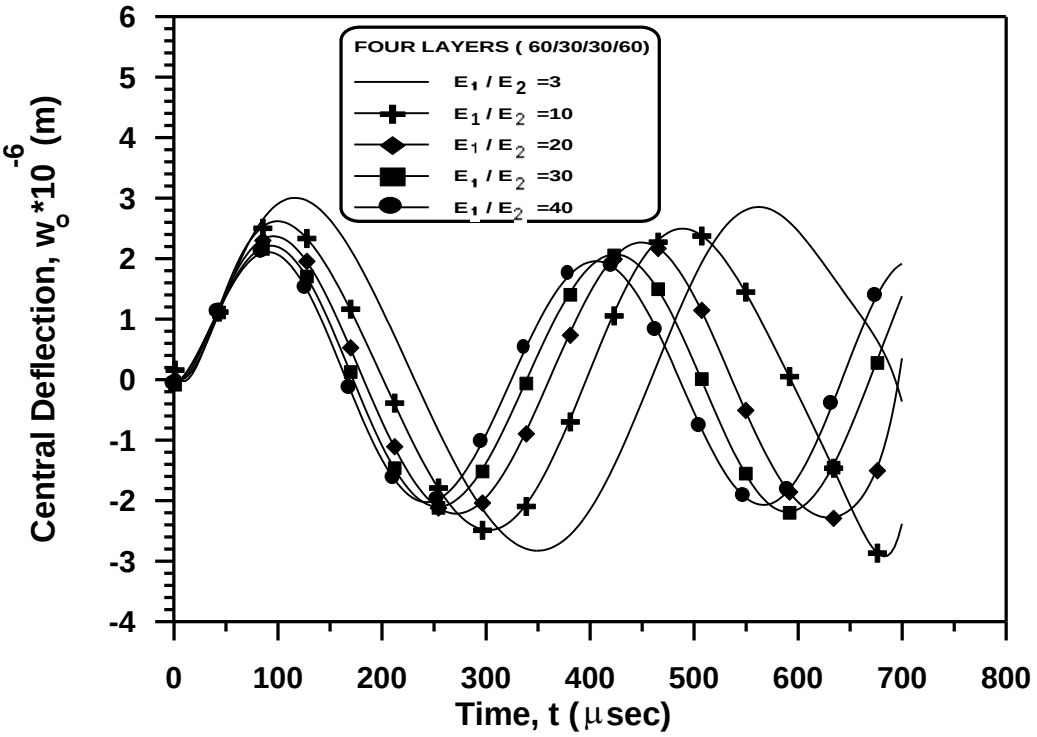

Figure (6.7): Effect of degree of orthotropy of individual layers on the dynamic response for a simply supported square laminated plate under impulsive loading.

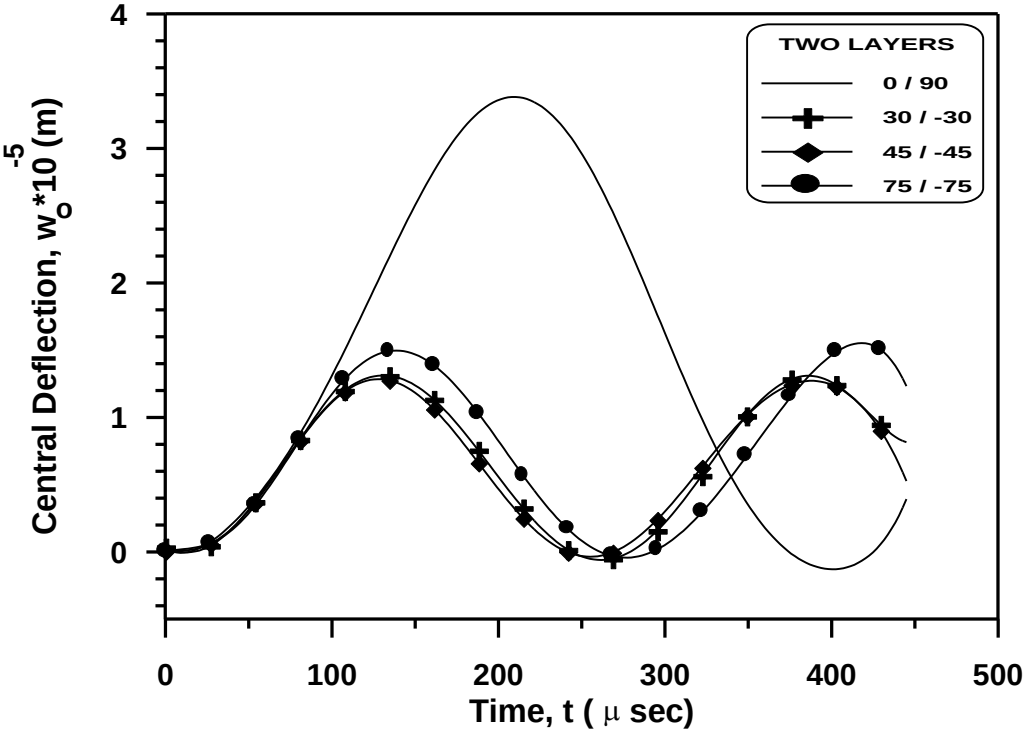

Figure (6.8): Effect of fiber's orientation angle on the dynamic response for a simply supported square laminated plate under pulse loading.

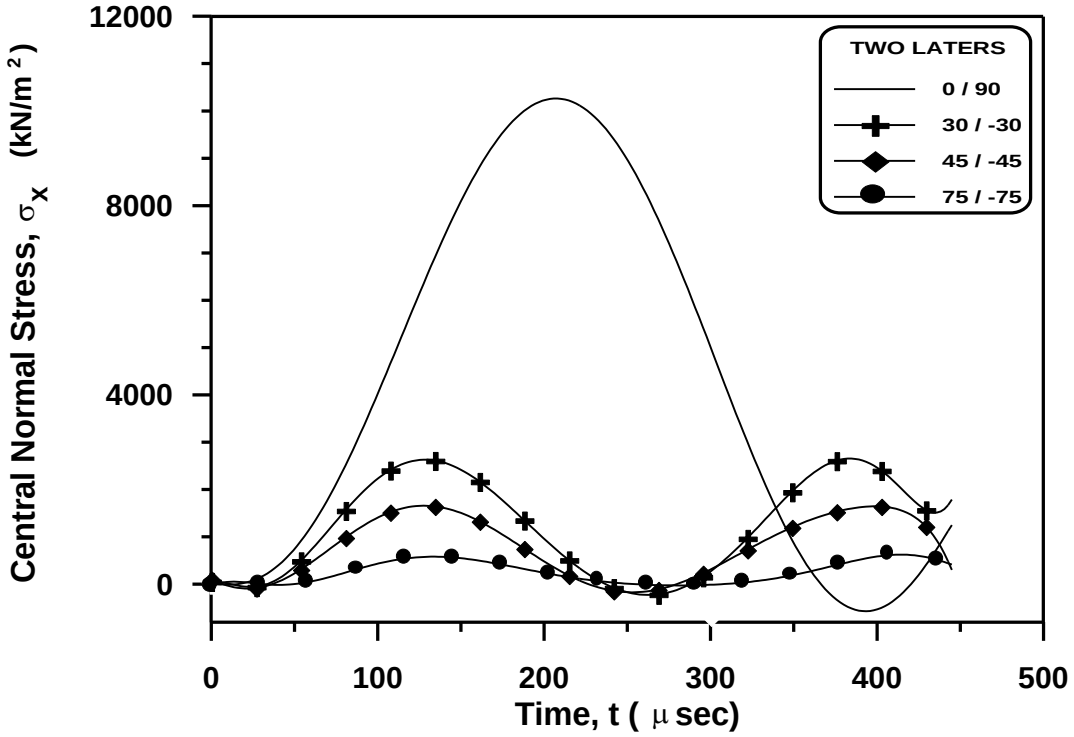

Figure (6.9): Effect of fiber's orientation on central normal stress (σ_x) for a simply supported square laminated plate under pulse loading.

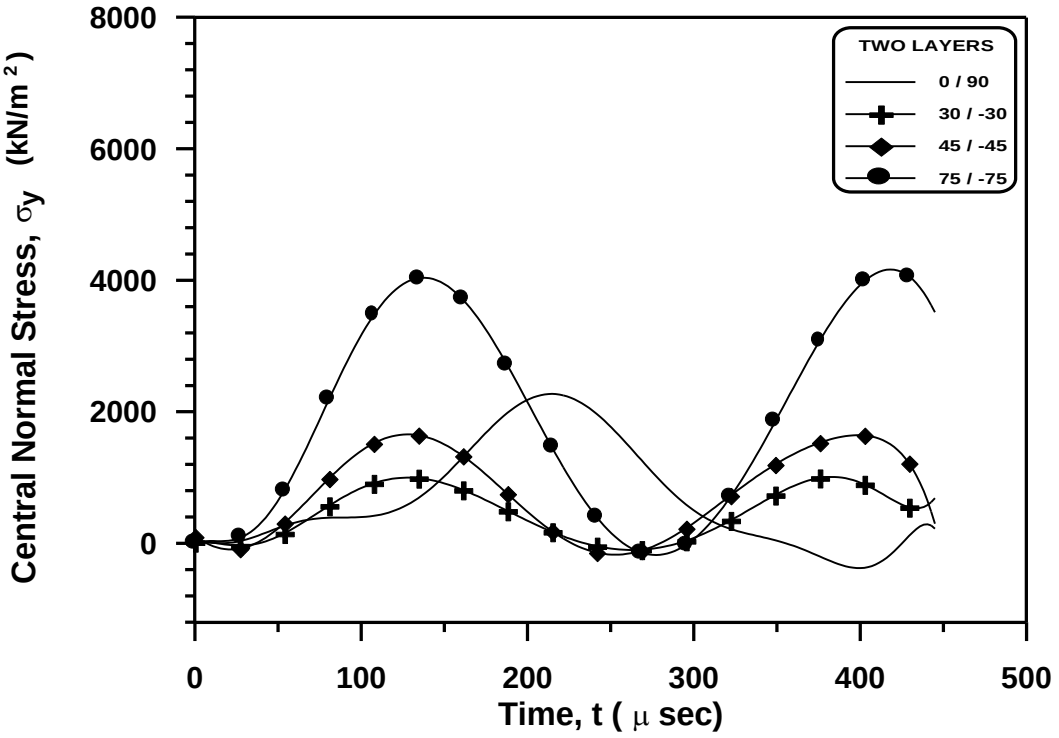

Figure (6.10): Effect of fiber's orientation on central normal stress (σ_y) for a simply supported square laminated plate under pulse loading.

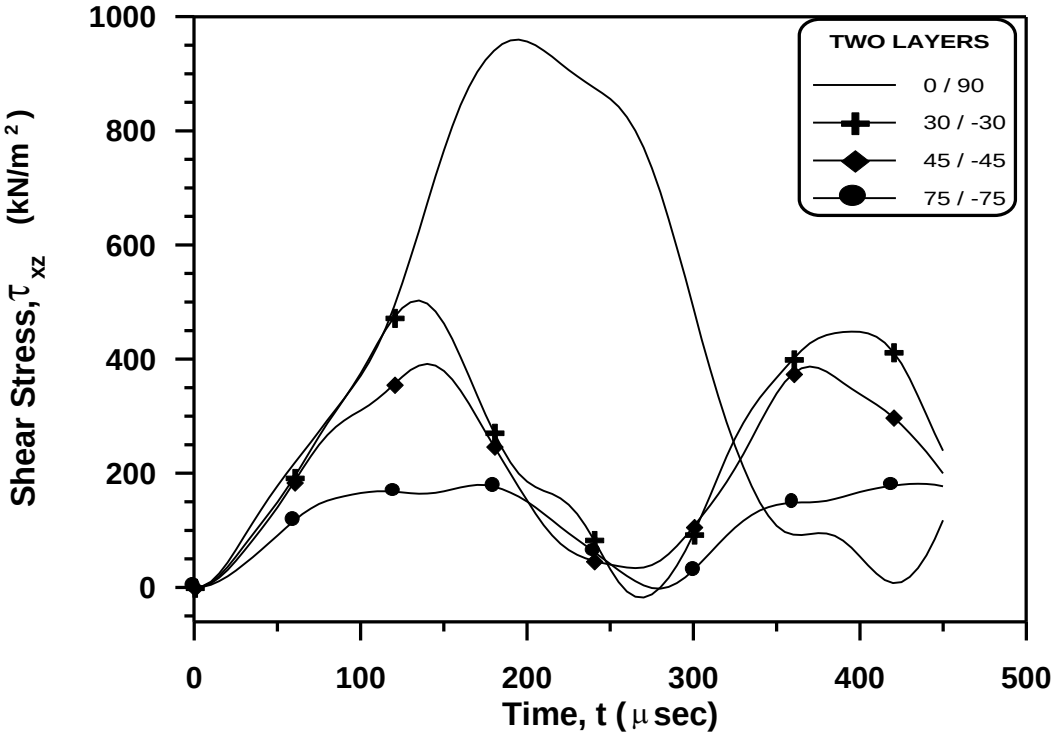

Figure (6.11): Effect of fiber's orientation on shear stress (τ_{xz}) for a simply supported square laminated plate under pulse loading.

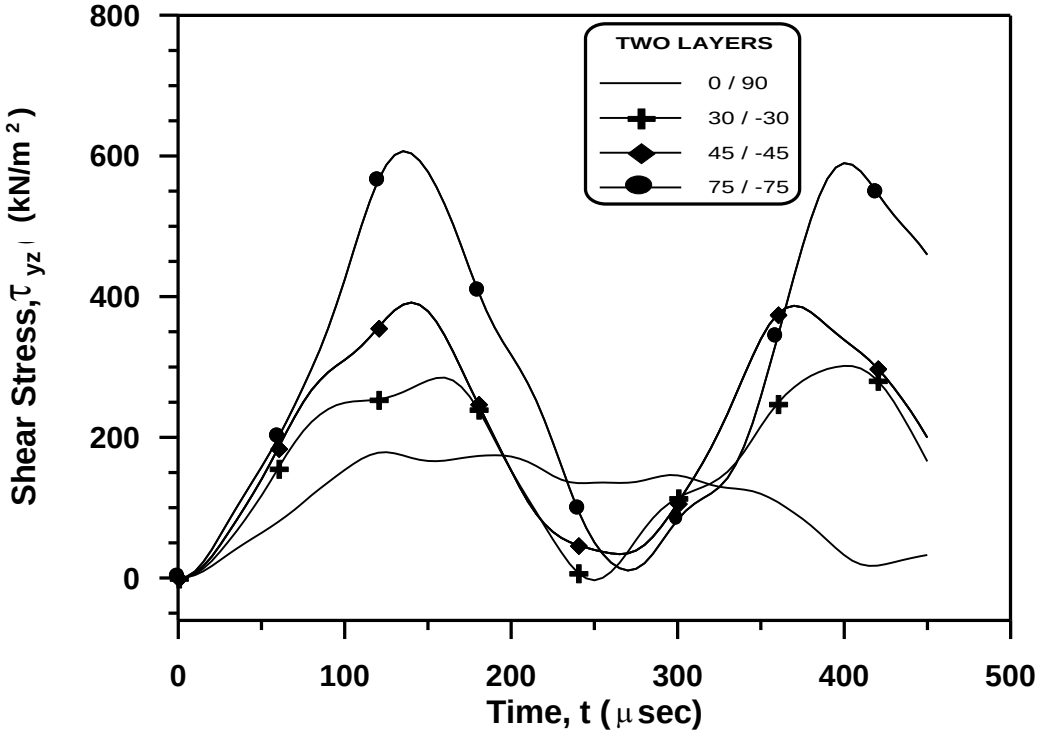

Figure (6.12): Effect of fiber's orientation on shear stress (τ_{yz}) for a simply supported square laminated plate under pulse loading.

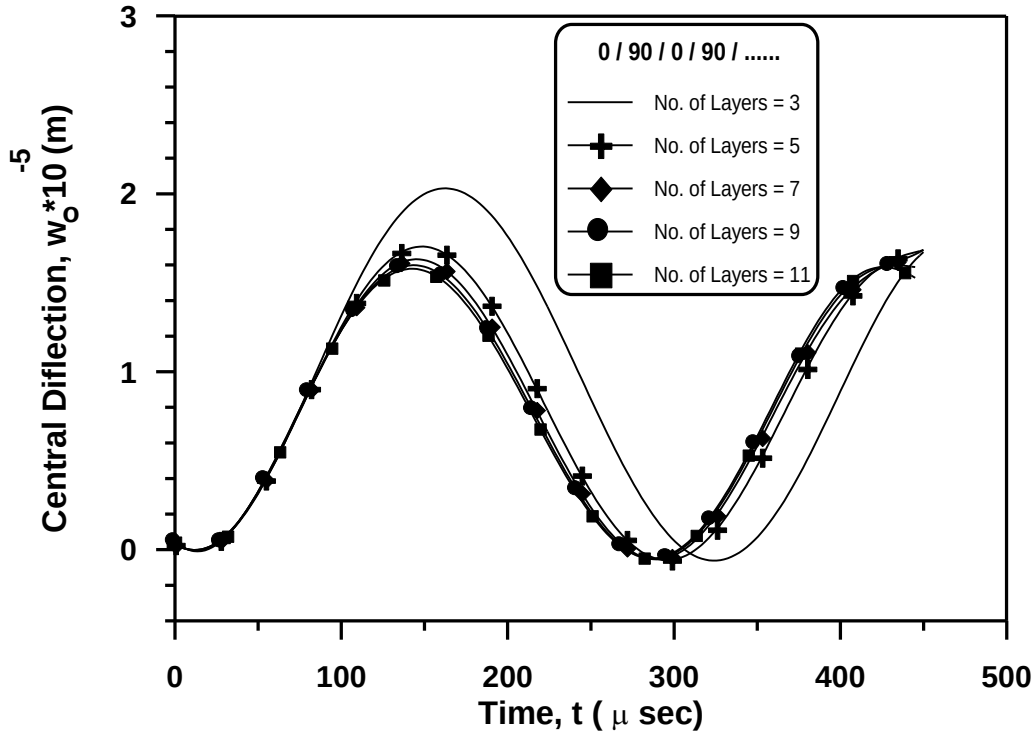

Figure (6.13): Effect of number of layers on central deflection for a simply supported square laminated plate under pulse loading.

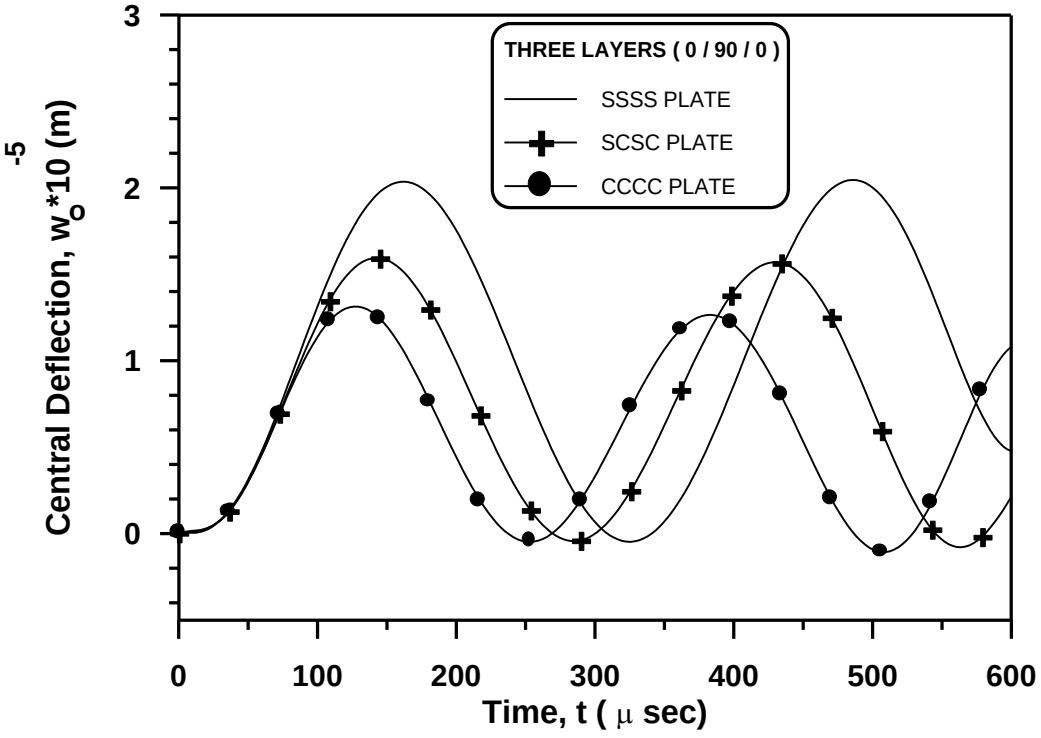

Figure (6.14): Effect of boundary condition on the dynamic response of a square laminated plate under pulse loading.

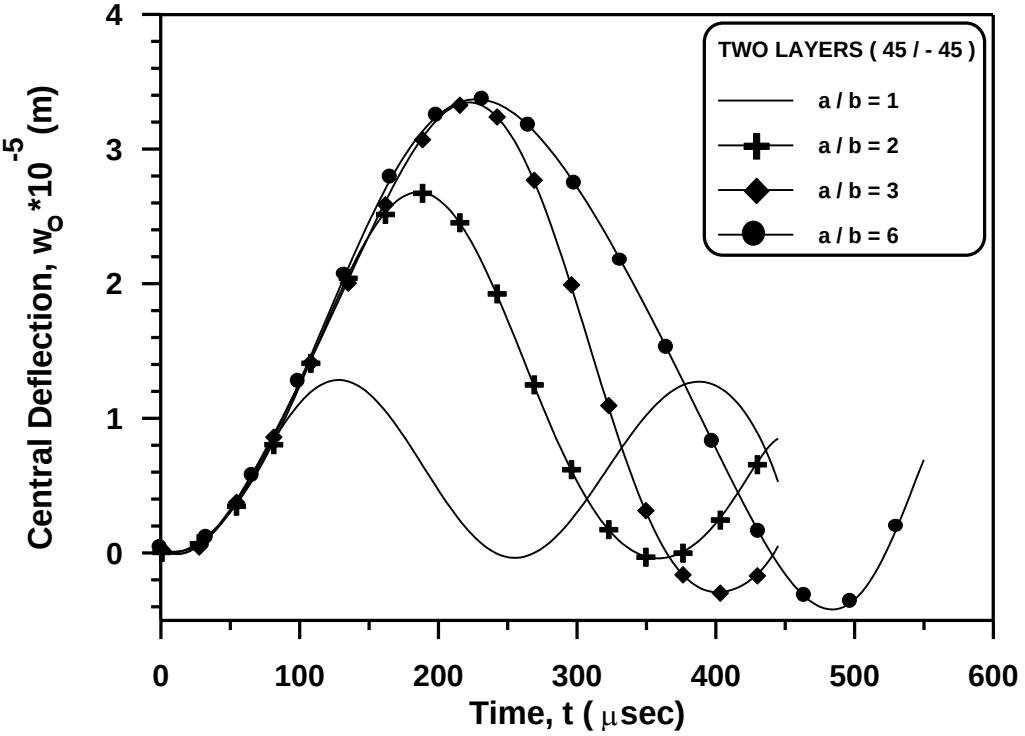

Figure (6.15): Effect of plate aspect ratio (a/b) on the dynamic response for a simply supported laminated plate under pulse loading.

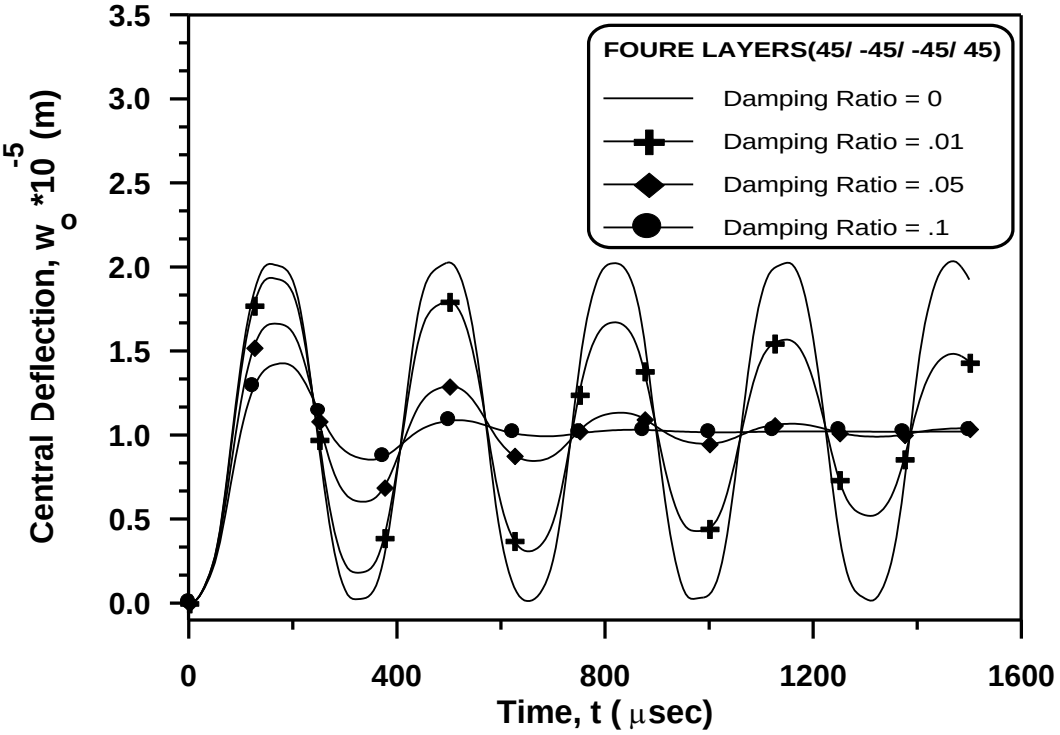

Figure (6.16): Effect of damping ratio on the dynamic response of a simply supported square laminated plate under pulse loading.

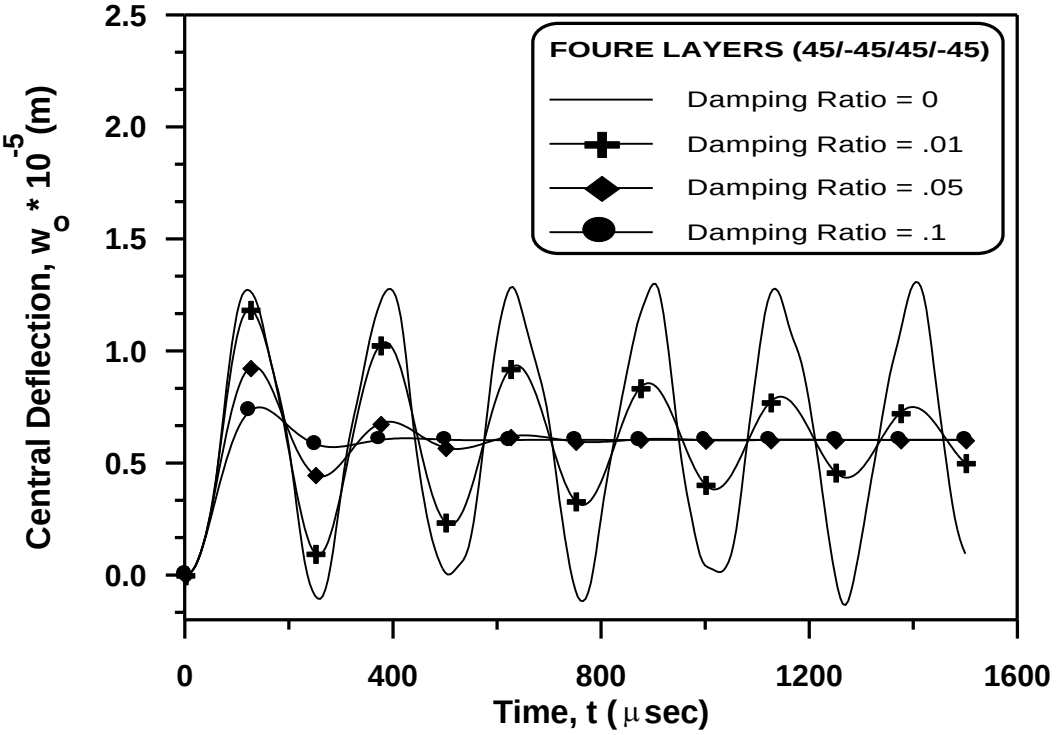

Figure (6.17): Effect of damping ratio on the dynamic response of a simply supported square laminated plate under pulse loading.

CHAPTER SEVEN

CONCLUSIONS AND RECOMMENDATIONS

7.1 Conclusions

Based on the results obtained from the present analysis procedure, the following conclusions can be drawn:

1. The results of present approach (two-dimensional layered approach) associated with the finite element method with higher order shear deformation theory show that this approach which is adopted in this study is suitable for prediction of the static and dynamic behavior of laminated composite plates.

2. The present higher order shear theory of plates represents an efficient theory in analysis of thick sandwich or laminated plates when compared with first order shear deformation theory and classical lamination theory since this theory leads to realistic parabolic variation of transverse shear stress through the plate thickness.

3. The comparison between the present higher order theories (HOST 7 and HOST 9) and the available exact and closed-form solutions shows good agreement. Also, as expected, the results of higher order shear deformation theory with nine degrees of freedom per node are more accurate than the theory with seven degrees of freedom per node. The maximum percentage difference of this theory (HOST 9), with exact and closed-form solution, is not more than (3.85 %, 1.78 %, 2.86 %) in the prediction of stresses of static analysis, the natural frequency , and the deflection of the dynamic analysis, respectively.

4. From the parametric studies, it can be concluded that increasing the degree of orthotropy of individual layers **(E_1/E_2)** by increasing **E_1** for constant **E_2** leads to increasing the stiffness of laminated composite plates for the same volume and number of layers. However, increasing the degree of orthotropy from **(3)** to **(40)** will reduce the central deflection by about **30%**.

5. The effect of fiber's orientation angle is found to have a significant effect on the deflection and stresses of laminated composite plates. It is found that the best angle at which one gets minimum deflection, minimum summation of normal stresses, and minimum shear stresses in plates is **45^o**.

6. The increasing number of layers for the same volume of plate shows a pronounced effect on reducing the maximum deflection of plates. However, for symmetric lamination this effect dies away when the number of layers become more than **(9)**.

7. According to the results obtained, it can be concluded that the antisymmetric lamination of plates has a damping rate faster than the symmetric lamination plate. Therefore, this lamination may be used in places, which are subjected to high intensity impact load and need to damp this wave in a shorter time of duration.

7.2 Recommendations

The following topics are suggested for future studies:

1. The finite element results could be compared with other results that can be obtained by using any other numerical method to evaluate the computational efficiencies.

2. This subject requires to be supplemented by experimental results to be obtained from laboratory tests under dynamic loads.

3. Extension of the present work to include the material non-linearity.

4. Studying the effect of delaminating on the dynamic behavior of laminated composite plates.

5. Studying the wave propagation effect in laminated composite plates.

6. Studying the dynamic behavior of laminated composite plates with woven fibers.